(4)

AFGL-TR-87-0109

IMPROVEMENTS IN EMPIRICAL MODELLING OF THE WORLD-WIDE IONOSPHERE.

Prof. Kurt Suchy
Inst. f. Theor. Physik II
Universitaet
Duesseldolf, W-Germany

Prof. Karl Rawer
Herenstr. 43
March, W-Germany

October 1986

Final Report

30 September 1983 - 31 July 1986

Approved for public release; distribution unlimited.

AIR FORCE GEOPHYSICS LABROATORY
AIR FORCE SYSTEMS COMMAND
UNITED STATES AIR FORCE
HANSCOM AFB, MASSACHUSETTS 01731

UNCLASSIFIED

SECURITY CLASSIFICATION OF THIS PAGE

REPORT DOCUMENTATION PAGE

Form Approved OMB No. 0704-0188

1a. REPORT SECURITY CLASSIFICATION: Unclassified	1b. RESTRICTIVE MARKINGS
2a. SECURITY CLASSIFICATION AUTHORITY	3. DISTRIBUTION/AVAILABILITY OF REPORT: Approved for public release; Distribution unlimited
2b. DECLASSIFICATION/DOWNGRADING SCHEDULE	
4. PERFORMING ORGANIZATION REPORT NUMBER(S)	5. MONITORING ORGANIZATION REPORT NUMBER(S): AFGL-TR-87-0109
6a. NAME OF PERFORMING ORGANIZATION: University of Dusseldorf; 6b. OFFICE SYMBOL (If applicable)	7a. NAME OF MONITORING ORGANIZATION: European Office of Aerospace Research and Development
6c. ADDRESS (City, State, and ZIP Code): Institute for Theoretical Physics, Universitatsstr. 1, D-4000 Dusseldorf, Federal Republic of Germany	7b. ADDRESS (City, State, and ZIP Code): Box 14, FPO New York 09510-0200
8a. NAME OF FUNDING/SPONSORING ORGANIZATION: Air Force Geophysics Laboratory; 8b. OFFICE SYMBOL (If applicable): LIS	9. PROCUREMENT INSTRUMENT IDENTIFICATION NUMBER: AFOSR 83-0369
8c. ADDRESS (City, State, and ZIP Code): Hanscom AFB, MA 01731-5000	10. SOURCE OF FUNDING NUMBERS: PROGRAM ELEMENT NO. 62101F; PROJECT NO. 4643; TASK NO 08; WORK UNIT ACCESSION NO

11. TITLE (Include Security Classification)
IMPROVEMENTS IN EMPIRICAL MODELLING OF THE WORLD-WIDE IONOSPHERE

12. PERSONAL AUTHOR(S)
Professor Kurt Suchy and Professor Karl Rawer

13a. TYPE OF REPORT	13b. TIME COVERED	14. DATE OF REPORT (Year, Month, Day)	15. PAGE COUNT
Final Scientific	FROM 30Sep83 TO 31Jul86	31 October 1986	120

16. SUPPLEMENTARY NOTATION

17. COSATI CODES		
FIELD	GROUP	SUB-GROUP

18. SUBJECT TERMS (Continue on reverse if necessary and identify by block number)
Electron density (profile), Epstein-functions, Ionosphere, International Reference Ionosphere, Optimization

19. ABSTRACT (Continue on reverse if necessary and identify by block number)

Using a method proposed by BOOKER one can describe the ionospheric electron density profile in a fully analytical way by using Epstein-functions. Since the practical application of this idea runs into serious difficulties a solution to the encountered problems is presented. A combined function LAY is introduced which allows the particular peak condition to be automatically respected. A larger set of empirical profiles measured in W-Germany were analysed and conclusions drawn how the function parameters could be determined for profile modelling. Numerical proposals are made with this in view. While these profiles are for the middle ionosphere similar analysis is also executed for typical lower ionosphere profiles and representative parameters are given.

20. DISTRIBUTION/AVAILABILITY OF ABSTRACT	21. ABSTRACT SECURITY CLASSIFICATION
☒ UNCLASSIFIED/UNLIMITED ☐ SAME AS RPT. ☐ DTIC USERS	Unclassified

22a. NAME OF RESPONSIBLE INDIVIDUAL	22b. TELEPHONE (Include Area Code)	22c. OFFICE SYMBOL
Jurgen Buchau	617-377-3121	AFGL/LIS

DD Form 1473, JUN 86 — Previous editions are obsolete. SECURITY CLASSIFICATION OF THIS PAGE

UNCLASSIFIED

TABLE OF CONTENTS

LIST OF TABLES

LIST OF ILLUSTRATIONS

IMPROVEMENTS IN EMPIRICAL MODELLING OF THE WORLD-WIDE IONOSPHERE

1. INTRODUCTION

Numerical Models of the ionosphere are needed for very different applications: radio wave propagation, environmental studies, estimates for theoretical considerations are a few of these. While for experiments with radio waves it is important to have a rather accurate vertical electron density profile at the interesting position, predictions of radio wave propagation often need this knowledge over a larger sector of Earth. For almost all radio problems the electrons alone are of importance, such that the composition of the heavier ions must not be known; also, in this context, the electron and ion temperatures are not important. These parameters are, however, of great interest for environmental studies and for checking aeronomic theories.

1.1 The CCIR Peak Program. Therefore, according to their uses, there exist different models. As for radio wave propagation in the hf range, the Comité Consultatif International des Radiocommunications (C.C.I.R.) has accepted in 1967 a computer program[1] specifying monthly median peak data of the ionosphere, namely: foF2, the critical frequency of the F2-layer and M(3ooo)F2, a propagation parameter used for computing the maximum usable frequency (MUF) for one-hope ionospheric propagation over a given distance. Both parameters are easily deri-

---

[1] C.C.I.R., Atlas of ionospheric characteristics, Rept. No.34o, Union Internationale des Télécommunications, Genève 1983 (original 1967/74).

ved from (bottom-side) ionograms[2]. From the square of foF2 one obtains directly the peak electron density, NmF2. M(3000)F2 is narrowly connected with the peak height, hmF2. Different connecting relations have been indicated in the literature[3-6].

The CCIR peak program[1] derives entirely from a large set of monthly mean data measured at about 100 ionospheric sounding stations all over the world and for many years. The geographic distribution of the stations is not uniform, since there were much less stations in the southern hemisphere than in the northern one and almost none in the oceans. The method of repre-

---

[2] W. Roy Piggott and Karl M.A. Rawer, U.R.S.I. Handbook of Ionogram Interpretation and Reduction, Elsevier, Amsterdam 1961 (and translations into french, japanese and russian languages). Secd. edition: Rept. UAG-23, World Data Center A S.T.P., Boulder, Co., U.S.A. 1972. Revision of chapts. 1-4 as Rept. UAG-23A, ibidem 1978.

[3] T. Shimazaki, World-wide daily variations in the height of the maximum electron density of the ionospheric F2-layer, J. Radio Res. Labs. (Tokyo) 2, 85-97 (1955).

[4] R.B. Bent and S.K. Llewellyn, Description of the 1965-71 ionospheric model used in the Definitive System (DODS), Rept. DBA-Systems, Melburne, Fl., U.S.A. 1970.

[5] P.A. Bradley and J.R. Dudeney, Vertical distribution of electron concentration in the ionosphere, J. Atmos. Terr. Phys. 35 2131-2146 (1973).

[6] D. Bilitza and R. Eyfrig, Modell zur Darstellung der Höhe des F2-Maximums mit Hilfe des M(3000)F2-Wertes des CCIR, Kleinheubacher Berichte 21, 167-174 (1978).

[1] C.C.I.R., Atlas of ionospheric characteristics, Rept. No. 340, Union Internationale des Télécommunications, Genève 1983.

sentation, due to Jones and Gallet[7], starts with a Fourier analysis (of seventh order) of the (monthly mean) diurnal variation. It ends up with 15 Fourier-coefficients for each station. Legendre (spherical functions) analysis is then applied separately to each of these conefficients, thus establishing 15 world-wide maps. None of these has a direct geophysical meaning, but all together with the relevant sine and cosine functions can be used to compose a world-wide map.

This rather complicated procedure, introduced after trials had failed to apply the Legendre procedure directly to foF2 or M(3ooo)F2. Such representation has an understandable tendency to smooth-out the very characteristic steep slopes which occur, in particular after sunrise.

The fact that the world-wide distribution of the basic inputs is far from being uniform forced Gallet and Jones to develope a special procedure for determining the Legendre coefficients. (The traditional procedure needs a uniform grid). However, when they applied their method to the measured data, they got negative values of foF2 in the Pacific (where their grid width was particularly large). In order to exclude such aberrations, they introduced so-called 'screen stations' by shifting coastal stations over some distance into the oceans, thus using the same data input twice. While this trick made the result more reasonable, it had a disappointing effect on the latitudinal variation over the oceans.

Feeling that shifting along circles of constant latitude was not appropriate because the upper ionosphere is under strong geomagnetic control, so that Rawer[8] proposed another latitudinal coordinate, now called MODIP (modified dip) which better

---

[7] W.B. Jones and R.M. Gallet, Telecomm. J. 29, 129 (1962); ibidem 32, 18 (1965).

[8] Karl M.A. Rawer, F2-layer ionization, in: B. Landmark (ed.), Advances in Upper Atmosphere Research, Pergamon, Oxford 1963, pp. 159-2o7.

takes account of this geophysical conditions. The CCIR program derives from an analysis made with this coordinate (instead of earlier geographic latitude).

1.2 The Profile Shape. Apart from this peak program, in view of absorption computations, CCIR accepted later a standard vertical profile following a proposal by Bradley and Dudeney[5,9]. This is a combination of two parabolas, one for the E- and one for the F-bottomside, linked by a linear transition range. Another vertical profile model is used in the Bent-model[4] which is applied in NASA practice for computing the different effects of ionospheric refraction on Earth-satellite radio links in the vhf and uhf ranges. These authors have a fourth order parabola for the bottom-side of the ionosphere, a second order parabola for the topside which on top is linked successively with three exponential sections. Since the bottomside enters into the computations only with its total electron content, the lower ionosphere is summarizingly taken account of by an increased thickness of the fourth order bottomside parabola. The Bent model is particularly important by the fact that it is the only readily accessible summary of a very large set of about 10.000 topside profiles derived from ionograms gathered by the ALOUETTE satellites. All these records are from receiving stations at different latitudes, but all in the longitude range of the American continent. The latitudinal variation in the Bent-model is discontinuous, admitting only three latitude ranges. It is unfortunate that the whole equatorial range ($\pm$ 30° geomagnetic) was thrown into just one latitude range. Thus, in the equatorial zone Bent's reproduction of the outer ionosphere profile cannot show the important variations with latitude which occur inside this zone.

---

[5] P.A. Bradley and J.R. Dudeney, Vertical distribution of electron concentration in the ionosphere, J. Atmos. Terr. Phys. 35, 2131-2146 (1973).

[9] J.R. Dudeney, J. Atmos. Terr. Phys. 40, 195 (1978).

[4] R.B. Bent and S.K. Llewellyn, Description of the 1965-1971 ionospheric model used in the Definitive System (DODS), Rept. DBA-Systems, Melbourne, Fl., U.S.A. 1970.

1.3 The International Reference Ionosphere.

The International Reference Ionosphere (IRI) is an international project which originated in COSPAR (the Space Research Committee of ICSU) and is co-sponsored by the International Union of Radio Science, URSI. In view of environmental applications, which are of first interest to COSPAR, apart from electron densities this model gives also electron and ion temperatures and the chemical composition of the positive ion population. The first IRI was published in 1978[10]; a later publication called IRI-79[11] corresponds, in fact, to the state of 1980. The model is fully computerized. During the years, the 'URSI-COSPAR Task Group on the IRI' has introduced different improvements and the computer program was, accordingly, refurbished several times. The actually valid version is IRI-9.

As for the main peak, the IRI electron density profile, Ne(z), depends entirely on the CCIR program[1]. So, the profile is given in reduced form comparing with the F2 peak density, NmF2. The logarithm of Ne/NmF2 is described layerwise by mathematical expressions which are smoothly connected at the interfaces. This is a rather involved procedure, but it has the advantage that measured characteristics like foE, foF1 etc. can easily be introduced.

---

[10] K. Rawer, S. Ramakrishnan and D. Bilitza, International Reference Ionosphere 1978, International Union of Radio Science (URSI), Brussels, B., 1978.

[11] K. Rawer (chmn.), J.V. Lincoln and R.O. ConKright (eds.), International Reference Ionosphere - IRI 79, World Data Center A (S.T.P.), Boulder, Co., U.S.A. 1981.

[1] C.C.I.R., Atlas of ionospheric characteristics, Rept. No. 340, Union Internationale des Télécommunications, Genève 1983.

1.4 Booker's Proposal. Right at the beginning of the IRI studies, Booker[12] proposed another reproduction of the Ne-profile which is fully analytic. It is apparent that such representation is advantageous for wave propagation computations. Booker starts from a graph of the logarithmic derivative of the profile, d log Ne/dz, which he approximates stepwise by constant values. In order to make this 'skeleton function' analytic, Booker replaces each of the discontinuous steps by one fully continuous Epstein-step-function, Eps_0, which is given by

$$Eps_0\ (z;HX,SC) = 1/(1 + \exp(-\zeta)) \qquad (1)$$

with $\zeta = (z-HX)/SC$.

It is evident that, asymptotically, Eps_0 approaches one at the right hand side and zero at left. The main variation occurs inside the width SC and is centered at HX, where the function takes the value 1/2. By linearly combining several functions Eps_0 with different, suitably chosen parameters (plus a constant), the original skeleton can quite well be approximated. The profile itself must then be found by integration. The integral function to Eps_0 reads[13]

$$Eps_{-1}(z;HX,SC) = \ln(1 + \exp(\zeta)) \qquad (2)$$

and is called Epstein-transition. It has for right hand asymptote the linear function $y = \zeta$ with slope 1, while the left hand asymptote is the z-axis (as for Eps_0). For completeness, we yet note the derivative of Eps_0 which reads

---

[12] H.G. Booker, Fitting of multi-region ionospheric profiles of electron density by a single analytic function of height, J. Atmos. Terr. Phys. 39, 619-623 (1977).

[13] K. Rawer, Replacement of the present sub-peak plasma density profile by a unique expression, Adv. Space Res. 2, No. 10, 183-190 (1982). (Printing error in formula for Eps_1).

$$Eps_1(z;HX,SC) = \exp(\zeta)/(1 + \exp(\zeta))^2. \qquad (3)$$

It peaks at $\zeta = 0$, i.e. $z = HX$, and has on both sides the z-axis as asymptote. It is, therfore, called Epstein-layer.

After integration, Booker's reproduction of the profile is a sum of Eps_{-1} functions plus a linear term (which stems from the constant in the skeleton). His fitting procedure is essentially layer-by-layer, i.e. by successive approximation.

Booker's proposal was discussed in the Task Group on IRI. Since in practice one has some characteristic values rather than the full derivative profile, it appeared difficult to meet these constraints when following Booker's proposal. It appeared at that time that a lengthy trial-and-error process applied to each individual profile was the only way to apply the Booker method with given constraints. A computer program going that way was besides presented in the first (1978) edition of IRI, but was not often used.

1.5 The Topside Profile. In the same edition, and in all that followed, a description in terms of two Epstein transition functions (plus a linear one) was, however, applied to the topside. This description (which is due to S. Ramakrishnan) was indirectly based on the data set gathered by the ALOUETTE satellites since the descriptive function was fitted to Bent's description. Although this latter is discontinuous, the new description was made continuous in all parameters (latitude, foF2, solar activity).

The IRI topside formula depends on eight parameters, namely one HX, one SC and one amplitude to each of the two Eps_{-1} members plus the two parameters of the additional linear function. These were fitted so as to have a peak at the given altitude hmF2. With the first Eps_{-1}, i.e. with HX1, SC1 and A1 Ramakrishnan approached the given Bent-profile in the 1oo to 2oo km

height range, just above the peak and with HX2, SC2 and A2, he adapted the function to the Bent-profile near 7oo to 8oo km of altitude. This was in agreement with Booker's proposal. However, in order to improve the description, a final correction was made taking simultaneously account of both functions together.

It was evident that a generalisation of this latter procedure to the whole ionospheric profile was not very promising, because one had then to deal with a considerable number of Eps_{-1} members (between seven and twelve) and, consequently, with quite a large number of parameters to be determined at one time (certainly more than twenty).

1.6 A Way to Ease Fitting. Later, Rawer made another proposal[14] in order to reduce the number of parameters to be fitted at one time. He felt that by subdividing the height range into, say three ranges, one might be able to come to a reasonable number of unknowns to be determined independently in each range. He applies filter functions by which a given height range might be selected. A function of the following kind is chosen:

$$Fi(z;z_{k-1},z_k) = Eps_o(z;z_{k-1},s) - Eps_o(z;z_k,s) \qquad (4)$$

where z_k is the upper, z_{k-1} the lower limit of the selected range and s is a scale which might be of the order of a few km. Apart from small ranges near $z=z_{k-1}$ and $z=z_k$, Fi_k is essentially one in the range $z_{k-1} < z < z_k$, and zero outside. Now, if for this range any description of the profile has been established as an anlytic function, Ne(z), this latter might take values far away from the given profile outside this range. However, when multiplying Ne(z) by the relevant filter function Fi, the product is essentially zero outside that range and

---

[14] K. Rawer, Analytical description of profiles through planetary atmospheres, Acta Astronaut. 11, 6o7-6o8, 1984.

identical with Ne(z) inside it. Applying this procedure separately in each range and adding up the different products, one obtains a correct reproduction of the whole electron density profile, though fitting was applied individually and independently in each range.

At the range limits one has a continuous change-over from one to the next individual description. In order to have continuity in value and slope, it is requested that at the cutting height the two individual functions take the same value and derivative from both sides. It is proposed to have the peaks of F2- and E-layer as range limits, such that one has three subranges: topside - middle ionosphere - lower ionosphere. The values at the limits are then NmF2 and NmE, with zero derivative at both limits.

1.7 Two Different Fitting Methods. Booker's method of successive fitting ('layer-by-layer') is rather easy to apply. It has, however, an important disadvantage, because each Eps_{-1} function describes the profile only in a subrange within which the logarithmic derivative should essentially be constant. This is so because the skeleton function is piecewise approached; an overlap of the individual Eps_0 functions is not allowed in Booker's method. It is evident that then the number of subranges and that of individual functions might become rather large. This might be acceptable at profile analysis where it is intended to reproduce just one given profile, but it is not suitable at profile synthesis, i.e. for use in a model.

The number can be considerably reduced when overlap of the different functions is admitted. In that case, however, the fitting can no more be made successively, function by function, but has to be made simultaneously for all functions which are needed in a given range. This method[15] will be applied in the

---

[15] K. Rawer, D. Bilitza and T.L. Gulyaeva, New formulas for the IRI electron density profile in the topside and middle ionosphere, Adv. Space Res. 5, No. 7, 3-12 (1985).

following. It was, in fact, applied for the first time with the final adjustment of the IRI topside formula.

1.8 Siting the Main Peak. With our choice of the range limits at hmF2 and hmE, there exists for each range one peak at one of the range limits. Its height and value are a priori given by an external input, e.g. the CCIR program or a formula of geophysical character. It is important that these values are correctly reproduced.

The value problem is easily resolved because in each range we reproduce a reduced (logarithmic) profile, namely log(Ne(z)/Nem).

Consequently, the profile function should be zero at hm. Further, the derivative d logNe/dz should also be zero there. In order to fulfill these two conditions, we need two parameters which can be freely adapted. The linear member is adequate to this end. So, the peak condition might be satisfied by suitably choosing the linear member. Apparently, this can only be done after determining the parameters of the different Eps_{-1} functions because these appear in the detailed formulation of the two above conditions. On the other hand, the linear member is of non-negligible importance in the fitting procedure itself. Thus, an iterative computation schedule would be needed. Rawer[14] has shown how such cumbersome procedure can be avoided. Instead of fulfilling the peak conditions at the end, this can be done before the fitting procedure, provided an individual linear term is added to each member Eps_{-1} in such way that each so formed function fulfills the peak conditions individually. This function is called LAY and reads

$$LAY(z;HX,SC) = Eps_{-1}(z;HX,SC) - Eps_{-1}(HM;HX,SC) - \\ - (z-HM) \cdot Eps_{0}(HM;HX,SC) . \qquad (5)$$

---

[14] K. Rawer, Analytical description of profiles through planetary atmospheres, Acta Astronaut. 11, 6o7-6o8, 1984.

HM is the given peak altitude. By definition, LAY and its derivative as well are zero at z=HM, not withstanding the values of the geometric parameters HX and SC. Figure 1 shows the dependence of LAY-functions on different HX and SC values. It appears that the main curvature occurs, as it must be, near z=HX. If HX is much lower than HM, the function takes quite small values in between, though the peak (of value zero) occurs exactly at z=HM.

When analyzing a profile in terms of a number NFU of LAY-functions, the number of free parameters is 3 ·NFU. Of these, a set of NFU amplitudes enter the analysis as linear parameters, while twice that number of geometric parameters, HX and SC, go in non-linearly.

1.9 Objective of the Study. When ionospheric electron density profiles are to be reproduced along the lines indicated above, it is important that the geometric parameters, HX and SC, of the different LAY-functions can be predicted. In order to achieve this goal, representative values must be derived from a suitable data base. Since, in the functional representation

$$\log(Ne(z)/Nem) = \sum_{i=1}^{I} A_i \cdot LAY(z;HX_i,SC_i) \qquad (6)$$

the amplitudes A_i enter linearly, these can easily be adapted to given constraints in a synthesis program[16]. Not so, however, the geometric parameters HX_i and SC_i. These should be known a priori before synthesis is undertaken, i.e. when the model is used. So, the emphasis of our study shall be on these geometric parameters. It is also important that the minimum number I of members in Equation (6) (needed to obtain a usable representation) should be discussed for the different geophysical situations which are of interest in our context.

---

[16] K. Rawer, Determining electron density profiles for the middle ionosphere, Adv. Space Res. 5, No. 1o, 43-49 (1985).

2. DATA BASE

2.1 Middle Ionosphere. Our main data base is a large set of profiles which were computed from good quality ionograms recorded at Lindau/Harz (51.62°N, 1o.o9°E) by W. Becker[1]. The final profile is tabulated with high resolution (plasma frequency steps of 1/1oo of foF2). Of course, the lowest part of the profile is extrapolated (by a cosine function) since there were no measured data below a sounding frequency of 1 MHz. Considering this fact in our evaluation, we avoided the use of height values relative to plasma frequencies below o.5 MHz.

Becker's computation method[2] applies the often used parabolic approximation for the part of the profile immediately below the peak. The critical frequency is obtained very accurately by this fit which is repeatedly applied whenever needed. In the middle part of the profile he applies splining (generally of second order). The reading frequencies are individually chosen so that to each step in frequency corresponds roughly the same height step. The "underlying ionization" is taken account of by an assumed cosine extrapolation towards zero plasma frequency.

Though Becker has a particular sub-routine for taking account of an E-F-valley (i.e. a minimum of ionization above the E-peak) this was not applied in almost all of the profiles we have received. So, his results are "lowest acceptable" profiles. This means: in case a valley was present, the real heights are higher than given by his profile. The difference is the valley width just above the E-layer critical frequency, foE; it decreases

---

[1] We are grateful to Dr. Walter Becker for giving us two magnetic tapes containing a large number of such profiles.

[2] W. Becker, Die Bestimmung der Feinstruktur der Ionosphäre aus Ionogrammen, Kleinheubacher Berichte 13, 37-44 (1969).

with increasing frequency. Nevertheless, the error at the F2-peak, i.e. in hmF2, might be about 1o km.

Otherwise, most of the profiles on the tapes are reliable. There is probably some smoothing introduced by the second order splining, but this is on line with our intentions: most original ionograms show small deformations of the trace which are mostly due to gravity waves in the upper atmosphere. For our purpose, these must be considered as unwanted perturbations of the intended undisturbed profile. So, the kind of smoothing introduced by the splining is just waht we need in order to get representative profiles.

In a very large data set as Becker's it is extremely difficult to exclude that a small number of the results is in error. We have found a few profiles with apparent errors in height scaling (e.g. E-peak at 5o or 15o km). Some day-time profiles show no E-region - probably because the corresponding trace was not visible on the ionogram. Profiles with apparent errors of this kind were omitted from our evaluation.

The data set covers day and night about equally well. For most evaluated dates, ionograms had been taken at hourly intervals or even more often so that the diurnal variation is covered. While the density of observations is high in this respect, the periods treated are not uniformly distributed over seasons and years. Two periods are particularly well covered, namely:

- summer (27.6. - 1.7.) of 1954
- spring (21.3. -28.4.) of 1958.

Quite clearly, 1958 was a year of extremely high solar activity while 1954 was about minimum. This is not too bad for our present purpose, because we can expect that the range of parameters can be estimated when comparing the two periods.

The total number of points on tape determining the profile is too large for our purpose of fitting the profile with a small

number of functions. Also, thanks to smoothing, the information about the profile does not correspond to such large input. We have made the first fitting trials with every second point, i.e. 5o in total. Since the computer time increases considerably with the number of points to be fitted, we finally used every fourth point, i.e. 25 in total. This number further is reduced because the lower frequency data (sounding frequency below o.5 MHz) are omitted. However, this was done by putting the weight to zero so that the number of points in the algorithm remained 25 always.

Our aim with these data is getting characteristics for the middle ionosphere. So, sounding results referring to regions below the E-peak are of no interest. To take account of this, the weight individually attributed to a profile point was cut below 1o5 km by an Epstein-step filter centered at that altitude (with scale s=4 km). Since bottom-side ionograms give no data from above the F2-peak, filtering at the upper end of the height scale was not needed.

2.2 Lower Ionosphere. The electron density profile shape below the E-peak is rather similar to that in the middle ionosphere with the difference that the profile is almost always monotonous. The occurrence of a minimum seems to be very rare, but a turning point around 8o km is typical. So, the same methods of representation can be applied as for the middle ionosphere.

a. McNamara's data base. By very detailed literature survey, McNamara[3] was able to produce a large collection of lower ionosphere electron density profiles observed with different

---

[3] L.F. McNamara, Ionospheric D-region profile base, a collection of computer accessible experimental profiles of the D- and lower E-regions, Rept. UAG-67, WDC A (S.T.P.), Boulder, Co., U.S.A. 1978. /We thank for granting us a magnetic tape containing these data/.

methods. His profile set contains, of course, data of very different quality. The elder in-situ measurements are very doubtful and even the more recent ones have yet problems with absolute calibrations. This latter is, unfortunately, often height-dependent so that even the relative profile shape is not guaranted.

Y.V. Ramanamurty, who has taken over to check this data set, established several groups according to the standard of the observations. Since our fitting procedure depends strongly on the peak value - the E-peak here - a large number of observations is not useful, because the E-peak is not covered and the absolute accuracy of the pretended density values is very poor. Therefore, only a small selection of profiles of this collection could be used for our purpose. It was, of course, obtained at very different locations and times. There is, however, a clear preference for day-time and northern middle latitudes. Night observations are quite rare.

b. Thumba probe data. Subbaraya et al.[4] have published a set of rocket measurements made at Thumba in southern India (8.53°N), near the magnetic equator (dip o.4o°S). The data set is much more homogeneous than McNamara's though, of course, rather restricted. The measurements were all made with comparable equipment and cover the altitude range from 6o (day) or 85 (night and twilight) up to 16o km. For day-time (near noon), a total of twelve rocket ascents was available. Night measurements were made at six occasions and twilight ones at seven, three in the morning, four in the evening. The authors give a mean electron density profile for day-time. For the other three groups, we produced medians from the given profiles.

---

[4] B.H. Subbaraya, Satya Prakash and S.P. Gupta, Electron densities in the equatorial lower ionosphere from the Langmuir probe experiments conducted at Thumba during the years 1966-1978, Rept. ISRO-PRL-SR-15-83, Indian Space Research Organisation, Bangalore, 1983.

So, for each of the four groups we have obtained a more or less representative profile. The definition of this latter is best for day and not too bad for night. Understandably, the original twilight profiles show rather important differences one against the other. This must be accepted, noting the quick changes occurring during these periods. Nevertheless, we feel that these four profiles might, provisionally, be taken as representative low-latitude profiles.

Since our analysis has to assume an E-peak, we identified this point individually on the given profile knowing, of course, the standard height range of region E. By day, the experimental profiles between 1oo and 14o km are sometimes monotonous, sometimes they show shallow minima, all with rather small variation in this height range. The mean day-time profile is monotonous. In individual night profiles, however, above a peak at a height between 1o4 and 114 km up to at least 155 km, there is a large range of definitively lower electron density. This is also shown in the median.

c. Singer's profiles. In his thesis Singer[5] produced profiles which, by a kind of trial and error methods, were fitted with a rather large number of propagation data. The question whether such 'conversion' is unambiguous has often been discussed. The author[5] feels that his inputs are so numerous that the final profile should be quite well defined. While medians of in-situ observations necessarily must be smoother than the individual profiles, Singer's technique probably has a tendency to produce rather sharp structures in the profile. This seems to be particularly so for night time. The relevant Singer profile is, in fact, a profile with rather sharp steps. We cannot decide here, whether this is a well-based result but have some doubts about this particular profile.

---

[5] W. Singer, Doktor-Dissertation, Humboldt-Universität Berlin, 1976. /We thank for forwarding us the profile tables/.

3. MATHEMATICAL TOOLS

We intend to reproduce a given profile, i.e. a set of between 15 and 3o profile points by a linear combination of three or, at most, four LAY-functions /Equation (6)/. Each function contains two geometric parameters, HX and SC, and is multiplied in the combination by a coefficient which might be called amplitude A. The task is to find an optimum set of the (unknown) parameters and amplitudes.

3.1 Reduced Error Sum. First of all, we must define a criterion for "best fitting". In the almost always used method of 'least squares' one takes the sum of the squared individual errors as the quantity which should be minimized in the procedure. However, since we attribute different weights, W, to the points, these weights must be used at the summation of the squared errors. So, we should consider

$$\sum_{k=1}^{M} W(k) \cdot (Y(k) - F(k))^2$$

where Y is the given value (at point k) and F is the corresponding value of the fitting function. This expression is well suited as criterion for fitting.

However, since the weight function W gives little weight to out-of-range points (below a lower limit, HW), the number of the mainly contributing points is different for different profiles. For example, in Becker's data set HW=1o5 and the reading points are at equal steps of the ratio f/foF2 where f is plasma frequency and foF2 the peak plasma frequency of the F-region. Thus, with a small foF2 a greater number of points falls below the E-peak than with a large foF2. For this reason, we have to expect a smaller sum for small foF2, i.e. low peak density. Since we intend to have a reliable measure giving comparable results under different conditions, a suitable reduction of the

above expression is needed. It can be obtained by dividing the above sum by the sum of the individual weights (which in the Becker schedule is smaller for small foF2). So, we define:

$$S = \sum_{k=1}^{M} W(k) \cdot (Y(k) - F(k))^2 \Big/ \sum_{1}^{M} W(k) \qquad (7)$$

as reduced error sum. It gives the average of the weighted squared error per point.

3.2 Problems with Optimization.

a. Linear or non-linear. Optimization is quite easy if the unknown parameters appear linearly in the fitting function F. In that particular case, the method of least squares leads to a system of linear equations with the different parameters as unknowns. Since the error sum is differentiated separately after each parameter, the number of equations equals the number of unknowns. The resolution is then obtained by standard methods provided the determinant of the coefficient matrix is different from zero. This condition is, however, only satisfied when all the different parameters are mutually independent. If there exists a (linear) connection between two of them, the determinant becomes zero such that no unique solution can be found.

In our fitting problem with Equation (6) the amplitudes go in linearly, but not so the geometric parameters, HX and SC. So, we have to face a non-linear problem. There exist different methods of optimization with non-linear parameters, all of which are necessarily iterative. The criterion expression - for us: the reduced error sum - as function of a number, L, of different parameters defines an L-dimensional surface in an (L+1)-dimensional space. An optimum means that there exists a minimum of the criterion at some combination of parameters. When the

entries are empirical data, there is not necessarily a unique minimum. If more than one appear, we encounter a serious difficulty.

b. Interdependence of parameters. Another problem which might become serious occurs when the parameters are not fully independent from each other. In particular, with empirical data such connections might only be valid in certain ranges of the relevant parameters. In that case, instead of a clear and unique 'crater-like' minimum, the criterion surface shows a more or less elongated 'minimum trench'. Note, that this can in practice occur without strict mathematical interdependence; it is sufficient that there exists no notable change of the criterion value along the 'trench'. An example can be seen on Figure 2 where we consider only one member in the sum and so have L=2, i.e. only two variable parameters, HX and SC, are admitted. Lines of constant reduced error sum S in an HX vs. SC diagram were drawn. We call such diagram 'error map'. In such case, no unique optimization result can be reached. The final result of an optimization procedure can then be any point at the bottom of the rift. In that case, the final result depends on the assumed entry values of the iteration.

c. Admissible number of unknowns. The iterative procedure starts usually with first determining the direction of steepest descent on the criterion-(error-) surface (arrows in Figure 2). L direction cosines must be determined to this end. If the assumed function allows it, these can be obtained by functional differentiation. The next step consists in a first correction, i.e. changing the parameters in a way that this direction is consistently followed. A step width SW must be assumed, it is usually decreased with increasing order of the iteration. Though this looks quite promising, the execution becomes more and more involved when the number L of unknown parameters increases. In practice, there exists a limit above which the iterative process might be unable to find the best possible

set of parameter values. It is rarely hopeful to let L go up to 1o.

In our case, we have 9 unknowns if the number, NFU, of LAY-functions is three, 12 if it is 4. Further, the parameters are not independent. In particular, the amplitude A and the transition height HX are de facto interrelated. With a larger A and a correspondingly decreased HX, one might come to a rather similar profile as with the original values, see Figure 3. Note, that the comparison is only made at a limited number (less than M) of given points and mainly over not much more than 1 decade from peak value.

d. Failure of differentiating procedure. Therfore, we could not apply one of the usual optimization methods unchanged. At first, we tried to find the direction of steepest descent, as usual, by differentiation, in our case after the geometric parameters, HX and SC. When doing so, the functions EPS_0 and Eps_1 are needed. Since the amplitude A - noting that it is not independent of HX - was held constant, the so found HX \SC direction was not really that of steepest descent in an absolute sense. In fact, by adjusting A to its optimum value a smaller error sum would be achieved. On the other hand, due to the interdependence, a method admitting all three variables would not lead to a clear answer, because the iterative process might develop towards extreme values of one or the other parameters.

With this result in mind, we finally decided to build an optimization procedure of our own, avoiding functional differentiation and taking account of the quasi-interdependence stated above.

3.3 Our Own Optimization Procedure.

a. Elimination of the amplitudes. In view of the above, we rearranged the iterative process applying it only to the geometric parameters, taking, however, care that the optimum amplitudes for all three or four LAY-functions, Equation (6), were re-determined at each step. So, independent from the applied set of geometric parameters, the amplitudes were step by step optimized so that they were no more considered as variables in the iteration itself. Since they enter linearly in F, these coefficients can straightforward be found by resolving a system of linear equations. With three or, at most, four unknowns this needs not very much computing time.

b. Parabolic extrapolation. Many optimization programs apply a linear extrapolation along the line of steepest descent. We had not much success with such a method, because it has a dangerous tendency: just when the minimum is approached, the extrapolation towards zero error pushes the iteration to often larger aberrations on the other side of the rift. We, therfore, finally preferred a parabolic extrapolation towards zero error.

In order to determine this parabola (with distance on the line of steepest descent as abscissa), we need three points, one more than for a linear extrapolation. We divide the given step-width SW by 2 and make two consecutive steps along the given direction. Together with the start position, this triple determines a parabola which either is concave and has a minimum somewhere (inbetween the three points or outside) or it is convex. In the latter case, the program identifies that of the three positions with error sum lowest and then takes one more step (of SW/2) in the direction beyond this point. The so found fourth position together with the two others next to it, is then used as another triple and another parabolic extrapolation is undertaken. The same is done when, in a concave situation, the computed minimum is too far distant (situation 'FLAT':

for us: beyond six forward or two backward steps). The forward or backward shift of the triple is arranged by the subroutines SHIFTA and SHIFTR , respectively. The number of these shift operations (during one iteration act) must, of course, be limited (we used a limit of 5).

Once a suitable parabolic minimum is found, this position is taken as starting point for the next iteration act (with halved step width).

c. Memorizing best conditions. Since it is not certain that this position has really a better error sum than reached formerly, during the whole iteration process we always had to remember the best condition found. In the subroutine RERRSS, which computes the reduced error sum, we have a final disjunction asking whether the new error sum is smaller than the smallest one reached before (which is in the memory). If it is, then instead of the memorized set, the new reduced error sum together with the corresponding set of all geometric parameter and amplitudes is commemorated. In case no improvement was reached the next iteration act starts from this "provisionally best" position (with renewed determination of the steepest descent direction, and halved step width).

d. Finding the steepest descent. When applying differentiation after HX and SC, we took the amplitude as fixed which is not justified. This could be corrected for, if the relation between A_i and HX_i a priori was known. But it is not and its coefficients depend on the individual data set. Therefore, the direction we found was not really that of steepest descent when A is allowed to vary too. This direction error was found to be quite appreciable so that the optimization advanced quite slowly.

In order to get this direction correctly without admitting A as an independent variable, we decided to use a non-differentiating

approach, replacing functional differentiation by a numerical one, i.e. by determining quotients of differences. This must, of course, be done with adequate small steps. At start, we take o.5 and 1 km (for SC and HX, respectively); in later iteration steps, when the iteration step SW decreases, we take care that the 'differentiation' step remains small against it. Designating the parameter values by Pj (j = 1 ... L, according to the number of variables chosen), we have a set P_j at the start position. We then make a displacement by ΔP_j in just one direction j so that we get a set of L auxiliary points, each on one of the R_j-coordinate axes.

To each of these L positions the error sum is computed (with optimized amplitudes always); from its difference against that of the start position the direction cosine (quotient of differences) can easily be computed. The ΔP_j define a multidimensional plane and its direction of steepest ascent is determined. This does subroutine ASCENT. The direction of steepest descent is then obtained by inverting the signs.

e. Description of the main program. The most important particularities of our optimization routine APTR have been described in the foregoing. A flux diagram, showing the most important actions in this program, can be found in Figure 4a. The important subroutines in APTR are shown in the subsequent Figures 4. The full text of subroutine APTR is reproduced as Figure 5 (in computer language SIMULA,of the ALGOL family).

By virtue of the subroutine CODELL, different combinations of variables can be selected. Instead of applying the optimization routine at once to all geometric parameters, it was in most conditions more advantageous to apply it several times with each time another suitably chosen set of variables. The last time we then admitted all geometric parameters as variables, but now starting from a rather good position and applying a small step width. In case of NFU=3, this means 6, for NFU=4, however, 8 variables. CODELL allows to go up to NFU=5 and offers 2o different combinations.

4. RESULTS MIDDLE IONOSPHERE

Our data source for this height range are W. Becker's profiles (see chapter 2.1). In the two tapes we have received from this author, for each profile he has evaluated he gives several presentations, the most useful for out purpose being one in height and normalized plasma frequency, the latter in units of 1% of the critical frequency foF2, thus with 1oo points per profile. For the purpose of our work and in view of the increase of computing time with increasing number of data points, we retain only every fourth data point which makes 25 per profile. This should be enough for defining a profile with good enough accuracy. It must, however, be noted that even so the lowest sampling frequency (4% of foF2) is quite a low one on which actual ionosonde measurements could actually not be made: either - at night - by the lower frequency limit of the instrument, or - by day - by absorption in the ionosphere. In fact, Becker has applied extrapolation towards the lowest frequencies. In particular, at night, this is misleading because the 'nite E' layer is known to exist, but does not show up on the ionogram and so not in Becker's profiles. Therefore, we have given zero weight to all data points at plasma frequencies below o.5 MHz. On the other hand, a decreased weight has been attributed to data points at altitudes below 1o5 km by putting $W=Eps_0(z;1o5,4)$.

As explained in our earlier report, there are, amongst Becker's profiles, quite clearly cases where something went completely wrong with the height scale or with extrapolation so, that geophysically improbable positions of the E-layer appear from time to time. Or, this layer is known to be the most regular of all and to appear in the same height range always. These errors are probably due to ionogram scaling or occurred during digitizing.

4.1 Night Profiles. At night, ionosondes only see an F-region trace with a minimum true height well above 1oo km. It is, however, known from other sources that an E-region is always

existing, but with rather low peak electron density so, that it cannot be readily detected with a normal ionosonde. Piggott and Rawer[1] give values of foE which lie between 1.o and o.55 MHz /Ne between 12.4 and 3.75 · $1o^9$ m^{-3}/. This should held from 1 h after sunset to 40 min before sunrise. Becker's tables, however, give curves ending with 1% of foF2 at heights well above 1oo km, the lowest points of which have certainly been obtained by extrapolation and cannot be correct. In our computations we always disregard those points of Becker's at which the plasma frequency is below o.5 MHz.

a. Odd conditions. At times, the bottom part of a profile may show a steep gradient, at other times, however, an almost linear decrease of plasma frequency with height. We have some doubts about these latter cases, because it is known that a deep valley exists at night so, that a sharp gradient should appear somewhere in the F2-profile. Our doubts are increased by the observations that such cases often appear for a short peri- or amongst 'regular' ones. Looking through a dense series of summer night measurements (about every half hour), we found many cases of "switching" between the two types in a 3o min interval. Apparently, some non-stationary condition of the F-region must have occurred. May-be, as by day, gravity waves produce short-lived deformations of the ionogram trace which, at data reduction, are smoothed and appear in the final profile as an extension towards lower altitudes.

This odd kind of night profiles in Becker's set has a large range of almost linear variation of plasma frequency with height. Figure 6 shows a normal and an odd profile for comparison.

---

[1] W.R. Piggott and K. Rawer, URSI Handbook of Ionogram Interpretation and Reduction, Elsevier, Amsterdam 1961, p. 127.

When fitting with just one LAY-function, the normal profiles use to be very well reproduced, the odd ones not so well. This appears clearly from the corresponding error maps which we show in Figure 7. The normal profile of Figure 6a shows a clear-cut 'trench' in the error map (Figure 7a). Since HX and A are interrelated, the optimum condition can be realized with different combinations of both as shown by the 'trench'. The odd profiles (Figure 6b), however, show instead of a 'trench' a broader 'valley'. The absolute scale values, SC, are much larger in odd cases, more than twice those found with parabolic shapes. This stems from the fact that our "best fit" is one which covers the over-all width of the layer rather than to reproduce best its high-density (peak) range.

As expressed above, we have doubts whether these conditions which occur only for short time sections should be taken as representative. Rather, we shall base our summary on "quasi-parabolic" conditions only. This is the more justified since we should anyway disregard the doubtful information, given at lower frequencies in Becker's profile. In the synthesis of night-time middle ionosphere profiles, we might then introduce a deep valley and "nite-E".

Just in order to demonstrate how the normal and the odd types behave, in Figures 7 we have shown error maps (arbitrary units) for these two conditions. Both are only 3o min apart. The corresponding profile shapes can be seen from Figures 6. The profile at 2oh3o is odd, that at 21 h normal. The quick change of types might be seen from the following table:

Table 1: Variation of scale, SC, for two night periods (25/27 June, 1954). NFU = 1: one LAY-function only. (Clearly odd profiles underlined).

(a) Night 25/26 June:

Hour	19.3o	2o	2o.3o	21	23	23.3o	00.3o	01
SC/km	23	14	<u>34</u>	8	4	6	<u>23</u>	2o

(b) Night 26/27 June:

Hour	2o.27	2o.57	22	23.57	00.27
SC/km	<u>4o</u>	24	1o	<u>47</u>	21.5

It is a merit of Becker's dense series of profiles that such phenomena and their changes can be seen at all which does, of course, not hold for averaged profiles. We feel that, in view of our final aim, we have to disregard these cases of 'linear decrease' because, what counts for our purpose, are stable conditions.

On the other hand, comparing with density-averaged profiles, the individual profiles in Becker's set have somewhat smaller thickness. We conclude that <u>averaging</u> over all conditions leads to <u>thicker</u> layers than does a selection of <u>stable profiles</u>.

b. Normal conditions at night. Apart from short-lived deformations, normal night profiles use to be of almost 'parabolic' shape. This is valid at all latitudes. Therefore, for reference purpose at least the night profiles can be reproduced by just one LAY-function. When trying with two such functions, one amplitude happened to come out quite small so that the effect of the second member in Equation (6) was negligible. This might be different with odd shapes which sometimes do occur (see a. above). We, therefore, feel definitively that the <u>night-time F-region</u> profile should be reproduced with <u>just one</u> such function.

One LAY-function has only two geometric parameters, such that our mapping program gives the best answer directly without further assumptions. For the majority of profiles which are of almost parabolic shape, the HX versus SC map shows a straight "trench" of "valley" which lies vertically in the map, such that the scale where the minimum appears is well-defined. In the trench one obtains about the same error value with different transition heights HX. This structure is the simplest we found. At analysis, this means that while the scale must be optimized the transition height is left free in a large range (of 100 km or more).

This feature appears, of course, only with our schedule of redetermination of the amplitude A at each step. With a fixed amplitude one would obtain just one minimum, not a trench. Some examples of error maps can be found in Figures 8 (which we shall discuss below).

Along the trench there exists, of course, a quite appreciable variation of the amplitude A which decreases towards larger values of HX (downwards in the Figures). The 'trench' is, however, not unlimited in the HX-direction: at its lower end (large HX) there appears a quick increase of the error sum. At the other end, the amplitude becomes larger and larger and at a certain

limit there appears an even steeper increase of the error sum. So, for a given profile we have to accept a limited HX range with a rather well defined scale SC as optimum condition. In practice, it is preferable to have not too large amplitudes and, therefore, we shall propose for applications HX values near the lower end of the trench.

All night-time error maps (of which we have drawn a large number) show similar structure, though the width of the trench varies. It is important to note that the low amplitude limit (at the bottomside in our Figures) was always found well below the peak altitude HM, sometimes even below HM/2.

As for our optimization program, it reaches necessarily a correct and unique scale value SC, while the final value of HX, due to the particular configuration, usually remains near the start value of this parameter. This ambiguity is typical at profile analysis.

At profile synthesis, however, (which is later to be executed when applying our results in IRI) we have quite a bit of freedom in choosing HX but not so for SC. Since this is our final intention, we have studied in more detail where the low amplitude end of the trench occurs and whether the relevant HX-value can be specified. To this end, that value (designated as HX_1) was compared in turn with the peak altitude, HM, the half-density altitude, HHA, and the quarter density altitude, HQA. In Figures 9a, b, c the relevant ratios have been plotted against the peak altitude, HM. Data were from the solar minimum year 1954 on the one hand, and from the very high solar maximum in 1957 and 1958 on the other. The Figures show the ratios decreasing with increasing HM. A straight line connection of the median point of the two periods is given by the following Equations:

$$(+): \quad HX_1/HM = .795o - .59o\ HM/1ooo\ km \qquad (8a)$$

(o): $HX_1/HHA = .9810 - .690\ HM/1000\ km$ (8b)

(x): $HX_1/HQU = .9605 - .525\ HM/1000\ km$. (8c)

The dispersion of the individual points is rather large. Nevertheless, the decreasing tendency is certain. We have also plotted the corresponding height differences (in Figures 10a, b, c). This is, of course, increasing with increasing HM and the connection of the median points is given by:

(+): $HM - HX_1 = .6130\ HM - 70.30\ km$ (9a)

(o): $HHA - HX_1 = .3680\ HM - 48.40\ km$ (9b)

(x): $HQU - HX_1 = .2845\ HM - 38.65\ km$. (9c)

We leave it open which of these relations might be most helpful at profile synthesis. The above relations (..a) with HM have the advantage that they do not need another characteristic. HQU might not be available experimentally when the peak density is small. So, the choice would probably be HM (or HHA). However, since these are median lines half of our data ly on the unwanted side. For this reason, at applications we should not use the median line but one on the safer side, e.g. the appropriate <u>quartile line</u> (thin lines in the Figures). These obey the following Equations:

$$\left.\begin{aligned} HX_{q1}/HM &= 0.7184 - 0.5708\ HM/1000\ km, \\ \text{i.e. } HX_{q1} &= 0.7184 \cdot HM - 0.5708\ HM^2/1000\ km \end{aligned}\right\} \quad (10a)$$

$$\left.\begin{aligned} HM - HX_{q2} &= 0.6\ HM - 30\ km \\ \text{i.e. } HX_{q2} &= 0.4\ HM + 30\ km \quad . \end{aligned}\right\} \quad (10b)$$

Since it has been proposed to apply a simple proportionality re-

lation for deducing[1] HHA from HM, we investigated this ratio with our data. Figure 11 shows the result. For night conditions, in solar minimum and maximum as well, the ratio is quite near to o.8 as indicated by this author. Drawing, as above, the connecting line between the median points of both periods, we get

$$HHA/HM = 0.9075 - 0.255\ HM/1000\ km.$$

Since the dispersion is rather small, an oblique median line through all points should, however, be preferred; it reads:

$$HHA/HM = 0.91 - 0.25\ HM/1000\ km \quad . \qquad (11)$$

This is the bold line in Figure 11. The quartile ranges, as indicated by thin lines in the same Figure, show that the dependence on HX is significant. During solar minimum when the peak altitude used to be considerably smaller, the median value of the ratio was o.83 while only 0.785 during solar maximum.

c. Short term variations. Becker's data set covers some dates for which profiles were computed at hourly or even half-hourly intervals. These are well suited for answering the question after the short term variability of the parameters HX and, in particular, SC. In Figure 12 we show in some detail what happened during the late night of 24/25 June, 1954. Apart from the f_p (plasma frequency) vs. height profile, two cuts of the error map (around the minimum) are shown with HX fixed at HM/2 and HM/3, respectively. It appears from this Figure that the quick changes between "normal" (a,c,f,g,h) and "odd" (b,d,e) profile types are accompanied in the map by a switching between a narrow "trench" centered at a small SC (between 5 and 25 km) and a broader one with much larger SC.

---

[1] T.L. Gulyaeva, Implementation of a new characteristic parameter into the IRI sub-peak electron density profile, Adv. Space Res. 2, No. 1o, 191-194 (1983).

One might try to take care of the different behaviour of what we called above "normal" and "odd" layers by comparing with a layer thickness parameter, e.g. the thickness SH, given by HHA (the point of half peak density), or SQ, given by HQU (at half plasma frequency, i.e. quarter density). These points are shown on the profiles of Figure 12 (as cross and bar, respectively). It appears that SH = HM - HHA is not much different while the quarter-thickness SQ = HM - HQU is considerably larger whenever the layer shape is "odd". The drawings also show the presumed "typical" value of o.8 HM for Nm/2. It appears that - at night - this altitude is almost always below HHA such that, when applying the coefficient o.8, one makes the layer thicker than observed. /Compare also Figure 11 above/.

We have studied in more detail another night of the same month /26/27 June 1954/ producing error maps and cuts at HX_1 = HM/2 for 15 profiles which Becker has deduced for the period 18h3o through o5h3o LT. It appeared that, when arranging after the optimum SC value, we find three groups of profiles: a group (a) with SC between 5 and 12 km, a group (b) around 2o km and a group (c) above 25 km. At least in that particular night the groups are well distinguished. We show the error map cuts in Figures 13a, b, c according to these groups. (The order inside each group was chosen for convenience of the aspect of the drawing). Of course, the trenches are narrower in group (a) where the optimum SC is small. The width can become quite large in group (c). This means that we have a large range of acceptable SC values, while in group (a) the "optimum analysis" leads to a well defined value. The narrowest trench was found for o2 h with a quite low minimum error which, however, increases rapidly at both sides.

The main question on our context is whether on behalf of the optimum, SC(opt), there exists some regularity or a systematic variation during the night. In order to demonstrate that this is not so, we show in Figure 14 some characteristic features of the

error map cuts in chronological order. On the diagram on top, showing SC(opt), one easily identifies the three groups. Their appearance during that night is apparently at random, no systematic variation being visible. Also, there exists no relation whatsoever with the HX_1 value (HM/2, shown on the bottom diagram). The same holds for the minimum reduced error sum, Err, which was plotted in second position (in units of $1o^{-4}$). As mentionned above, there must exist a relation with the width of the trench. In Figure 14 we use two different definitions of width: δ_1 is the width for twice the minimum Err-value, while δ_2 is the width at the fixed value Err=5o $\cdot 1o^{-4}$. For future applications at profile synthesizing, δ_2 might be of greater interest because it means considering the same maximum acceptable error sum for all profiles equally.

For synthesizing application one might yet be interested to have the median values. In the particular case of Figure 14 these are found as:

$$HX_1 = 15o \text{ km}; \quad SC(opt) = 21 \text{ km}; \quad \text{Width } \delta_2 = 9 \text{ km}.$$

Summarizing our findings /in view of future synthesizing/ we may state that, at night, types and characteristics of the F2-profile are quickly variable in an irregular manner. Since, apparently, conditions can change seriously in an interval of 3o min, it is not helpful to ask for a regular variation with the hour. Therefore, median parameters should be adopted at night, which might, of course, yet depend on season and solar activity.

In this context, it might be indicated to apply a HX_1 value which follows the peak altitude HM. In the Figures above we simply used HM/2 (and also HM/3 in Figures 12). It might, however, be preferable to use the relation

$$HX_1 = HM - \Delta$$

where Δ could be taken from Equation (10b). (During the solar minimum year 1954, this value was rather near to HM/2).

d. Long term variations. We have quite generally found that, at night, for each individual profile which we have analyzed the optimum scale SC(opt) is well defined, though the statistical dispersion of all profiles is rather large. Going over Becker's profiles for each night of his data set, we studied a few around midnight. As mentionned above, the main data are from summer 1954 and from spring 1958. In Figures 8 we have shown eight typical error maps selected from the whole set. It appears that, though the position of the optimum SC-value can be largely different, the structure of these maps is always similar. It is characterized by a "trench" extending along the ordinate (HX) direction, but the extension of which is clearly limited at both ends. The end with largest HX admissible (bottom side in the Figures) has the smaller amplitudes and is of particular interest for future synthesizing of profiles. (This end was studied in Figures 9 and 1o, Subsection b).

It should be noted that, by night, our weighting covers all of Becker's profile points down to a plasma frequency of o.5 MHz. It is evident that another fit of the profile, limited to a small height range near the peak, might end-up with somewhat other values. Just this profile range is, however, in Becker's analysis determined by an assumed nose function (mostly a parabola). For a reference, it is certainly more important to fit the profile as whole, what we have done.

In order to recommend an SC1, we first felt that SC1 could be related with the half-density thickness SH (or the quarter-density thickness SQ). Figure 15 shows correlograms of the pairs SH vs. SC and SQ vs. SC. There is, apparently, some correlation for SC-values below about 4o km. For higher values, however, we cannot see any correlation.

It might, thus, be the best solution to recommend the median SC of the monthly sets. Se, we find (around midnight):

SC1 = 2o in summer 1954 (solar minimum), but
SC1 = 45 in spring 1958 (solar maximum).

It must yet be found out whether the effect of the solar cycle or that of the season is more important.

One might find it more appropriate to link the SC1-value with the peak altitude - which is much higher during solar maximum. Using the HM group medians from Figures 9 and 1o which are 314 and 481 km, respectively, and assuming a linear relation, we find

$$SC1 = o.15\ HM - 27.1\ km \qquad (12)$$

as a median relation to be used by night.

As for HX1, as we have seen, it can be chosen in a large range but must not come near to HM. In Subsection (b) we have investigated quite a few error maps determining the greatest admissible value of HX1. We propose to apply the quartile value of Δ , as specified in Equation (1@b). This ends up with a recommended HX1 after

$$HX1 = 0.4\ HM + 30\ km. \qquad (13)$$

This relation gives HX1 = 155 km as the 1954 (summer) median and 223 km for spring of 1958, the ratio to HM being o.5o and o.46, respectively.

It should be noted that the above two standard parameters do not yet fully determine a profile. One more parameter is left, namely the amplitude A. At synthesis, it could be chosen so as to satisfy one constraint, e.g. the half or quarter density point. Since the peak of a LAY-function is fixed, the profile goes through a predetermined HHA or HQU, provided A is chosen by the condition

$$A = -o.3o1/LAY\ (HHA;\ HX,SC) \qquad (14a)$$

or

$$A = -o.6o2/LAY\ (HQU;\ HX,SC). \qquad (14b)$$

It is, of course, important to find geophysical relations determining HHA and HQU.

A future night reference must, of course, also specify a valley and an E-region. These do not appear on ionograms. The relevant information must be taken from other sources (as in the present IRI). From an extended study of night ionograms (mid-latitude) Piggott[1] established the following table for the averaged night values of foE, depending on the time since sunset or before sunrise. One starts from an observed foE value, reached near sunset (first column in Table 2a), and goes towards a corresponding value, reached shortly after sunrise (last column in Table 2b).

Table 2. Night Values of E-Layer Critical Frequency/MHz (after Piggott).

a. h = hours after sunset (with first value of foE)

h	0	o.25	o.5	o.75	1.o	1.5	2.o	2.5	3.o	3.5	4.o	>4.o
	1.6	1.35	1.2	1.1	1.o	o.85	o.8	o.75	o.7	o.65	o.6	o.55
	1.5	1.3	1.15	1.o5	1.o	o.85	o.8	o.75	o.7	o.65	o.6	o.55
foE	1.4	1.25	1.1	1.o	o.95	o.85	o.75	o.7	o.65	o.6	o.6	o.55
	1.3	1.15	1.o5	1.o	o.9	o.8	o.75	o.7	o.65	o.6	o.6	o.55
	1.2	1.1	1.o	o.9	o.85	o.8	o.75	o.7	o.65	o.6	o.55	o.55
	1.1	1.o	o.95	o.9	o.85	o.75	o.7	o.65	o.6	o.6	o.55	o.55

b. h = hours before last value

h	>2.o	2.o	1.5	1.o	o.75	o.5	o.25	0
	o.55	o.65	o.75	o.9	o.95	1.1	1.3	1.6
	o.55	o.65	o.75	o.85	o.95	1.o5	1.2	1.5
foE	o.55	o.65	o.75	o.85	o.9	1.o	1.15	1.4
	o.55	o.65	o.75	o.8	o.9	o.95	1.1	1.3
	o.55	o.65	o.7	o.8	o.85	o.95	1.o5	1.2
	o.55	o.65	o.7	o.75	o.8	o.9	o.95	1.1

[1] W.R. Piggott and K. Rawer, URSI Handbook of Ionogram Interpretation and Reduction, Elsevier, Amsterdam 1961.

Determining the night-E peak by the values given in Table 2 and using standard values for the peak height hmE (1o5 km) and for the valley bottom (e.g. 14o km), we yet need a valley depth, e.g. log(NmV/NmE). It is known that the night time E-F-valley is quite deep, but the estimates cover a large range. In IRI the average results of Maeda's[2] study are used to this end, though they are based on rather old rocket measurements the calibration of which might be doubtful. This is still a difficult problem.

More recent investigations with the coherent scatter sounding technique are reported to have shown that, at night, in the broad valley range rapid and important short-term changes occur quite regularly. Transient (mostly descending) irregular layers might reach considerably increased electron density than average. For a reference, one should disregard such features and better give a quasi-minimum value.

Once the NmV/NmE ratio is fixed and standard geometric parameters are assumed for the second and third LAY-function, the night-F profile might be completed down to hmE. Since the main LAY-function represents the observable F2-layer down to low density, the two other functions can be determined with fixed geometric parameters, the two amplitudes being determined by three or four conditions(constraints). A solution can be found by applying the method of least squares. This is outside of the present study.

---

[2] K.-I. Maeda, Study on electron density profile in the lower ionosphere, J. Geomagn. Geoelectr. 23, 133-159 (1971).

4.2. Day Profiles. The fitting situation is quite different with day profiles. At night, the E-region is so poorly ionized that the F-region could independently be fitted. This was due to the fact that there was no overlap with the range of the main LAY-function. By day, however, for an optimum fit the ranges of the different LAY-functions are almost always overlapping. Therefore, the F-region profile cannot independently be fitted; the fitting procedure has to take account of all three or four functions and their parameters. This means that we have six or eight geometric parameters which must be optimized. The methods we applied to this end were described in Chapter 3.

There occur two classes of day-time profiles which must be discussed: when no F1-layer is visible, the middle ionosphere profile can quite well be fitted with three LAY-functions. The main function which has the largest scale SC1 reproduces the main (F2-) peak but covers the whole range. The secondary functions are needed to (i) reproduce a valley (or a turning point) somewhere around 14o km, and (ii) the peak of the E-region at about 1o5 km. These have smaller scales but, since their HX values are rather near together, they have overlap with each other (and, of course, with the main function).

The appearance of the F1-feature changes the situation. The corresponding turning point in the F1/F2 profile can only be reproduced with a fourth LAY-function.

a. Profiles without the F1 feature. These are represented by one main layer (F) and two secondary ones (V and E), thus with I = 3 /in Equation (6)/. Figures 16a,b show typical examples where an F1-layer did not appear at all. Figure 16c, however, shows F1, but this feature - by suitable starting conditions - was neglected at fitting. Apart from the height range where F1 occurs, the profile is certainly representative. A larger selection of profiles fitted with I = 3 is reproduced in

Figures 17. It cannot be denied that these profiles are all reproduced quite satisfyingly. So, I = 3 is the right choice under the assumed conditions. It is also apparent that the HX and SC values of the second and third LAY-function are quite stable.

The median geometric parameters of these secondary layers were found from a statistical evaluation of a number of day-time profiles obtained in spring of 1958 (a year of very high solar activity). The median values found for this period are:

HX2	SC2	HX3	SC3		
116	2	1o5	5	km.	(i)

As for the parameters of the main layer (1), there exists some interpendence as we have mentionned earlier. Thus, there is a certain freedom in choosing HX1; in the fitting procedure the result depends largely on the starting value. It appeared reasonable to admit proportionality with the peak altitude HM. We used to start fitting with a ratio HX /HM = o.9, and this was essentially conserved during the fitting procedure. So, we have with

HX1 o.9 HM and o.85 HM (ii)

found the median thickness scale to be

$\overline{SC1}$ = 63 km and 7o km, respectively. (iii)

Once the secondary LAY-parameters have been optimized /as in (i)/, one may proceed to draw an error map (with H vs. SC1 as coordinates). The details of the map are, of course, somewhat depending on the parameters taken for the secondary functions. There are, however, two typical features occurring rather regularly: one is that - quite different from night conditions - there ixists now a <u>lower</u> limit for HX1 (on top in our figures); secondly, there is again a trench which, however, extends up to HX1 values far beyond HM. The lowest Err-values are now found when HX is rather near to HM. Examples are shown in Figure 18.

As done above for night (Figure 15), we established correlograms between SC1 and the half-density-thickness SH and quarter density thickness SQ. For the considered period median values and dispersion (decile) ranges were found as shown in Table 3. Looking for correlations, none could be seen with SQ. With SH, though a median regression line was empirically found as SC1 = 5 SH - 525 km, it could not be taken as a satisfactory description since it gives negative values of SC1 for SH below 1o5 km. Although a line from the origin to the center of the distribution around this line is not symmetric but oblique. With other words, the ratio SC1/SH is not constant but decreases with increasing value of SH. We felt that a more involved relation had to be established taking account of this feature. By log vs. log plotting we found:

$$SC1 = (SH/42\ km)^4 \quad .$$

This formula also takes account of the fact that the ranges over which both parameters vary are rather different, as can be seen from Table 3.

Table 3. Thickness parameters (F-region, day, I=3)

	SH/km	SQ/km	SC1/km
median	123	187	63
quartile range	114-127	159-2o4	49-88
decile range	9o-15o	132-22o	3o-13o

b. Profiles with F1. We have shown that, generally, reproduction of a day-profile with three LAY-functions (I=3) is largely satisfying. We have shown by Figure 16c that this is true even with F1 present, provided one accepts some deviation from the original profile in a rather limited height range.

However, if it is intended to reproduce the F1 feature as such, a typical summerday profile cannot accurately be fitted with I less than 4. Becker's summer daytime profiles obtained in June/July 1954, also those of March/April 1958, when they showed some

indication of F1, were fitted with I=4 in order to see the difference against I=3. Figure 19 shows three examples where the fit was made with I=4 and I=3 as well. Error maps (in HX1 vs. SC1) were also computed and are shown in Figure 2o. The change between both I-values is important. With I=3 a "trench" appears at rather small SC-values (around 2o km). With I=4, however, the same original profile has its SC(opt) at much greater values, so that the trench is displaced and is now almost elongated along the SC1-axis. Thus, the optimum is now found in a rather narrow range of HX1. However, the error values show only little variation such that we have a large field in the map with almost equal Err-values. This means that (when always determining the optimum amplitude) there is a certain freedom in the choice of both, HX1 and SC1.

It should, therefore, be noted that the introduction of a secondary function at F-region heights, in addition to the main function, considerably changes the relation between SH1 and SC1, as mentionned above. Going from I=3 to I=4 makes, in fact, a considerable change in the reproduction of the F-region. As the above Figures show, a twice-incurved profile can quite well be reproduced when admitting two LAY-functions instead of only one. While the amplitude of the main function is always negative, the secondary one needs a positive amplitude. Since the transition heights HX1, HX2 were found to be not very much different, the effect of both functions must partially compensate each other in a certain height range which is determined by the smaller of the two scales, SC1, SC2.

Results of fitting day-profiles with I=4 are shown in Figures 21 through 23 for the years 1954, 1957 and 1958, respectively. The first of these years was at solar minimum, the last two were at the greatest activity maximum ever reached in our lifetime.

We have established statistics of our fitting results for the two periods where Becker has many profiles: summer of 1954 and spring of 1958. The main results of this statistics are shown

in Table 4 which might be useful at future synthesis.

Table 4. Statistical overview of the results of analysis with four LAY-functions /Sp = Spring: 21.3. - 28.4.1958; Su = Summer: 27.6. - 1.7.1954/

F-region:	HX1/km median	HX1/km quartile range	SC1/km median	SC1/km quartile range	HX1/HM median	HX1/HM quartile range
Sp	272	268-29o	9o	76-96	.74	.68-.8o
Su	175	152-2oo	88	75-92	.7o	.62-.82

F-region:	HX2/km		SC2/km		HX2/HM	
Sp	261	247-271	13	9-21	.69	.68-.73
Su	185	175-2o9	13	4-48	.75	.72-.81

Valley:	HX3/km		SC3/km	
Sp	117	113-118	7	5-9
Su	114	1o5-119	5	2-9

E-region:	HX4/km		SC4/km	
Sp	98	9o-1o1	5	4-8
Su	96	88-1o3	5	4-8

F Peak:	HM/km	
Sp	371	356-392
Su	249	231-26o

Our results show that there is a clear distinction between the main function (of negative amplitude) which has an SC1 around 8o km, and the other one (of positive amplitude) with an SC2 on-

ly slightly above 1o km. Median values and quartile ranges can be seen from Table 4. When compared with HM, the heights HX1, HX2 typically give a ratio around o.7 instead of o.9, found in the I=3 analysis:

$$HX1,2 \approx o.7 \cdot HM \qquad (iv)$$

$$\overline{SCT} \approx 97 \text{ km} \quad . \qquad (v)$$

With I=3, we also found a smaller SC1 (63 km); the larger value now needed for SC1 (with I=4) must be attributed to the partial compensation of the two LAY-functions in the F-region.

Like for I=3 we have also investigated whether the SC1-values found by fitting with I=4 are related with the thickness parameters SH and SQ. No good correlation could be found with SQ. For SH, however, there exists some correlation as can be seen from Figure 24. Separately from the two data sets we found the following linear relations:

$$SC1 = \begin{cases} o.65 \cdot SH & \text{in spring,} \\ o.83 \cdot SH & \text{in summer.} \end{cases} \qquad (vi)$$

When trying to combine both sets (as in Figure 24), we better use an incurved relation, for example (I=4, day):

$$SC1/km = 12o - o.oo66\ (SH/km - 19o)^2 \quad . \qquad (vii)$$

As shown above, we found quite different values with a three function fit. Both approaches should not be confounded therefore - except for the E- and V-fits which use to give comparable results. As for SC2 (of the "correction function" provoking the F1-feature) the dispersion of the points is larger, the median relation being:

$$SC2 = \begin{cases} o.1o \cdot SH & \text{in spring,} \\ o.o9 \cdot SH & \text{in summer.} \end{cases} \qquad (viii)$$

Thus, the value of SC2 lies between 15 and 11% of that of SC1.

It is a practical question whether a reference reproduction (e.g. in IRI) needs the F1-feature to be reproduced. Our results, apparently, show that one cannot simply add a secondary function in the F-region description without admitting some change in the parameters of the main function. Summarizing our findings: if HXO, SCO are the main layer parameters in an I=3 description, then - when going over to I=4 - one might make new specifications as follows:

$$\left\{ \begin{array}{ll} HX1 = 0.80 \cdot HXO; & HX2 = 0.76 \cdot HXO \\ SC1 = 1.4 \cdot SCO; & SC2 = 0.12 \cdot SC1 \end{array} \right\} \qquad (ix)$$

5. RESULTS LOWER IONOSPHERE

In the lower ionosphere we encounter a comparable situation as we found in the middle one. At the upper boundary peak height and density (now of the E-layer) are known; the profile has (very rarely a minimum but) almost always a turning point near 80 km. Mechtly and Bilitza[1] established a simple empirical rule for the day-time electron density NmD for that point which is used in IRI in the following shape:

$$NmD/m^{-3} = (6.05 + 0.088 \cdot R) \cdot 10^{8} \cdot \exp(-0.1/(\cos\chi)^{2.7}). \quad (15)$$

R is the Zuerich sunspot number and χ the solar zenith angle. The formula was obtained with a combination from a set of in-situ rocket measurements obtained with a combination of Langmuir probe and (ground-to-rocket) phase propagation experiment. The night value of NmD is fixed in IRI to $4 \cdot 10^{8}$ m^{-3}.

---

[1] E.A. Mechtly and D. Bilitza, Models of D-region Electron Concentration, Rept. IPW-WB1, Fraunhofer-Institut füer physikalische Weltraumforschung, D-7800 Freiburg i.Br., F.R.G., 1974

Though the lower ionosphere was not the principal field of the present investigation, we felt that we should at least investigate whether our proposed representation with LAY-functions is also applicable to that height range[2]. In the following we describe the results obtained with three different data sets[3].

5.1 McNamara's Data Collection. This is a rather complete collection[4] of all available measured profile data up to 1977. Most profiles are incomplete and the absolute calibration is often doubtful. Ramanamurty has selected a much smaller set of profiles, covering the whole height range including the E-peak. This latter is sometimes ill defined. Ramanamurty first tried to take the peak density NmE from empirical formulas describing the critical frequency foE, as evaluated on ionograms. However, the absolute calibration of the collected data used to be too bad, so that the disagreement between published profile density and that obtained from ionograms was too large.

Our method is not bound to absolute values - the description gives the logarithmic density ratio to the peak value. So, we work with relative densities anyway. Therefore, we finally decided to determine an NmE from the profile data themselves. This guess sometimes is difficult, particularly where more than one maximum is reported. We used to take that which was nearest to the standard peak altitude of IRI (1o5 km).

---

[2] An important part of this particular investigation was made in cooperation with Y.V. Ramanamurty (on leave from National Physical Laboratory, New-Delhi, India). His stay in Germany was sponsored by Deutsche Forschungsgemeinschaft, Bonn.

[3] Y.V. Ramanamurty and K. Rawer, Modelling of the lower ionosphere according to IRI guidelines, Adv. Space Res. 6 (to appear in 1987).

[4] L.F. McNamara, Ionospheric D-region Profile Data Base, A Collection of Computer-Accessible Experimental Profiles of the D- and lower E-region, Rept. UAG-67, WDC-A for Solar-Terrestrial Physics, NOAA, Boulder, Co., U.S.A., 1978.

Analyzing some 2o daytime profiles in terms of three LAY-functions, we found the dispersion of the resulting parameters rather large. A dependence on the solar zenith angle χ could not clearly be established. Since our aim is to get a set of significant average parameters, we feel that the median values of our selection might be considered as more or less significant. These are given in Table 5.

Table 5. Median lower ionosphere LAY representation (for day conditions).

	Main	secondary 1	secondary 2	
HX	8o.4	87	7o.3	km
SC	11	5.3	6.3	km
A	-22.4	1.2	4.5	

This is probably o.k. for the first two lines, i.e. the geometric parameters. As for the amplitudes it might not be helpful to take median values because the shape of the profile is very sensible to the exact values of the amplitudes. Also, in the future application the amplitudes will not be taken from past experience but be determined at the application itself (so as to satisfy certain constraints).

Studying this in more detail, we have computed quite a number of profiles with the geometric parameters HX and SC, given above, but with different combinations of amplitudes. It appeared that rather small changes of the amplitudes of the secondary functions might have the effect that an otherwise monotonuous profile is transformed into one with a peak somewhere around or even below 8o km. It is even possible to "overthrow" the schedule and produce a profile running with decreasing height towards always greater values.

However, since the future choice of amplitudes will be limited by strict constraints, it might be interesting to show how this

choice could influence the profile. In Figure 25 we show a few of our computed profiles, all with the same geometric parameters. It can be seen that, with an appropriate determination of the amplitudes, one can obtain very reasonable profiles.

5.2. Median Profiles from the Magnetic Equator. At low latitudes there exists a collection of rocket profiles from Thumba (India), near the magnetic equator[1]. All of these were obtained between 1966 and 1978 by the same measuring device, the PRL-Langmuir probe. The profiles cover the height range up to 160 km, starting at about 60 km by day and at about 85 km for twilight and night. They are averaged in four groups as described in Section 2.

The authors give a mean noon profile which we have analyzed. For the other groups we produced one median profile for each group and analyzed this profile. While individual profiles show some irregularities, the median profiles are reasonably smooth so that they may be taken as representative. The E-peak was always matched with the observed profile curve. The results of this analysis are shown on Table 6. The relevant profiles (measured and fitted) together with the contributing LAY-functions are shown in Figures 26.

---

[1] B.H. Subbaraya, Satya Prakash and S.P. Gupta, Electron Densities in the Equatorial Lower Ionosphere from the Langmuir Probe Experiments Conducted at Thumba during the Years 1966-1978, Scientific Rept. ISRO-PRL-SR-15-83, Indian Space Research Organisation, Bangalore, India, Dec. 1983.

Table 6. Low Latitude Profiles of the Lower Ionosphere[+]

Type	Hours	Number I		HX1	SC1	HX2	SC2	HX3	SC3/km
Day	1o4o -1415	12	3	1o1.2	13.4 (o.o64)	82.7	1.2 (o.322)	81.8	9.5 (-4.716)
Morning	o54o		2	1o1.2	6.7	89.3	-1.7		
		3			(-o.293)		(-1.1o2)		
twilight	-o615		1	85.7	3.o				
					(-4.17o)				
Evening twilight	183o -19oo	3	3	84.9	11.1 (-89.6o)	92.2	8.1 (38.49)	75.3	2.o (-1o6.o4)
Night	22oo -o215	6	2	85.6	3.9 (6.685)	93.5	4.6 (-5.547)		

[+]Numbers in parantheses give the amplitude found at fitting.

For the median daytime profile three LAY-functions are clearly needed. This profile peaks at 1o7 km and shows a turning point around 8o km at a density of about 1/3oo of NmE /i.e.: $\log (N/N_{max}) = -2.5$ /. Compared with the present IRI, this is not far from its NmD/NmE ratio. The lower boundary is at about 65 km /with -3.5, as for the present IRI/.

The twilight flights were so arranged that the solar zenith angle was between 9o and 1oo°. At morning twilight the (here alone interesting) profile below HmE can quite well be represented by one LAY-function only. As for evening twilight, the three basic profiles are more different so that the median profile might not be representative. So, we obtained an almost constant electron density between 9o km and the "peak" at 1o2 km. At least, two LAY-functions are needed ; for perfect description

three of these are preferable so that the flat peak can be better reproduced. In this special case our fit leads to rather large amplitudes (because the particular shape is brought about by compensation of functions of different sign).

Though we describe (in Figure and Table) the night profile of the Indian authors with the help of two LAY-functions, this is not really needed. A satisfying description could be obtained with one only.

We feel that the results of this homogenous set of measurements should be given preference in comparison with the inhomogeneous set, discussed in Subsection 5.1. They could directly be used for establishing a low latitude lower ionosphere reference profile.

It is hoped that similar sets of homogeneous measurements might be obtained for other latitudes too.

5.3. Median Profiles from Radio Wave Propagation Data.

Singer[1] has constructed profiles by trial-and-error comparison with data obtained from different techniques of probing the ionosphere with radio waves. We analyzed his profiles, mostly with three LAY-functions. Figures 27 show some results.

It must be emphasized that Singer's night profile is rather different from the in-situ measured profiles by the fact that it has a "staircase" aspect with almost discontinuous transitions from one level to the next one. It is explained that a good reproduction of the radio data from different working frequencies cannot be otherwise obtained. Under these circumstances our fitting method necessarily leads to a series of well distinguished short-scale bends, so that there is no difference against the

---

[1] W. Singer, Charakteristische ... Elektronenkonzentrationsprofile ..., Z.S. Meteorologie 26, 231-243 (1976)

original "step-by-step" method of Booker. One needs more than three LAY-functions with this very particular profile.

We feel that this profile should be considered as controversial. The special features, mentionned above, occur at very low electron density, i.e. at heights where in-situ measurements are very difficult. May-be that the present-time activity in the "Middle Atmosphere Program" could end-up with reliable data for this height range by night. In the actual IRI, these low electron densities are outside of the range of our particular interest.

6. CONCLUSIONS

Summarizing our findings, we state first of all that the proposed system of profile representation can very well be applied to all types of electron density profiles observed in both, middle and lower ionosphere.

For the middle ionosphere, we established in Chapter 4 numerical relations depending on the peak altitude HmF. These might provisionally be applied for mid-latitudes. By day, they give the geometric parameters for three (or, in the presence of F1, four) LAY-functions. By night, one function is enough for describing the upper profile part which refers to the F-region. The lower part, i.e. valley and E-region, must be inferred from other sources.

For the lower ionosphere, in Chapter 5 we could at least show that the description with three LAY-functions allows a very satisfying reproduction. From different data sets somewhat different sets of geometric parameters were obtained. The "Task Group on IRI" will have to decide which of these is to be preferred - or whether new basic data should be looked for. At night, the lowest electron density features at the base of the ionosphere (Singer's night profile) might provisionally be dis-

regarded. Then, one LAY-function describing the "nite-E" bottomside is good enough.

Finally, future application of our proposed system in IRI necessitates the establishment of suitable geophysical constraints from which the amplitudes should be determined individually, i.e. in the IRI computer program itself. These should not arbitrarily be distributed over the height range but must be chosen in a way, that to each LAY-function at least one relevant condition exists.

CAPTIONS TO THE FIGURES

Fig. 1. LAY-function of altitude z (ordinate), variation of geometric parameters:
(a) SC fixed to 1o km, HX varied;
(b) HX fixed to 25o km, SC varied.

Fig. 2. Error map, i.e. reduced error sum as function of HX (ordinate) and SC (abscissa). Arrows show directions of "steepest descent".

Fig. 3. LAY-function multiplied with amplitude A. Interdependence of A and HX for fixed SC. Amplitudes were so chosen that same curvature occurs at peak HM.

Fig. 4. Flux diagrams of optimization procedure APTR:
(a) Main program; (b) 1-6 Subroutines.

Fig. 5. Printouts of final optimization program APTR (in SIMULA computer language):
(a) Main program APTR;
(b1,2) Subroutines used in APTR;
(b3) Subroutine LSFURR followed by CHOLESKY (solving a system of linear equations).

Fig. 6. Night profiles: (a) normal; (b) odd.

Fig. 7. Error maps (see Figure 2) to Figure 6.

Fig. 8. Error maps for eight different night profiles of 1954, 1957 and 1958. (date and hour see lower left-hand corner).

Fig. 9. Ratio (as function of HM) of greatest admissible HX (from night-time error map), HX1, to (a) HM, (b) HHA, (c) HWU. Thick line: connection between median points of 1954 and 1958. Thin lines: delimit quartile ranges.

Fig. 1o. Difference (as function of HM) between greatest admissible HX (from error map), HX1, and (a) HM, (b) HHA, (c) HQU. /See caption to Figure 9/.

Fig. 11. Ratio of half density height, HHA, and peak height, HM, as function of HM. /See caption to Figure 9; o 1954, x 1957, + 1958/.

Fig. 12. Night-time plasma frequency profiles (right hand side) and cuts through the error map (one LAY-function only) at HX1 = HM/2 (full line) and at HX1 = HM/3 (broken line). /Becker's profiles from 00 to 04h on 25 June 1954; hour indicated inside profile drawing/.

Fig. 13. Cuts through error maps (one LAY-function) at HX1 = HM/2 for all night profiles given by Becker for 26/27 June 1954. /Hour in the left- or right-hand upper corner/. In Subfigures (a),(b),(c) the cuts are arranged after the value of SC at minimum.

Fig. 14. Survey to Figures 13 showing the variations of the optimum (i.e. position = SC for minimum, and minimum Err-value, Err min). Further, the width of the minimum: Delta$_1$ between 2·Err min points, and delta$_2$ at Err = 5o. HX1 = HM/2 in bottom line /(night 26/27 June 1954, 18-06h)/.

Fig. 15. Correlograms between optimum SC, abscissa, and lower half-density layer thickness, SH (top), or lower quarter-density thickness, SQ (bottom). Night profiles from 1954 (solar activity minimum) to 1958 (maximum).

Fig. 16. Reproducing day profiles[1] with three LAY-functions:
(a) Reference profile with an E-F valley;
(b) Becker's profile 886 with no F1 indicated;
(c) Becker's profile 74 with F1 indicated (but overlooked in the fitting procedure).

Fig. 17. Six day profiles without F1 fitted with three LAY-functions (I=3). Becker profiles numbers: 541, 661, 761, 826, 953, 1325.
/G = Gulyaeva's estimate of HHA/.

Fig. 18. Error maps: isolines of reduced error sum in HX vs. SC coordinates of main LAY-functions. Example for day-time profile without F1 (I=3).
(a) Large scale survey;
(b) Neighbourhood of minimum, small scale.

Fig. 19. Three profiles with F1-features fitted with I=3 (a,c,e) and I=4 (b,d,f) for comparison. Becker profiles numbers 74 (a,b), 114 (c,d), 1484 (e,f).

Fig. 2o. Error maps for three profiles with F1-feature, fitted with I=3 (a,c,e) and with I=4 (b,d,f). Same Becker profiles as in Figure 19.

---

[1] In our profile drawings the original data points are drawn as circles. The individual contributions of the different LAY-functions, A · LAY, are shown with different symbols. Their sum, i.e. the approximation finally reached, is given by triangles ▲. Note that the drawing program gives straight line connections such that the marked points only should be considered.

Fig. 21.[2] Six day-time profiles with F1-feature fitted with four LAY-functions (I=4): Becker profiles numbers: 122, 177, 18o, 185 (two versions), 294, 3o7. All of 1954 (solar minimum).

Fig. 22. Day-time profile of 1957 (Becker number 541, solar maximum) fitted with four LAY-functions (I=4).

Fig. 23. 15 day-time profiles of 1958 (solar maximum) with four LAY-functions (I=4). Becker profiles numbers: 661, 761, 821, 826, 953, 957, 11o4, 1223, 1275, 1325, 1365, 1428, 1545, 1613, 166o.

Fig. 24. Correlograms between the optimum scale SC_1 of the main LAY-function (ordinate) and the lower half-density thickness SH (abscissa), obtained from day-time Becker-profiles fitted with I=4.

Fig. 25. Lower ionosphere profiles (day) computed with three LAY-functions (I=4) using the median geometric parameters obtained by analysis of McNamara profiles (Table 5) and different amplitude combinations.
(a)-A_1 = parameter, A_2 = 5.2, A_3 = 4.3;
(b) A_1 = -22.4, A_2 = parameter, A_3 = 4.5;
(c) A_1 = -22.4, A_2 = 4.8, A_3 = parameter.

---

[2] Since the representative function is fitted to the input points (circles), it might show some deviations in between, which are not necessarily shown by the measured profile. The two versions of profile 185 show what might happen in the E-F valley when the height difference of the data points becomes too large. This can be avoided by introducing intermediate data input at these critical intervals.

Fig. 26. Median profiles after rocket measurements at Thumba (India - magnetic equator, see Table 6). Standard analysis with up to three LAY-functions for:
No. 1 = noon; 2 = night; 3 = morning twilight.
No. 5 is the same night profile as No. 2 analyzed, however, with the upper peak appearing around 160 km.
/This example shows that our analysis is also suited for abnormal conditions/.

Fig. 27. Analysis of standard ionosphere profiles as established by W. Singer.
(1-4) Summer, Covington index F = 75; solar zenith angle (sza):(1) 80°, (3) 60°, (4) 40°.
(5-8) Winter, F = 75; sza:(5) 85°, (6) 80° average quiet conditions, (8) 80° low absorption.
(10) Summer, F = 150; sza 70°.
(13-15) April, F = 75; sza:(13) 80°, (15) 60°.
(16) F = 75; - night conditions -.

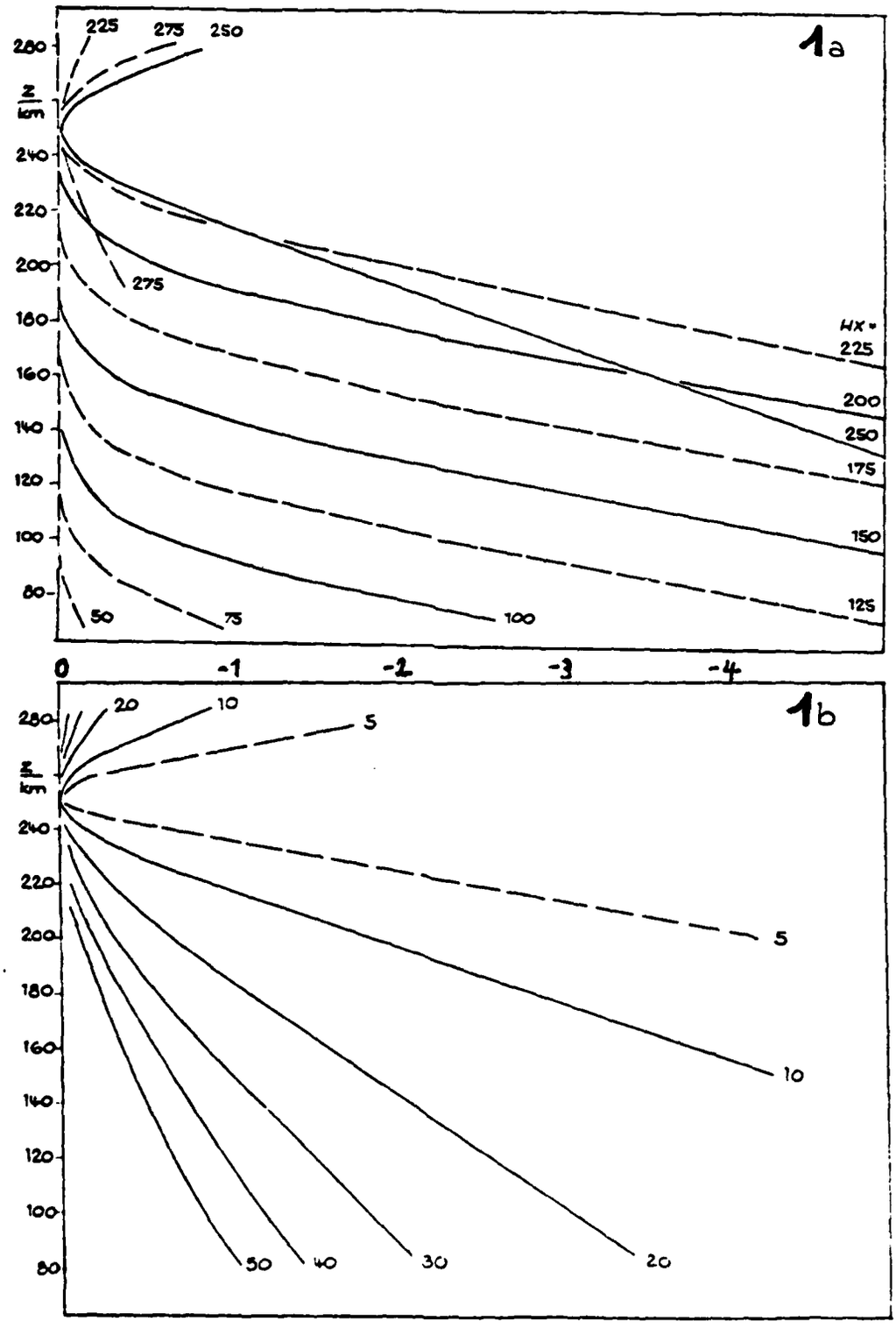
1a
225
275
250
280
240
220
200
180
160
140
120
100
80
275
Hx =
225
200
250
175
150
125
50
75
100
0
-1
-2
-3
-4
1b
20
10
5
5
10
50
40
30
20

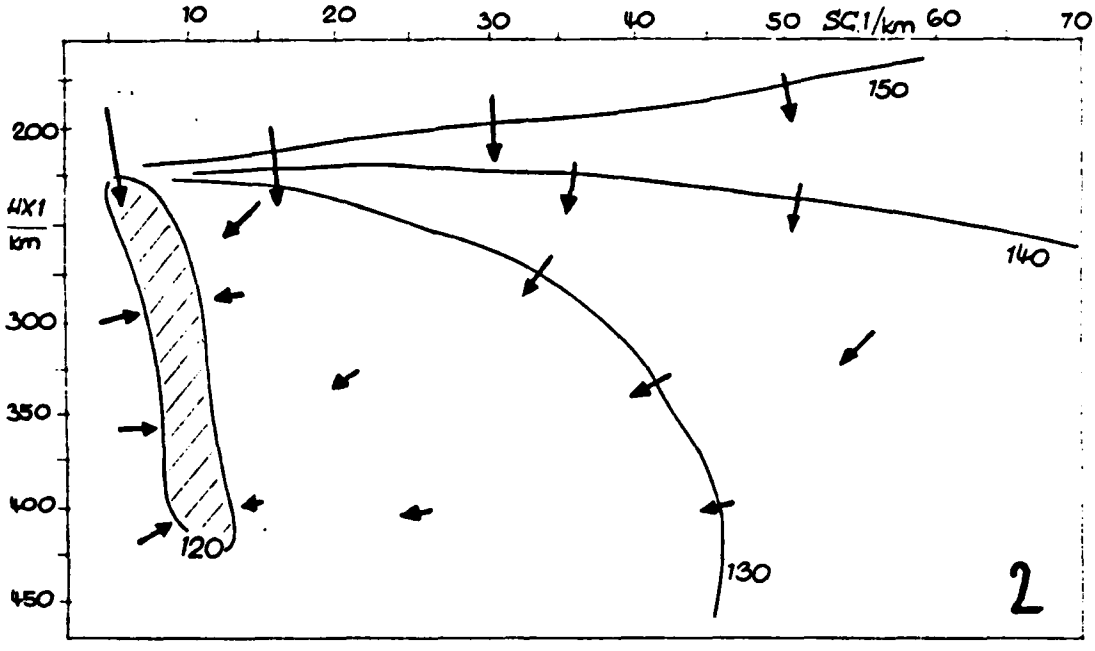
10
20
30
40
50
SC.1/km
60
70
200
HX1
km
300
350
400
450
150
140
120
130
2

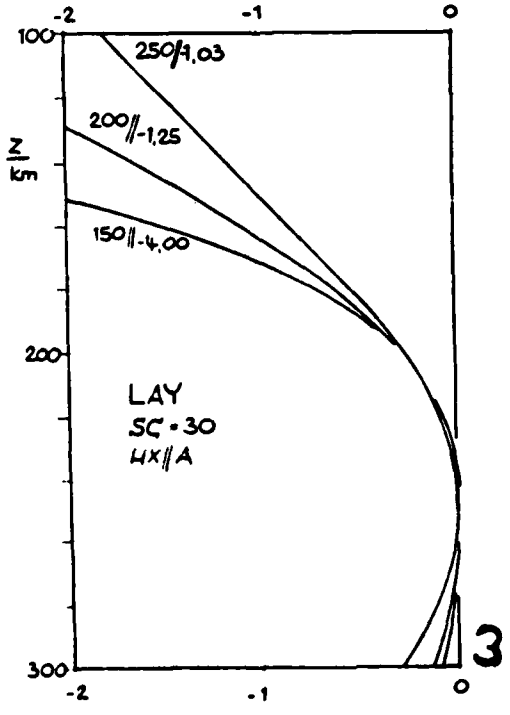
-2
-1
0
100
250/1,03
200//-1,25
Z
km
150//-4,00
200
LAY
SC = 30
HX// A
300
3

APTR

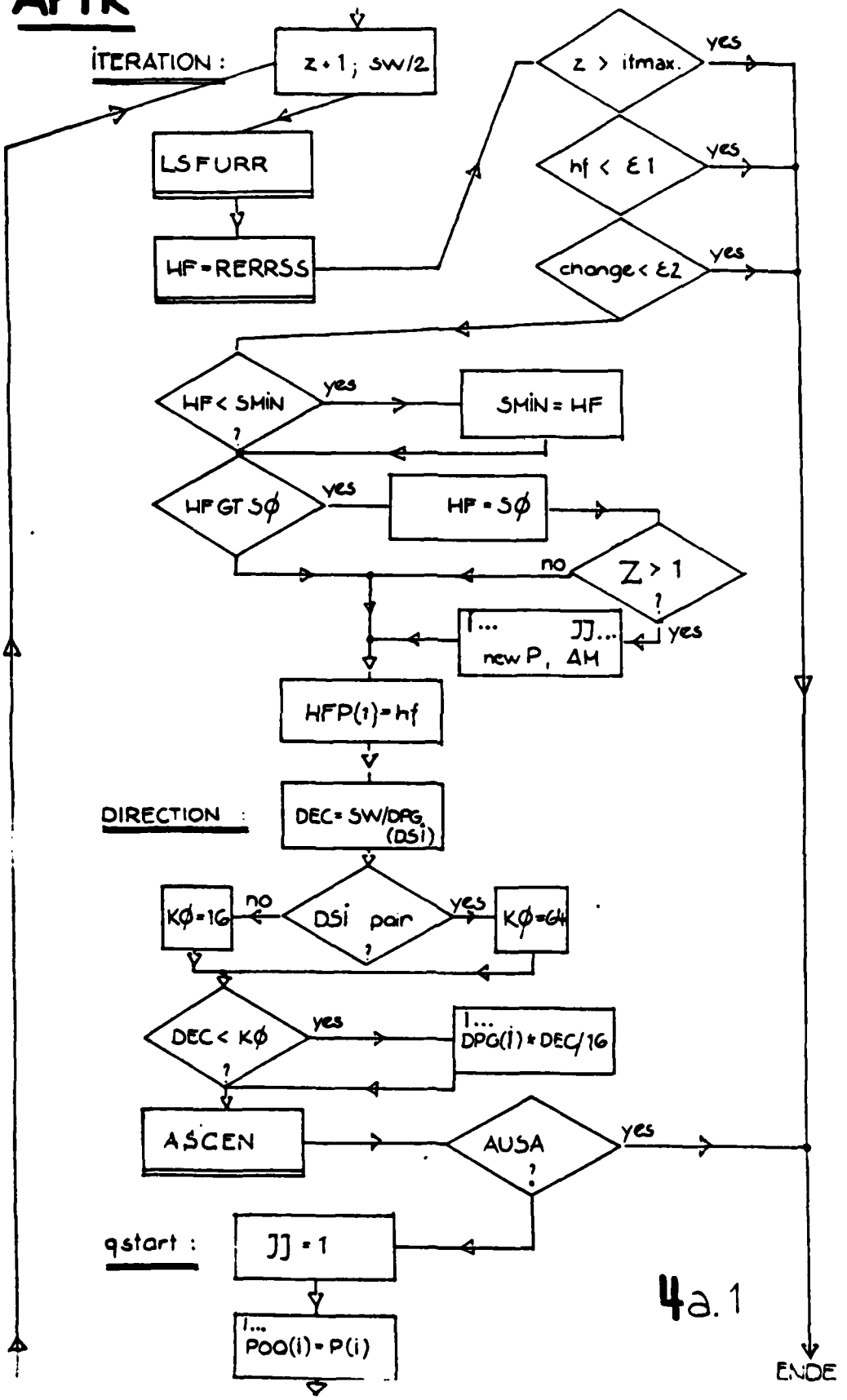
ITERATION :
z + 1 ; SW/2
LSFURR
HF = RERRSS
z > itmax.
yes
hf < ε1
yes
change < ε2
yes
HF < SMIN ?
yes
SMIN = HF
HF GT Sφ ?
yes
HF = Sφ
Z > 1 ?
no
yes
I... JJ... new P, ΔH
HFP(I) = hf
DIRECTION :
DEC = SW/DPG (DSI)
DSI pair ?
no
yes
Kφ = 16
Kφ = 64
DEC < Kφ ?
yes
I... DPG(I) = DEC/16
ASCEN
AUSA ?
yes
qstart :
JJ = 1
I... P00(I) = P(I)
ENDE

4a.1

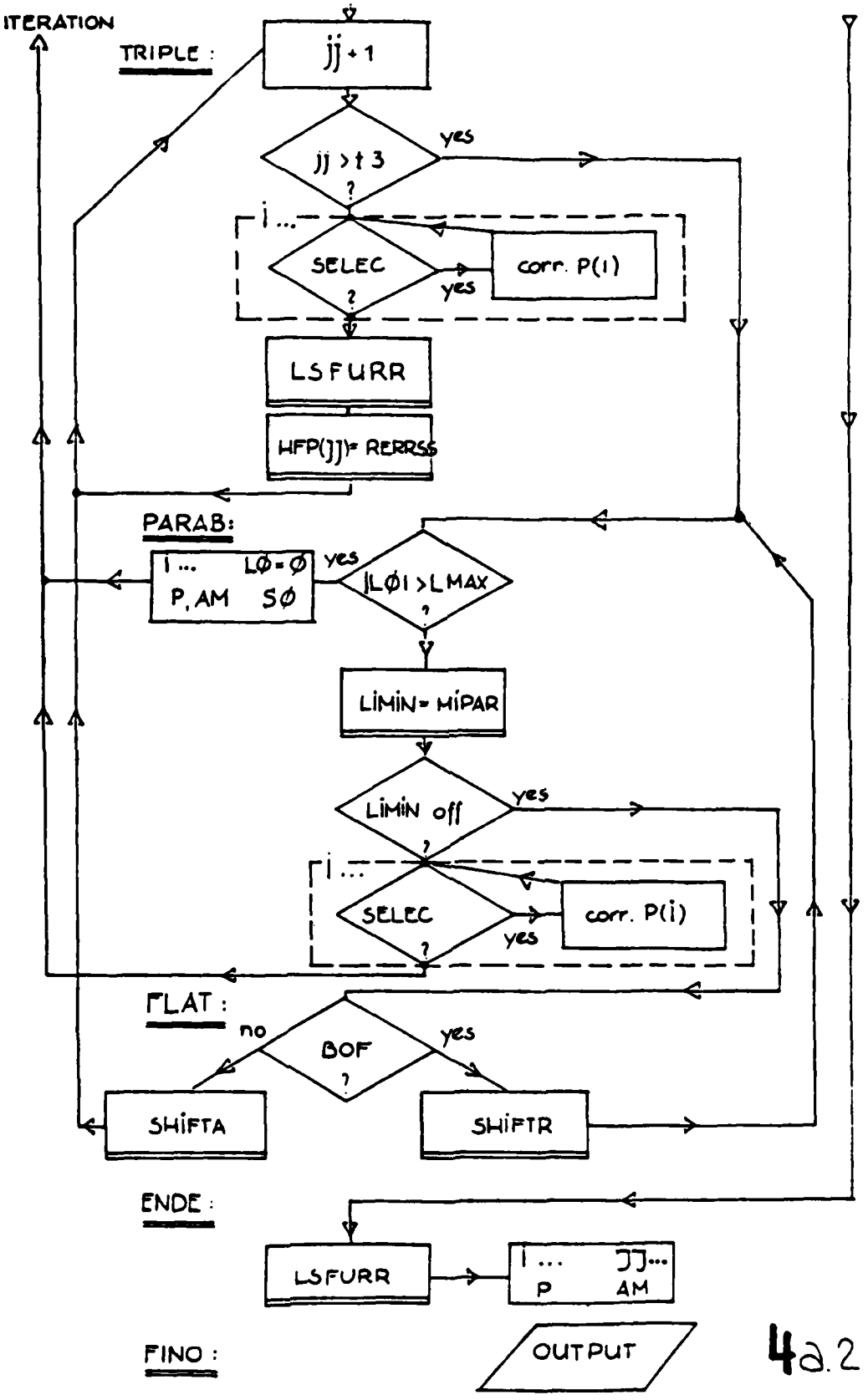
ITERATION
TRIPLE :
jj + 1
jj > t 3
?
yes
i ...
SELEC
?
corr. P(i)
yes
LSFURR
HFP(JJ)= RERRSS
PARAB:
i ... LØ = Ø
P, AM SØ
yes
|LØI > LMAX
?
LIMIN = HIPAR
LIMIN off
yes
?
i ...
SELEC
?
corr. P(i)
yes
FLAT :
no
BOF
?
yes
SHIFTA
SHIFTR
ENDE :
LSFURR
i ... JJ...
P AM
FINO :
OUTPUT

4a.2

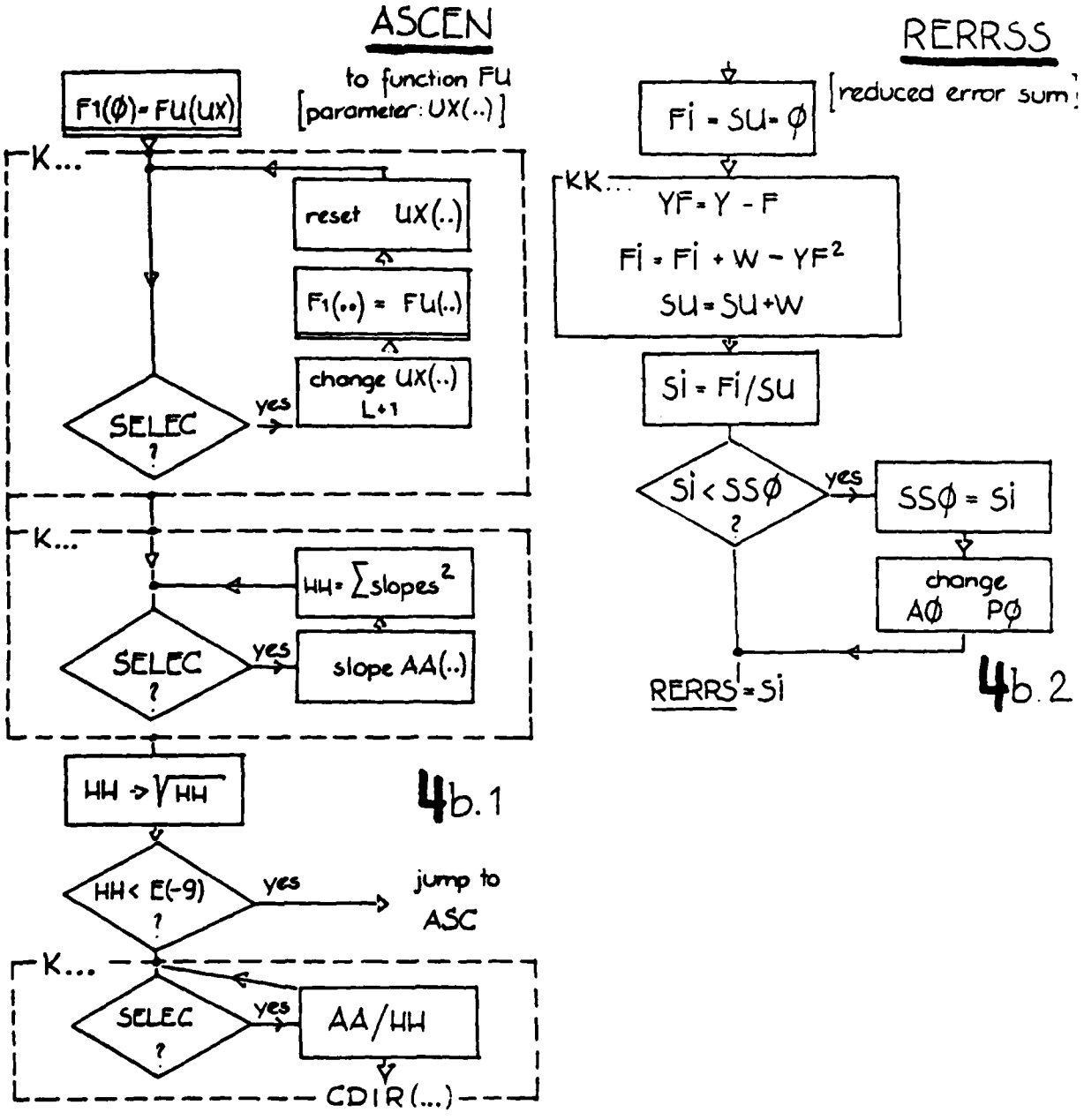
ASCEN
to function FU
[parameter: UX(..)]
F1(Ø) = FU(UX)
K...
reset UX(..)
F1(..) = FU(..)
change UX(..)
L+1
SELEC ?
yes
K...
HH = ∑slopes²
SELEC ?
yes
slope AA(..)
HH -> √HH
4b.1
HH < E(-9) ?
yes
jump to ASC
K...
SELEC ?
yes
AA/HH
CDIR(...)
RERRSS
[reduced error sum]
Fi = SU = Ø
KK...
YF = Y - F
Fi = Fi + W - YF²
SU = SU + W
Si = Fi/SU
Si < SSØ ?
yes
SSØ = Si
change AØ PØ
RERRS = Si
4b.2

MIPAR

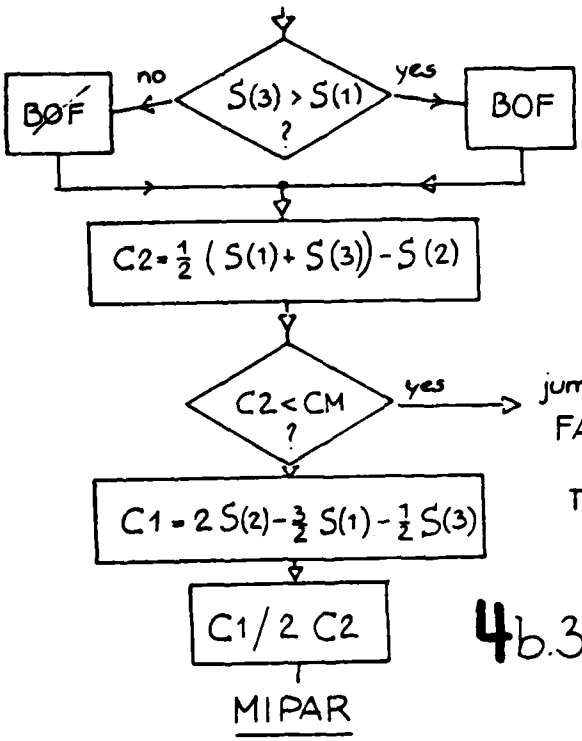

4b.3

SHIFTA

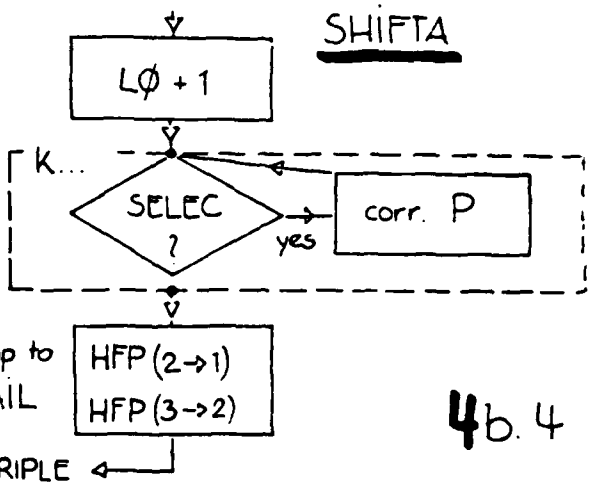

4b.4

SHIFTR

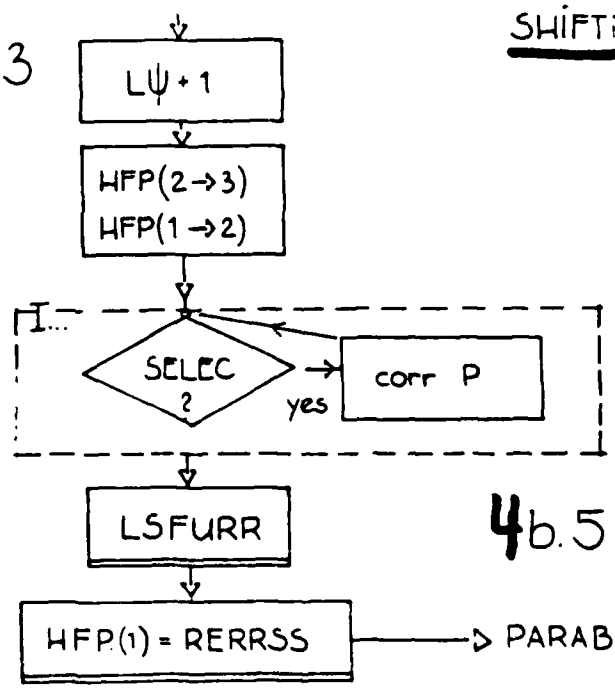

4b.5

LSFURR

To given arrays X, Y and prescribed function F [= set of LAY-functions with given parameters $P(\ldots)$] first computes [by least squares] optimum set of coefficients AMPL such that reduced error sum [of F against Y] is minimized; then computes array of function values F to given array X.
Least squares optimum searched with method of CHOLESKY. Jump-out if no solution achieved

4b.6

5a

```
1 COMMENT START   A       P       T       R ;
2 S0:=S00;    LMAX:=5;     LC:=Z:=0,
3 XM:=MA; KEMA:=10; SMIN:=SU:=S, PAUS:= TRUE; LIN:= TRUE;
4 FOR I:=1 STEP 1 UNTIL N66 DO DPG(I):= IF SELEC(I) EQ 0 THEN 0
5 ELSE IF (I/2-I//2) LT 0.1 THEN 0.25         ELSE 1;
6 COMMENT IF AT ALL SELEC=1 THEN DPG=1 FOR ALL MX BUT 0.25 FOR ALL SC,
7 I:=0;FOR I:=I+1 WHILE ABS(DPG(I)) LT 0.0001 DO DSI:=0,DSI:=1;
8 COMMENT IDENTIFIES FIRST POSITION WHERE DPG(I) DIFFERENT FROM 0,
9 I.E. SELEC = 1;
10 FOR I:=1 STEP 1 UNTIL N66 DO P(I):=P0(I),
11              ITERATION: Z:=Z+1;  SU:=SU/2,
12          LSFUNR(NI,P,XM,P,AP,N,Y,W,F);
13    MF:=RERRSS(NI,P,P,PGP,AR,APG,Y,F,W,SD);
14  IF  Z  GT  ITMAX  THEN  BEGIN  KEMA:=2;  GOTO  ENDE  END ;
15 IF MF LT EPS1 THEN BEGIN OUTIMAGE;OUTTEXT("KEMA=1, S=  ");
16 OUTREAL(MF,5,11),  GOTO ENDE   END,
17 IF ABS(1-MF/SPIN) LT EPS4 THEN BEGIN OUTIMAGE,KEMA:=0;
18 OUTTEXT("KEMA=0, S=  ");OUTREAL(MF,5,11),GOTO ENDE   END;
19 IF MF LT SMIN THEN SMIN:=MF;
20 IF MF GT SC THEN BEGIN MF:=SU;
21 IF Z GT 1 THEN BEGIN FOR I:=1 STEP 1 UNTIL N66 DO   P(I):=PMP(I),
22 FOR JJ:=1 STEP 1 UNTIL N, GO AR(JJ):=ARM(JJ), S:=SL END;  END;
23          MFP(1):=MF;
24 DIRECTION: DEC:=SW/DPG(0,I);
25 LC:=IF (DSI/4-DSI//2) LT 0.1 THEN 64 ELSE 16,
26 COMMENT THE FIRST SELEC-POSITION IS EITHER AN MX - THEN DSI UNPAIR,
27 LC=16 - OR AN SC - THEN PAIR,NO UREATER :0;
28 IF DEC LT 0 THEN
29 FOR I:=1 STEP 1 UNTIL N66 DO DPG(I):=DEC*DPG(I)/16,
30 COMMENT MAKES ASCEN-INTERVAL DPG SMALL AGAINST STEPWIDTH S0;
31 ASCEN(NI,P,XM,APGPR,SELEC,P,DPG,A,Y,W,SDI,AUSA);     GOTO BSTART,
32 AUSA: OUTTEXT(" #### FLATLIN #### "), GOTO ENDE;
33 COMMENT COSB:RECT.OF STEEPEST ASCENT IN LIN.VAR. AND SDI(I);
34 BSTART: JJ:=1;  FOR I:=1 STEP 1 UNTIL N66 DO  PG0(I):=P(I);
35 TRIPLE:JJ:=JJ+1;          IF JJ GT 3 THEN GOTO PARAB,
36 FOR I:=1 STEP 1 UNTIL N66 DO IF SELEC(I) EQ 1 THEN P(I):=P(I)-SDA(I)*S0,
37          LSFUPR(NI,P,XM,P,AM,N,Y,W,F);
38        MFP(JJ):=RERRSS(NI,M,P,PGP,AR,ARM,Y,F,W,SD),
39        GOTO TRIPLE,
40 PARAB: IF ABS(LC) GT LMAX THEN BEGIN
41 FOR I:=1 STEP 1 UNTIL N66 DO  P(I):=PMP(I),
42 FOR I:=1 STEP 1 UNTIL NI DO AM(I):=ARM(I);S:=S0;
43 LC:=0;  GOTO ITERATION END,
44 LIMIN:=PIPAR(MFP,DDF,E-8,FLAT),
45 IF LIMIN GT 0.0 OR LIMIN LT -2.0 THEN GOTO FLAT;
46 COMMENT STEEPEST DESCENT TO PARAB. MINIMUM FROM STARTING POINT P0,
47 FOR I:=1 STEP 1 UNTIL N66 DO
48 IF SELEC(I) EQ 1 THEN P(I):=PG0(I)-LIMIN*SDI(I)*S0,
49 KEMA:=4;    GOTO ITERATION ;
50 FLAT:   IF DDF THEN     SHIFTR   ELSE     SHIFTA ,
51 ENDE:    LSFUNR(NI,M,XM,P,AM,N,Y,W,F);
52 FOR JJ:=1 STEP 1 UNTIL NI DO AR(JJ):=ARM(JJ),
53 FOR I:=1 STEP 1 UNTIL N66 DO BEGIN P0(I):=PMP(I) , COMMENT COPY.MIN,   END,
54 FINC: COMMENT BLOCK 0 ENDE    A       P       T       R     ,   END, END,
```

5b-1

```
PROCEDURE SHIFTA; COMMENT SHIFT AVANT IN ARRAY MFP;
BEGIN INTEGER K;
  LG:=LG+1;
FOR K:=1 STEP 1 UNTIL NGG DO PGG(K):= IF SELEC(K) EQ 1 THEN
P(K)+SDR(K)*SW ELSE P(K);          COMMENT NEW START NOTED;
FOR K:=1,2 DO MFP(K):=MFP(K+1);JJ:=2; GOTO TRIPLE
END;    COMMENT ENDE    S    H    I    F    T    A  ,

PROCEDURE SHIFTR; COMMENT SHIFT RETOUR IN ARRAY MFP,
BEGIN INTEGER I,K;
LG:=LG+1;
FOR K:= 3,2 DO MFP(K):=MFP(K-1);
FOR I:=1 STEP 1 UNTIL NGG DO PGG(I):=IF SELEC(I) EQ 1 THEN
P(I)+3*SDR(I)*SW ELSE P(I);          COMMENT NEW START NOTED;
          LSFLPR(NI,P,NR,P,AP,X,Y,W,F);
    MFP(1):=REGRESS(NI,P,P,PGP,AR,APG,Y,F,..,[illegible]);     GOTO PARAP
END;    COMMENT ENDE    S    H    I    F    T    R  ;

PROCEDURE ASCEN(NJ,PR,MPA,SFU,SELE,NU,DU,X,Y,W,CDIR,ASC);
COMMENT RAUER JUNE 73.DIRECTION OF STEEPEST ASCENT(AS NU-VECTOR CDIR,NN
COMP.NE 0) DETERMINED FOR FUNCTION SFU OF NU VARIABLES BY DETERMINING
SFU AT NU NEIGHBOUR POINTS EACH SHIFTED BY DU(1:NU),ALONG ONE COORD.ONLY.
IF NO APPRECIABLE VARIATION IN SFU(LT 1-6) JUMP TO LABEL ASC.
SELECTION OF NU VARIABLES OUT OF LARGER ARRAY [illegible](1:NU) BY INTEGERARRAY
SELE (OUT OF PROC. CORELL). ARRAYS X,Y,W AS INPUTS TO SFU.
[illegible]. NU INTERNALLY FROM SELE,
NAME CDIR; INTEGER NJ,MP, REAL MPA; INTEGER ARRAY SELE;
ARRAY CDIR,DU,P,DU,X,Y,   REAL PROCEDURE SFU;   LABEL ASC;
    BEGIN INTEGER K,L,NU,NN,  REAL RR,MM,A;
NU:=NJ-MP,  COMMENT BLOCK,
    BEGIN ARRAY PA,F1(0:NU),PR(1:NJ),UR(1:NU),
FOR A:=1 STEP 1 UNTIL NU DO UR(K):=PR(A),
F1(0):=SFU(NJ,MP,MPA,UR,X,Y,W),
L:=0;     FOR K:=1 STEP 1 UNTIL NU DO
IF SELE(K) EQ 1 THEN   BEGIN
L:=L+1,          UR(K):=PR(K)+DU(K);
F1(K):=SFU(NJ,MP,MPA,UR,X,Y,W),
UR(K):=UR(K)-DU(K)     END          ELSE F1(K):=F1(0),          NN:=0,
NN:=0;FOR A:=1 STEP 1 UNTIL NU DO IF SELE(A) EQ 1 THEN
BEGIN RR:=PA(A):=(F1(A)-F1(0))/DU(A);
     NN:=NN+RR*RR                      END;
NN:=SQRT(NN),
IF NN LT 1-9 THEN GOTO ASC,
FOR A:=1 STEP 1 UNTIL NU DO IF SELE(A) EQ 1 THEN
K:=CDIR(A):=PA(K)/NN,                                         END,
COMMENT BLOCK & ENDE     A      S      C      E      N  ,          END;

REAL PROCEDURE MIPAR(S3,RO,CR,FAIL);
COMMENT PLACE OF MINIMUM OF PARABOLA THROUGH 3 ORDINATES
S3(1...3) AT EQUIDISTANT ABSCISSAS 1...3 IN SOME UNITS.
IF CURVATURE INAPPROPRIATE(CR),LABEL FAIL OR RO. [illegible],
NAME RO;BOOLEAN RO;REAL CR,ARRAY S3,
LABEL FAIL,
BEGIN REAL C1,C2,
RO:=IF S3(3) GT S3(1) THEN TRUE ELSE FALSE,
C2:=0.5*S3(1)-S3(2)+0.5*S3(3);
IF C2 LT CR THEN GOTO FAIL,
C1:=-1.5*S3(1)+2*S3(2)-0.5*S3(3),
MIPAR:=-C1/(2*C2);        END;
COMMENT    ENDE        M        I        P        A        R,
```

5b-2

```
REAL PROCEDURE LAY(MX,SC,X,XM),  COMMENT ONE LAY,PARAM.MX,SC,
UNIT AMPLITUDE,WITH LOG(LAY)=0 AT XM.  RAUER JUL. 83,
REAL MX,SC,X,XM;        BEGIN
LAY:=EPTR(X,SC,MX)-EPTR(XM,SC,MX)-(X-XM)*EPST(XM,SC,MX)/SC END;
COMMENT   ENDE     L      A       Y        ;

REAL PROCEDURE AFURR(NI,ML,MMA,PG,X,Y,W);
COMMENT RAUER JUNE 83.LPR.SUM,REDUCED,OF LSFURR [NO MEMORY FOR OPTIMUM];
INTEGER ML,NI;     REAL MMA;
 ARRAY PG,W,X,Y;
  BEGIN INTEGER KK,NG;     REAL FI,YF,SU;
   ARRAY AMP(1:NI),F(1:ML)     ;
NG:=2*NI;
LSFURR(NI,ML,MMA,PG,AMP,X,Y,W,F),
IF PRAFAUS THEN   BEGIN
OUTIMAGE;       OUTTEXT("   X             Y");
FOR KK:=1 STEP 1 UNTIL ML DO                         BEGIN
OUTIMAGE; K:=E3*X(KK); OUTINT(K,10);
 K:=E6*Y(KK); OUTINT(K,10)   END;  END;
SU:=FI:=0;   FOR KK:=1 STEP 1 UNTIL ML DO
BEGIN YF:=Y(KK)-F(KK); FI:=FI+YF*YF*W(KK); SU:=SU+W(KK)  END;
      AFURR:=FI/SU;
COMMENT ENDE        A        F        U        R        R;         END;

REAL PROCEDURE EPTR(X,B1,X1),
COMMENT RAUER MAY 82.EPSTEIN TRANSITION FROM 0 AT LEFT
TO LINEAR WITH SLOPE 1/B1 AT RIGHT. B1 MUST BE NE 0;
REAL X,B1,X1,
BEGIN REAL D1;D1:=(X-X1)/B1;
IF ABS(D1) GT 40 THEN BEGIN
EPTR:=IF D1 GT 0 THEN D1 ELSE 0 END ELSE
EPTR:=LN(1+EXP(D1)) END;
COMMENT ENDE        E          P           T              R;
REAL PROCEDURE EPST(X,B1,X1);
COMMENT RAUER MAY 82.
EPSTEIN STEP FROM 0 AT LEFT TO 1 AT RIGHT.  EPST=DERIVATIVE OF EPTR.
B1 MUST BE NE 0;
REAL X,B1,X1,
BEGIN REAL D1; D1:=(X-X1)/B1;
IF ABS(D1) GT 40 THEN
   BEGIN EPST:=IF D1 GT 0 THEN 1 ELSE 0 END      ELSE
EPST:=1/(1+EXP(-D1))        END;
COMMENT ENDE      E          P           S             T,

          REAL PROCEDURE REGRSS(N1,M1,PG,PG0,A3,A03,Y,F,W,SS0);
COMMENT RAUER MAY/JUL.84.SI=REDUCED ERRORSUM(1..M1)=AVERAGE SQUARED DEV.
N1 NO.OF LAY-TERMS WITH NGN=2*N1 GEOM.COEFF.PG(1:NGN). F=SUM[AMPLIT*LAY]=
INPUT.  REGRSS MEMORIZING OPTIMUM CONDITION AS PG0,A03,SS0.
WEIGHT REDUCED NUMBER COUNT,
NAME A03,PG0,SS0; INTEGER M1,N1, REAL SS0, ARRAY A3,A03,F,PG,PG0,W,Y;
BEGIN INTEGER II,KK,NGN,    REAL FI,SI,SU,YF;                NGN:=2*N1;
 SU:=FI:=0;     FOR KK:=1 STEP 1 UNTIL M1 DO BEGIN YF:=Y(KK)-F(KK);
FI:=FI+W(KK)*YF*YF;    SU:=SU+W(KK)            END;
                 REGRSS:=SI:=FI/SU,
IF SI LT SS0 THEN                                 BEGIN   SS0:=SI;
FOR KK:=1 STEP 1 UNTIL N1 DO A03(KK):=A3(KK);
FOR II:=1 STEP 1 UNTIL NGN DO PG0(II):=PG(II)     END;              END;
COMMENT ENDE        R        E        G        R        S        S,
```

5 b-3

```
1 PROCEDURE LSFURR(NI,PL,HMA,PL,AMPL,X,Y,*,F);
2 COMMENT RAWER JUNE 65 WITH GIVEN COEFF ARRAY PL(1...2*NI) AND NI
3 MEMBERS IN REPRESENTATIVE FUNCTION F(1..*L) FINDS BY LEASTSQUARES
4 (CHOLESKY) OPTIMUM AMPLITUDES AMPL(1...NI) SO THAT *EIGHTED[1...ML]
5 REDUCED SQUARED ERROR SUM [OF F AGAINST MEASURED VALUES Y] IS MINI-
6 MIZED.  THEN FUNCTION [ARRAY F] COMPUTED WITH THESE AMPLITUDES.
7 PROCEDURE CHOLESKY &  REAL PROCEDURE LAY NEEDED;
8 NAME AMPL,F;     INTEGER NI,ML;   REAL HMA;
9 ARRAY AMPL,F,PL,W,X,Y;
10        BEGIN INTEGER I,J,K,L,NG,    REAL FIL,FUAIJ,FUIL,P2I,P2IM;
11 NG:=2*NI;  BEGIN            COMMENT    B  L  O  C  K   ;
12  ARRAY FFI(1:NI,1:ML),FUA(1:NI,1:NI),FUB(1:NI),PU(1:NG);
13 FOR J:=1 STEP 1 UNTIL NG DO PU(J):=PL(J);
14   FOR I:=1 STEP 1 UNTIL NI DO       BEGIN
15    K:=2*I;P2I:=PU(K);P2IM:=PU(K-1);
16 FUIL:=0;   FOR L:=1 STEP 1 UNTIL ML DO BEGIN
17       FIL:=FFI(I,L):=LAY(P2IM,P2I,X(L),HMA);
18       FUIL:=FUIL+Y(L)*FIL*W(L)                              END;
19 FUB(I):=FUIL                                                   END;
20 FOR I:=1 STEP 1 UNTIL NI DO                                      BEGIN
21 FOR J:=1 STEP 1 UNTIL NI DO                                    BEGIN
22 FUAIJ:=0;
23 FOR L:=1 STEP 1 UNTIL ML DO                                 BEGIN
24 FUAIJ:=FUAIJ+FFI(I,L)*FFI(J,L)*W(L)                         END;
25 FUA(J,I):=FUA(I,J):=FUAIJ                                       END;
26                                                                    END;
27 CHOLESKY(1,NI,FUA,FUB,AMPL,SINGA);
28 GOTO CHOLA,
29 SINGA: OUTTEXT(" AMPL.SING. ");
30 CHOLA: FOR L:=1 STEP 1 UNTIL ML DO              BEGIN
31 F(L):=0;     FOR J:=1 STEP 1 UNTIL NI DO
32 F(L):=F(L)+AMPL(J)*FFI(J,L)                     END;   END;
33 COMMENT BLOCK & ENDE     L       S       F       U       R       R;   END;
34
35  PROCEDURE  CHOLESKY (N1, N2, A, B, X, SING),  COMMENT RESOLVES LINEAR
36  SYSTEM OF EQS., EXCEPT WHEN SINGULARY;
37  NAME  X;  INTEGER  N1, N2; ARRAY  A, B, X;  LABEL  SING;
38  BEGIN   INTEGER  IC,JC,KC,   REAL  H;
39  FOR  IC:=N1  STEP  1  UNTIL  N2  DO
40  BEGIN  X(IC):=B(IC); FOR JC:=IC-1  STEP  -1  UNTIL  N1  DO
41  BEGIN  H:=A(JC,JC)*A(IC,JC),
42  A(IC,IC):=A(IC,IC)-H*A(IC,JC),  X(IC):=X(IC)-A(IC,JC)*X(JC);
43  FOR KC:=IC+1 STEP 1 UNTIL N2 DO A(KC,IC):=A(KC,IC)-H*A(KC,JC)
44     END;              IF  A(IC,IC)  LE  0.0  THEN   WOTO  SING;
45  FOR KC:=IC+1 STEP 1 UNTIL N2 DO A(KC,IC):=A(KC,IC)/A(IC,IC) END ;
46  FOR IC:=N2 STEP -1 UNTIL N1 DO  BEGIN  X(IC):=X(IC)/A(IC,IC);
47  FOR KC:=IC+1 STEP 1 UNTIL N2 DO X(IC):=X(IC)-A(KC,IC)*X(KC) END;
48 END;        COMMENT  ENDE    C   H   O   L   E   S   K   Y   ;
```

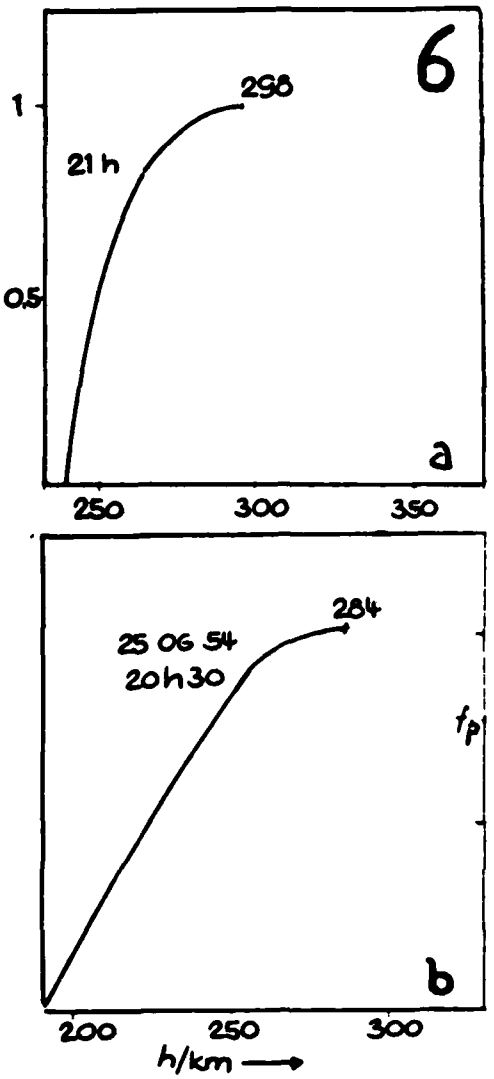
6
1
0.5
298
21 h
a
250
300
350
284
25 06 54
20h30
fp
b
200
250
300
h/km

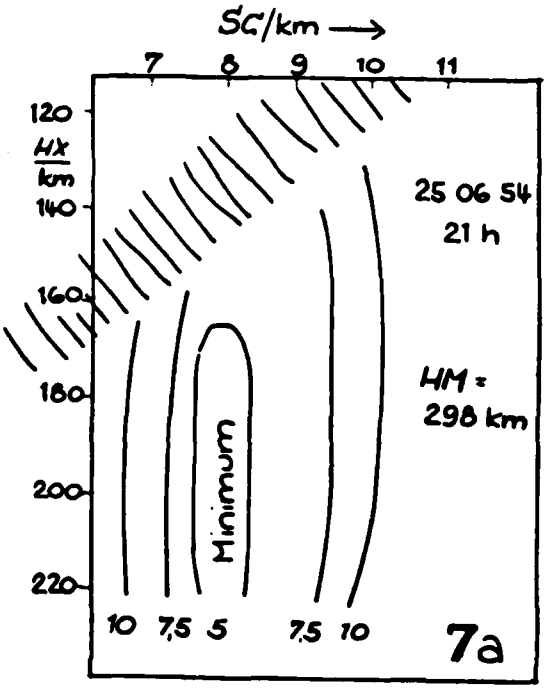
SC/km
7
8
9
10
11
120
Hx/km
140
160
180
200
220
25 06 54
21 h
HM = 298 km
Minimum
10
7,5
5
7,5
10
7a

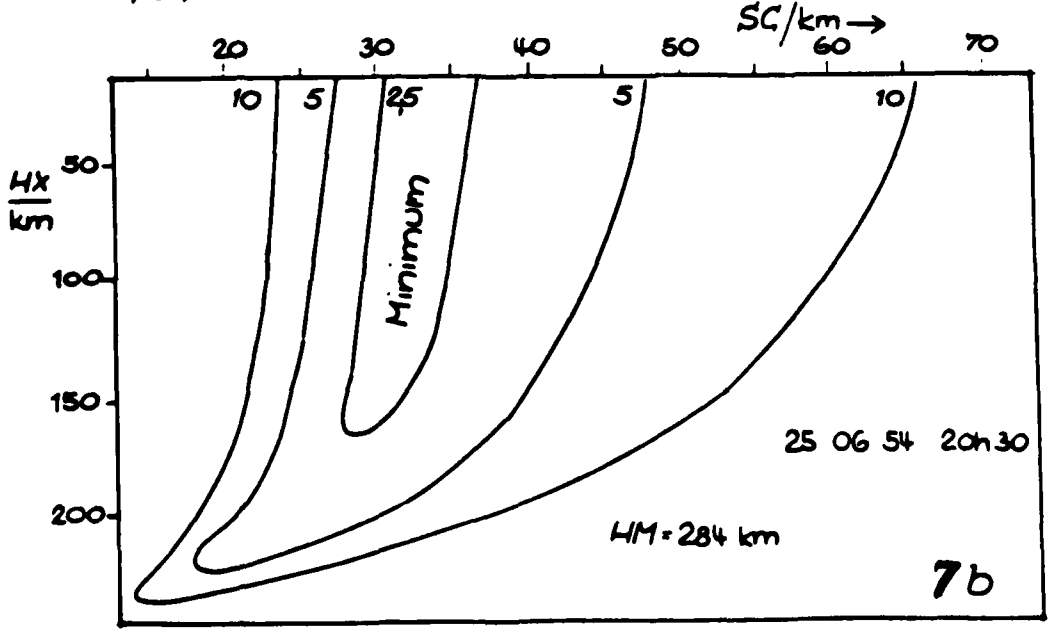
SC/km
20
30
40
50
60
70
10
5
25
5
10
Hx/km
50
100
150
200
Minimum
25 06 54 20h30
HM = 284 km
7b

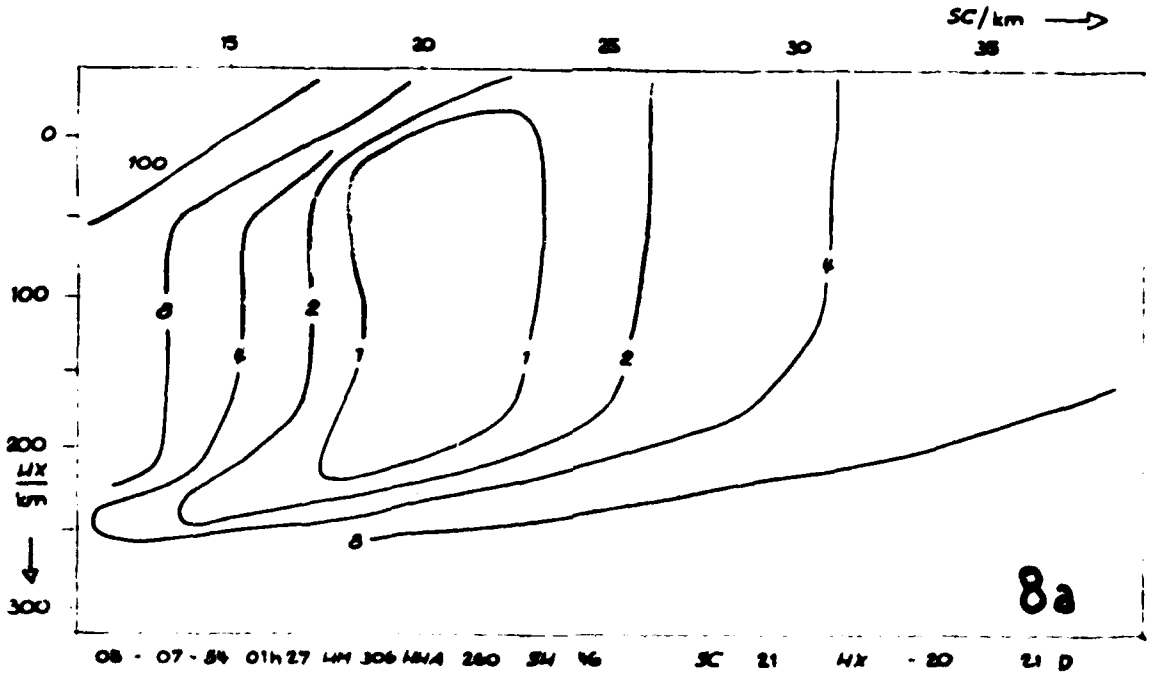
SC/km
15
20
25
30
35
0
100
200
MX
km
300
100
6
2
1
1
2
6
8
8a
08 - 07 - 84 01h27 LAM 306 HMA 280 SM 96 SC 21 MX - 20 21 D

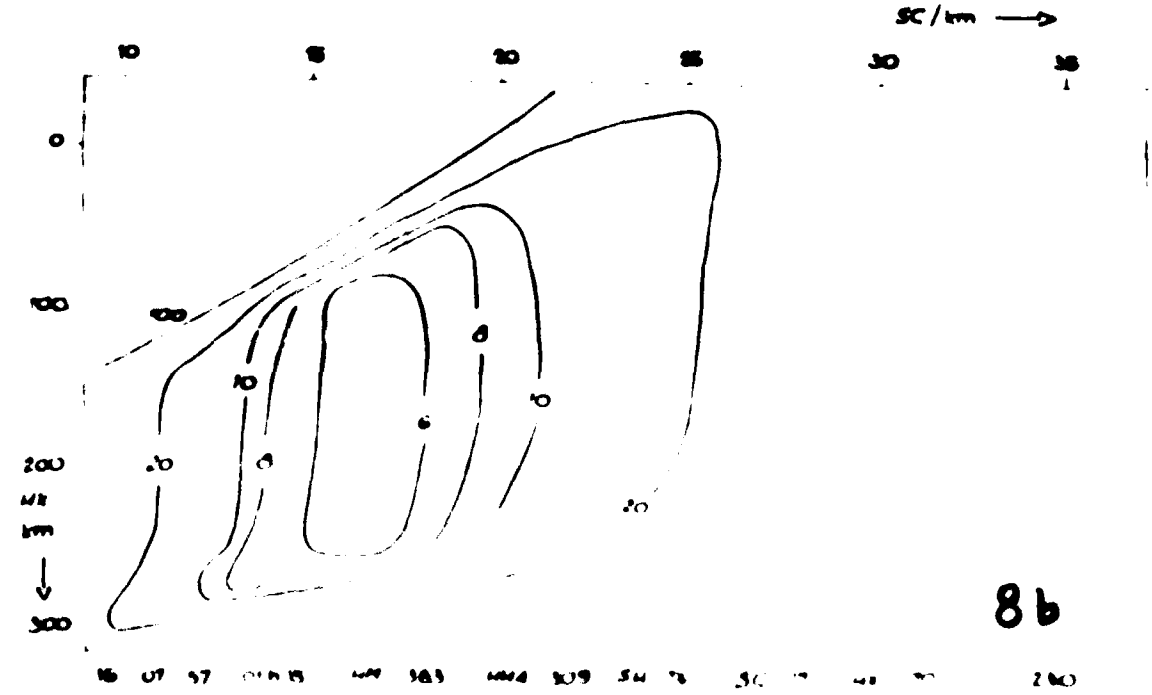
SC/km
10
15
20
25
30
35
0
100
200
MX
km
300
100
10
6
8
10
20
8b

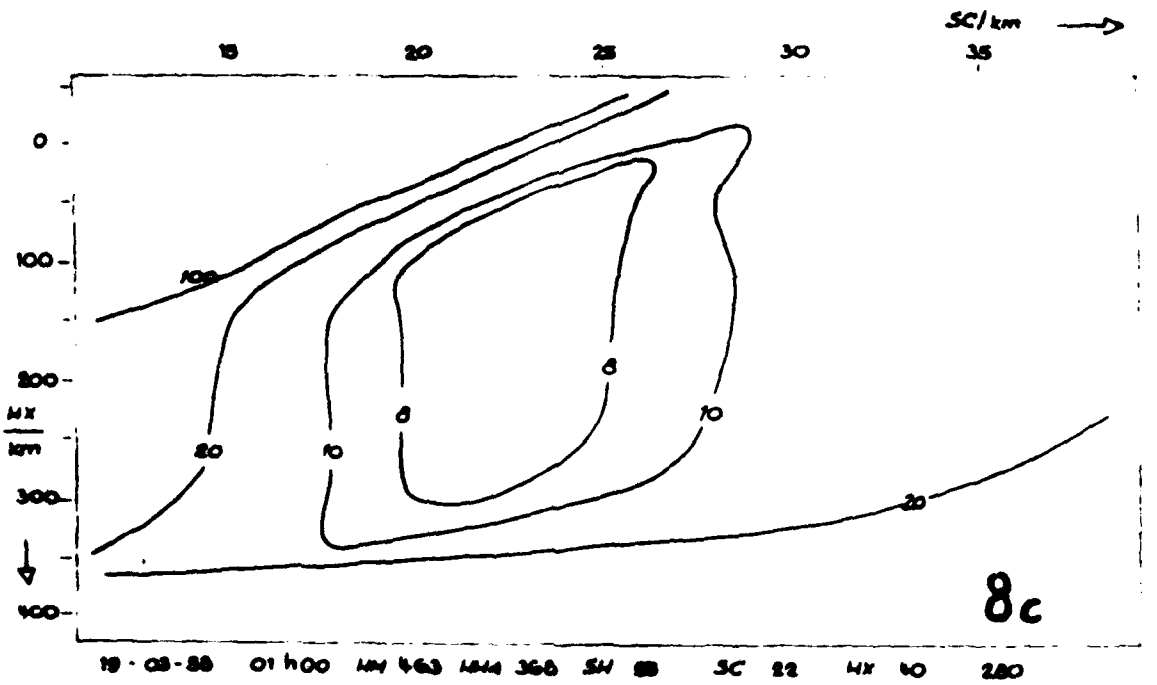
SC/km
15
20
25
30
35
0
100
200
Mx
km
300
400
100
80
10
6
6
6
10
20
8c

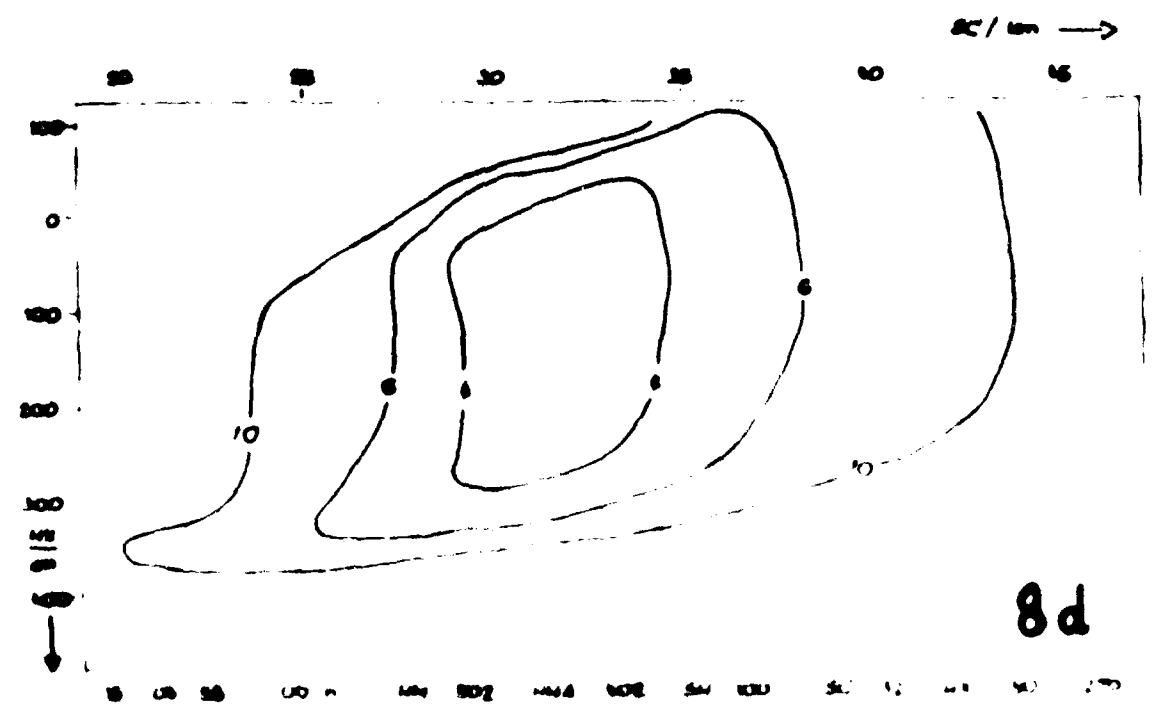
SC / km
6
6
6
6
10
10
8d

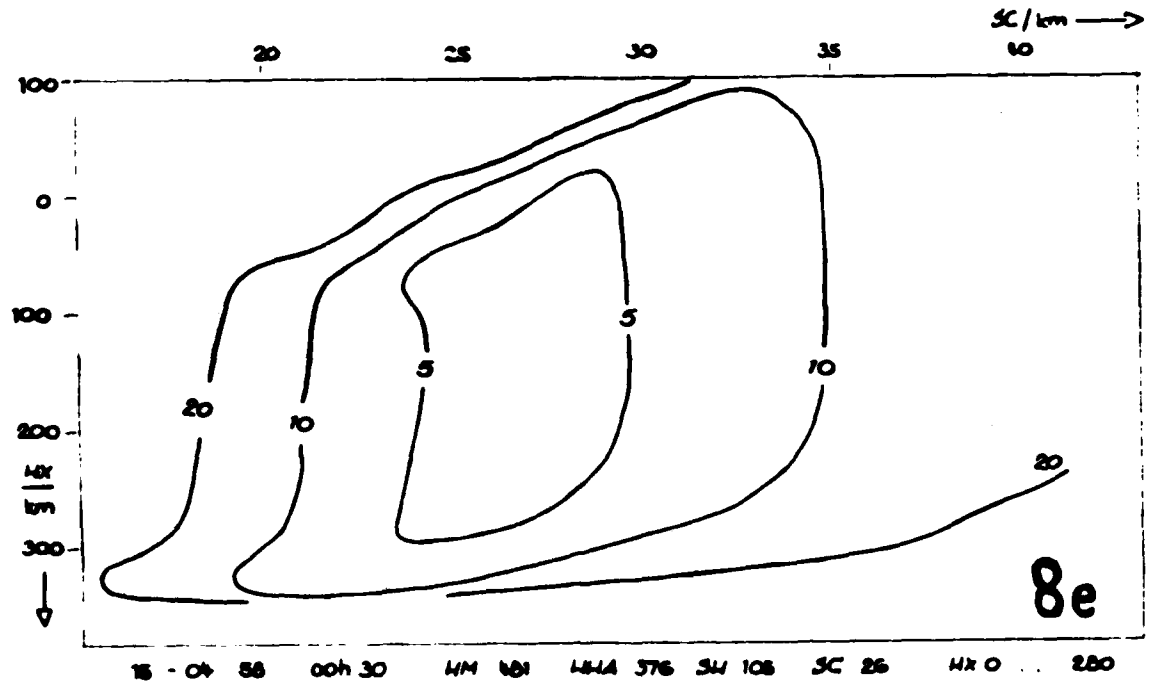
SC/km
20
25
30
35
40
100
0
100
200
300
20
10
5
5
5
10
20
8e

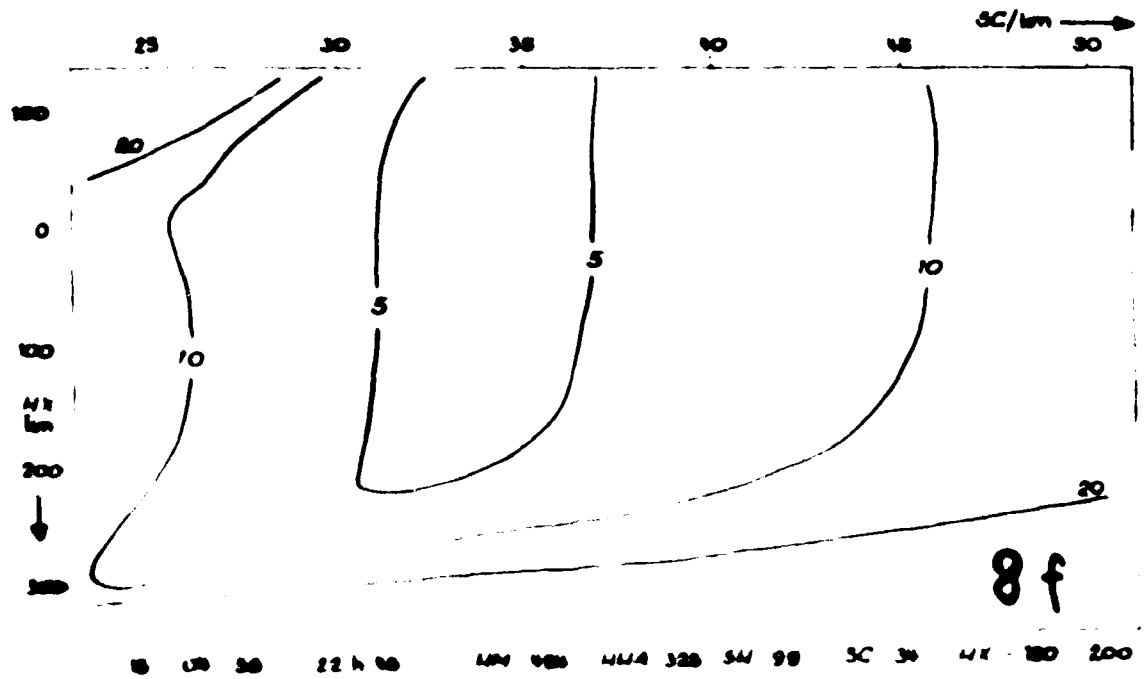
SC/km
25
30
35
40
45
50
80
0
5
5
10
10
20
8f

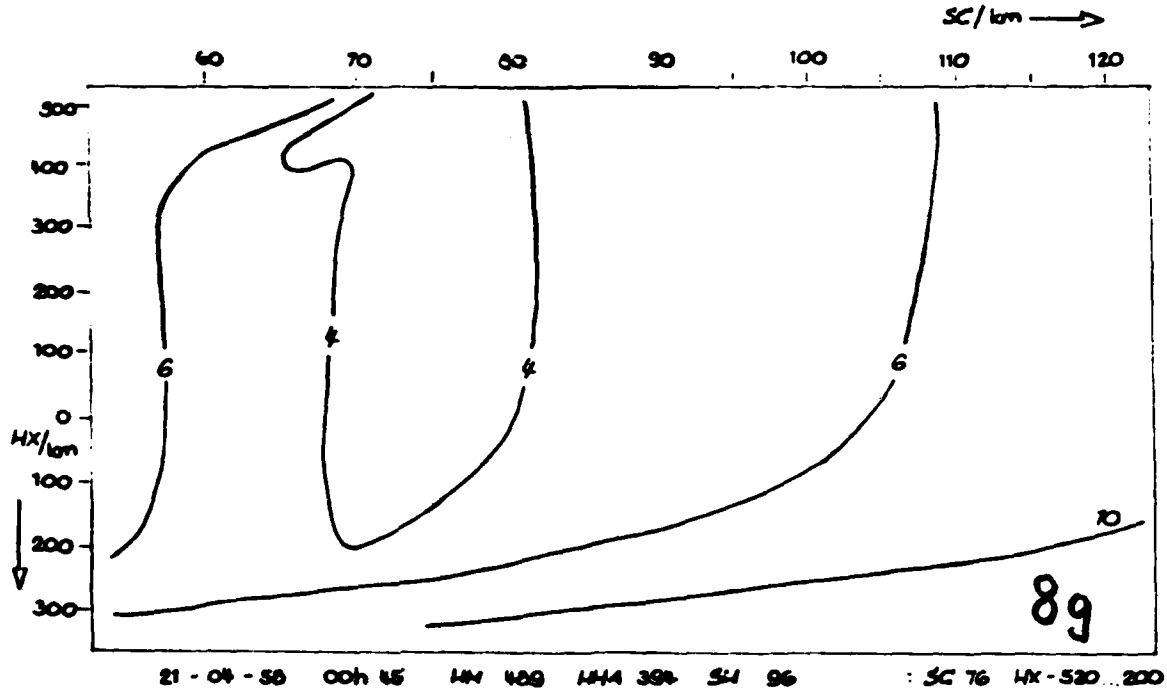
SC/km
60
70
80
90
100
110
120
HX/km
0
100
200
300
6
4
4
6
10
8g
21 - 04 - 58 00h 45 MM 488 MM4 398 SM 96 : SC 76 HX - 520 ... 200

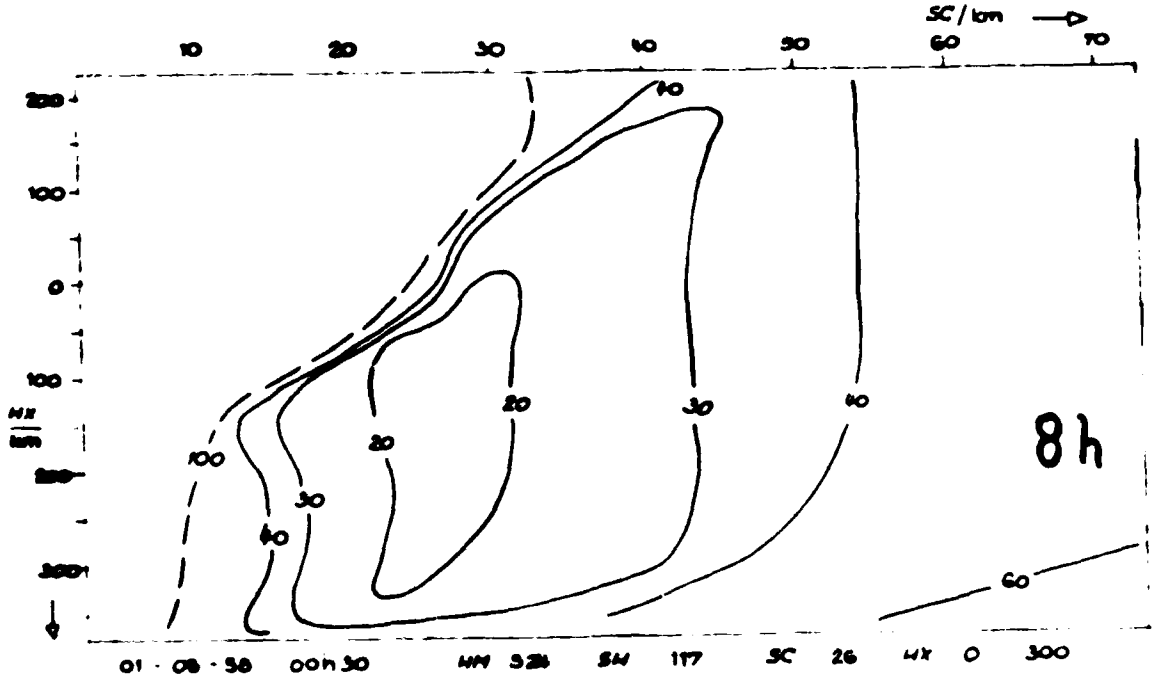
SC/km
10
20
30
40
50
60
70
HX/km
0
100
200
300
40
20
30
40
100
20
30
40
60
8h
01 - 08 - 58 00h 30 MM 528 SM 117 SC 26 HX 0 300

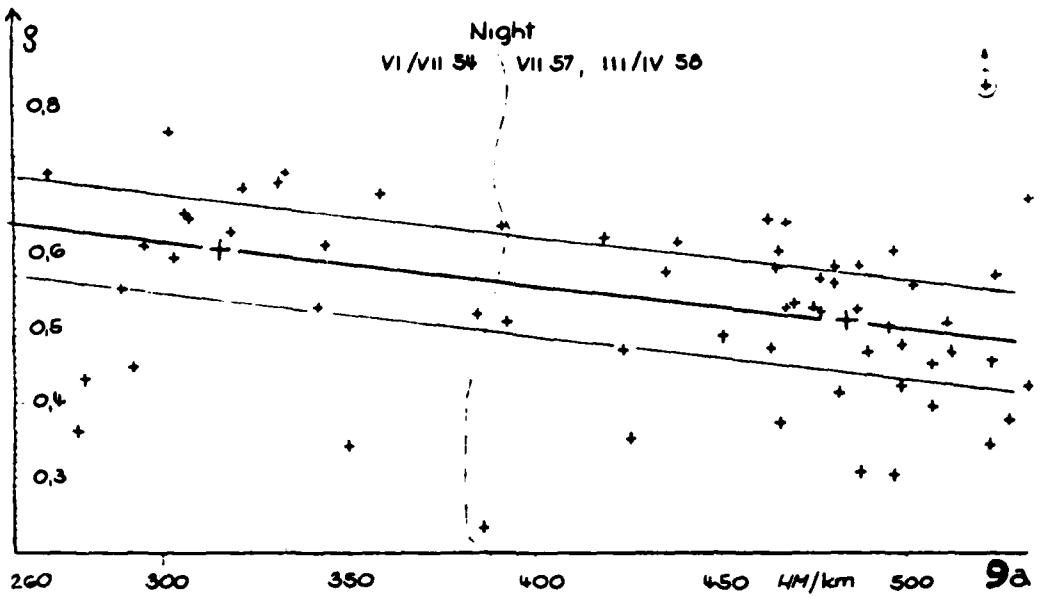
Night
VI/VII 54 VII 57, III/IV 58
0,8
0,6
0,5
0,4
0,3
260
300
350
400
450
HM/km
500

9a

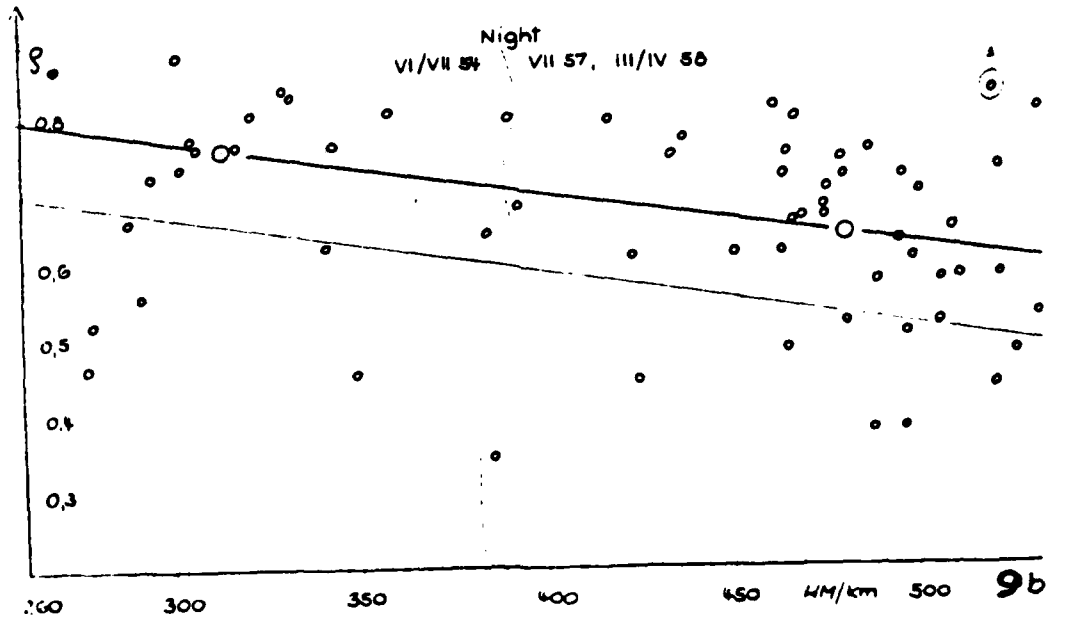
Night
VI/VII 54 VII 57, III/IV 58
0,8
0,6
0,5
0,4
0,3
260
300
350
400
450
HM/km
500

9b

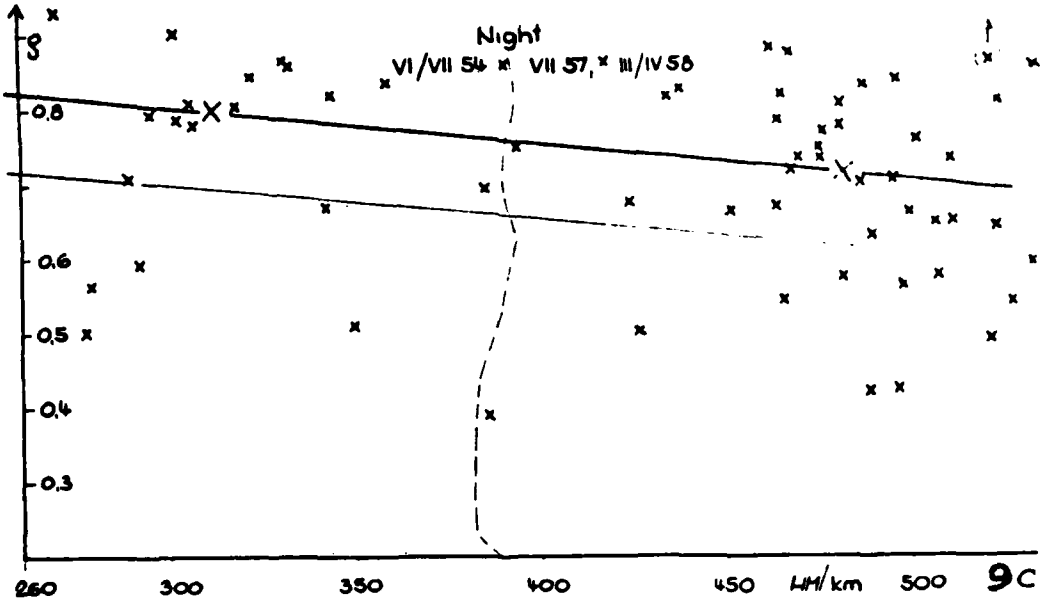
Night
VI/VII 54 VII 57, III/IV 58
g
0,8
0,6
0,5
0,4
0,3
260
300
350
400
450
HM/km
500
9c

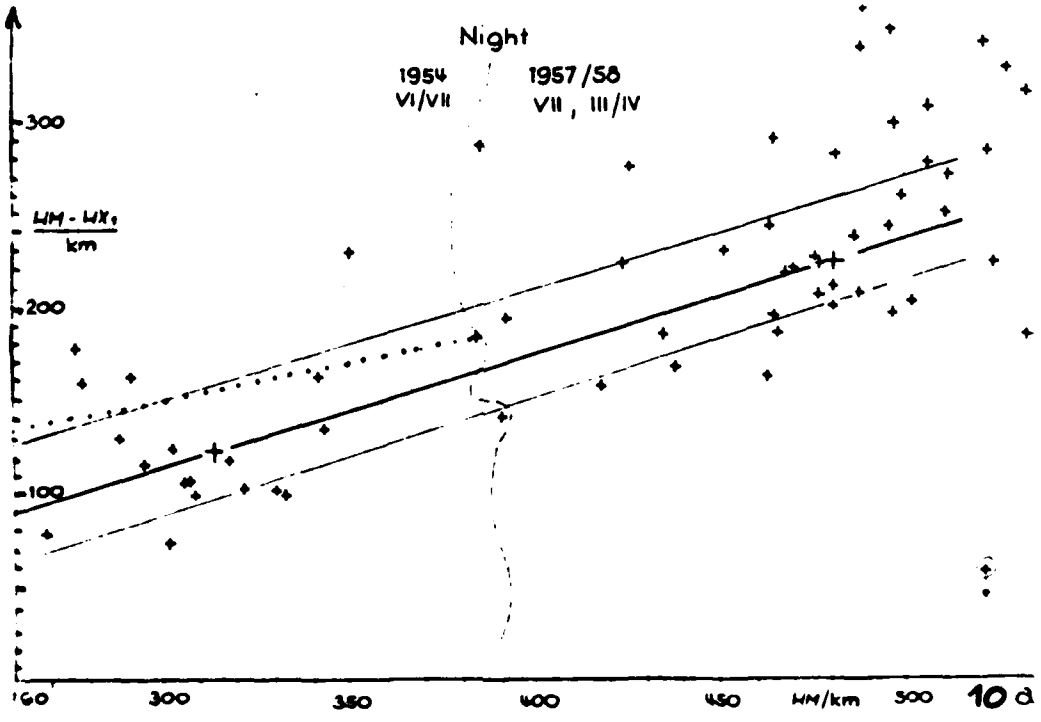
Night
1954
VI/VII
1957/58
VII, III/IV
300
HM - HX
km
200
100
60
300
350
400
450
HM/km
500
10 d

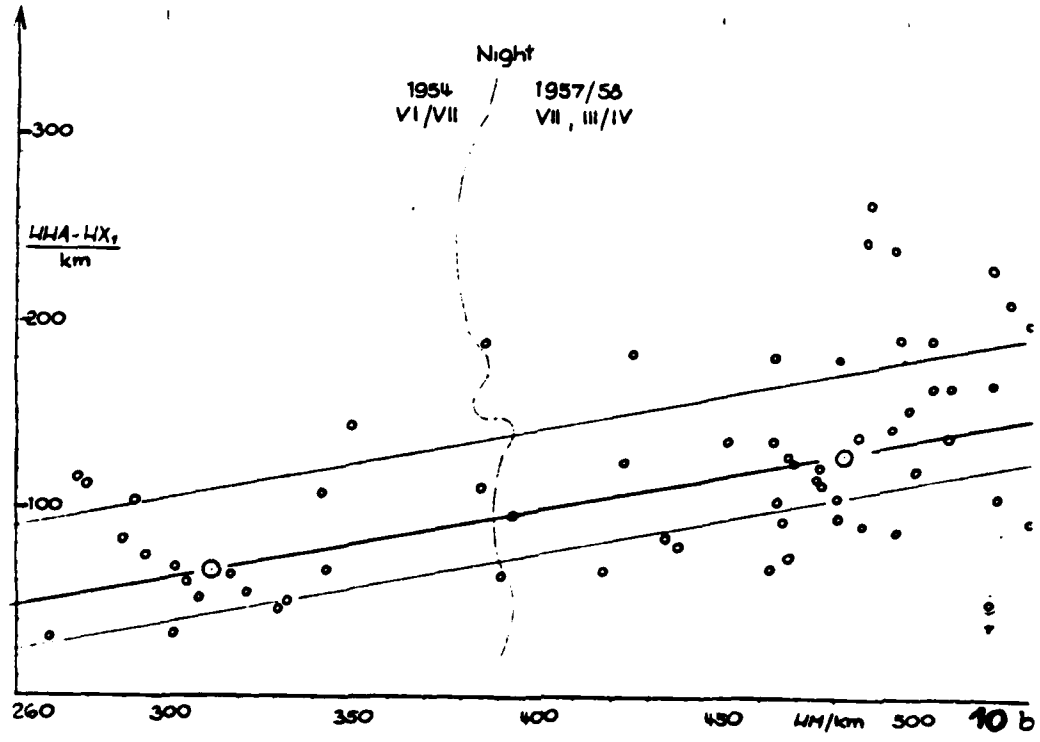
Night
1954
VI/VII
1957/58
VII, III/IV
300
HHA - HX1
km
200
100
260
300
350
400
450
HH/km
500
10 b

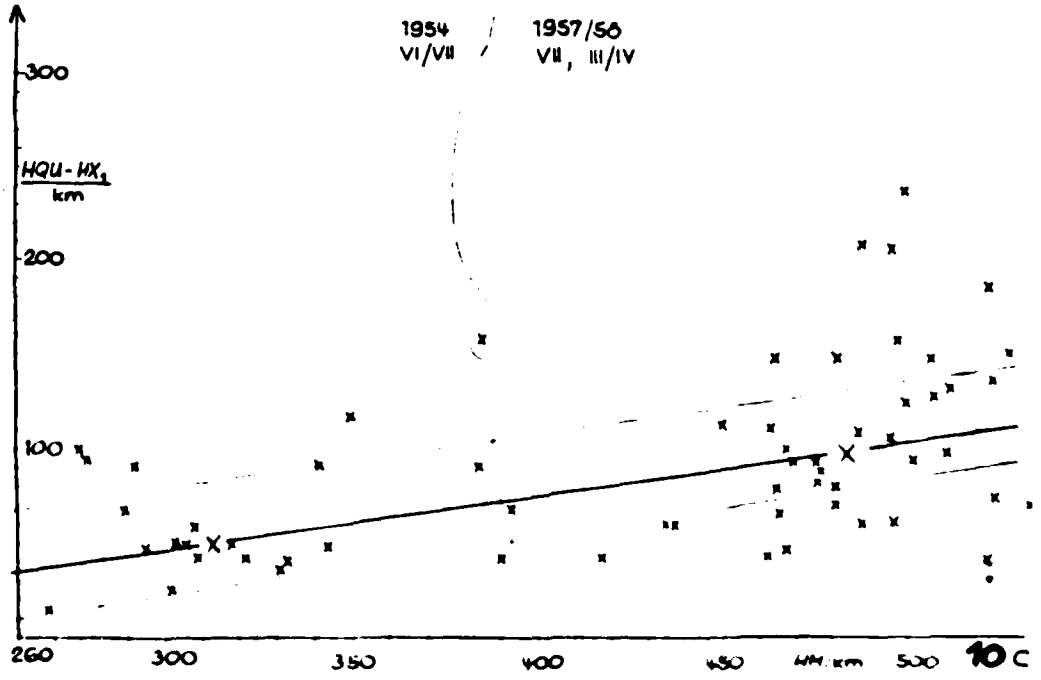
1954
VI/VII
1957/58
VII, III/IV
300
HQU - HX1
km
200
100
260
300
350
400
450
HH km
500
10 c

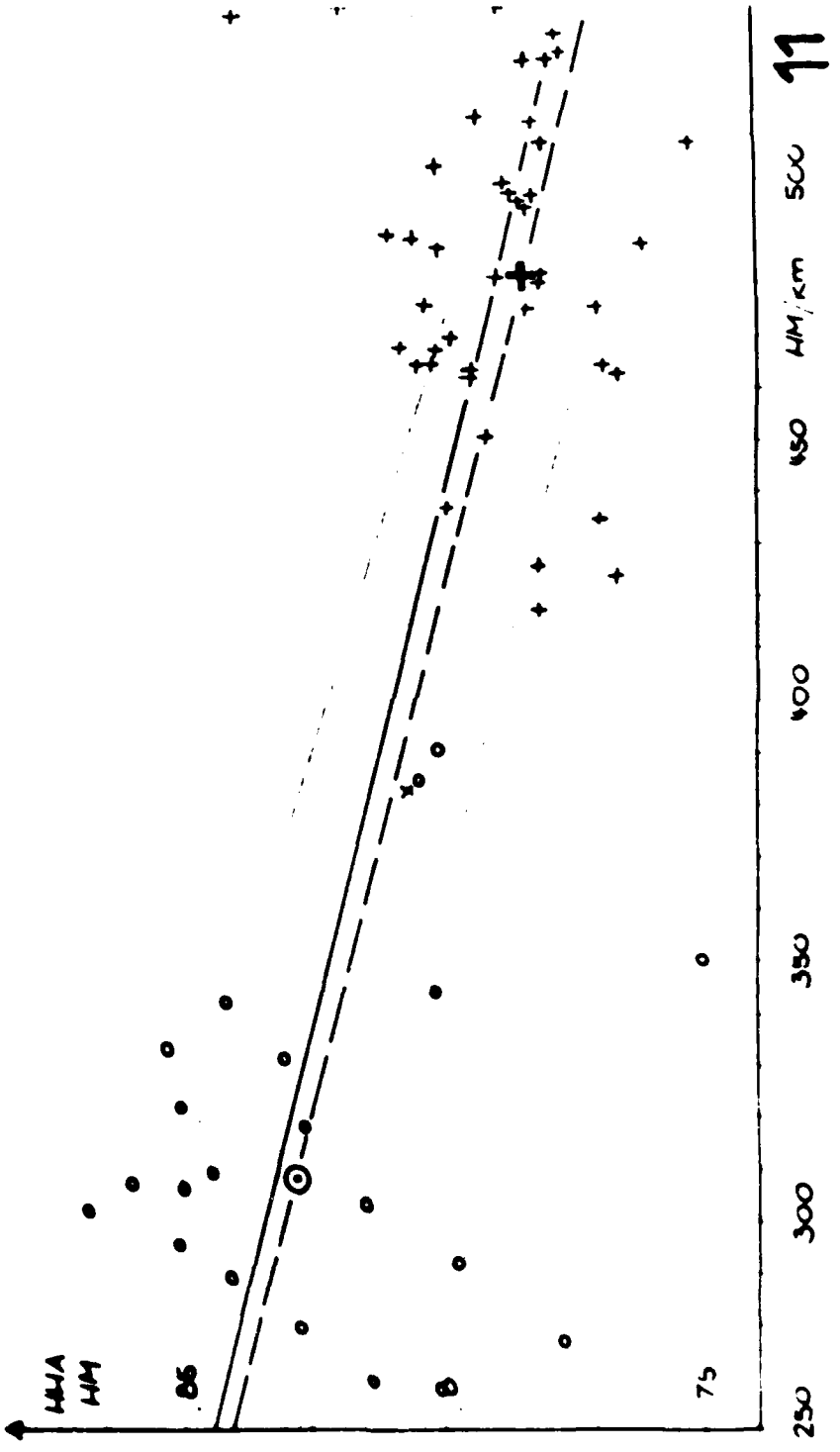
11
MM/KM
250
300
350
400
450
500
85
75
MM/A

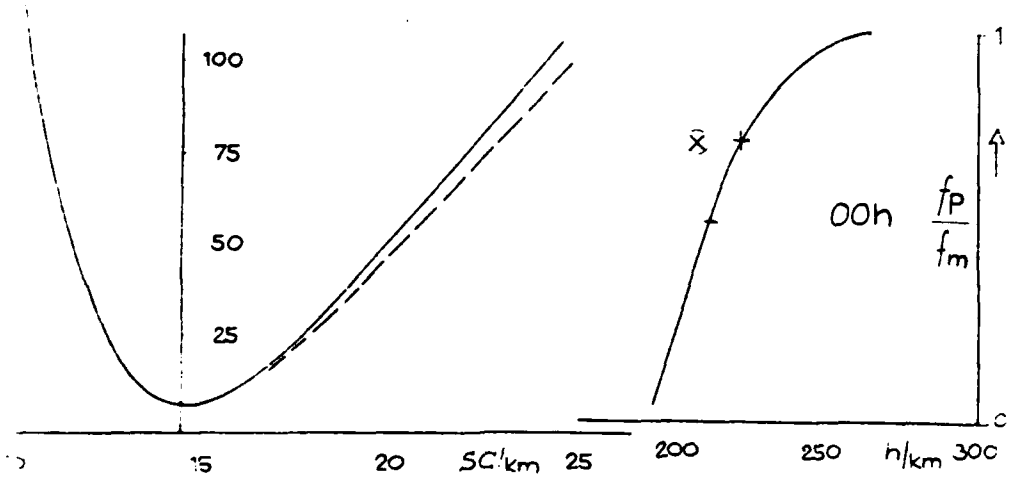
100
75
50
25
15
20
SC/km
25
200
250
h/km
300
1
0
00h
fp/fm

12a

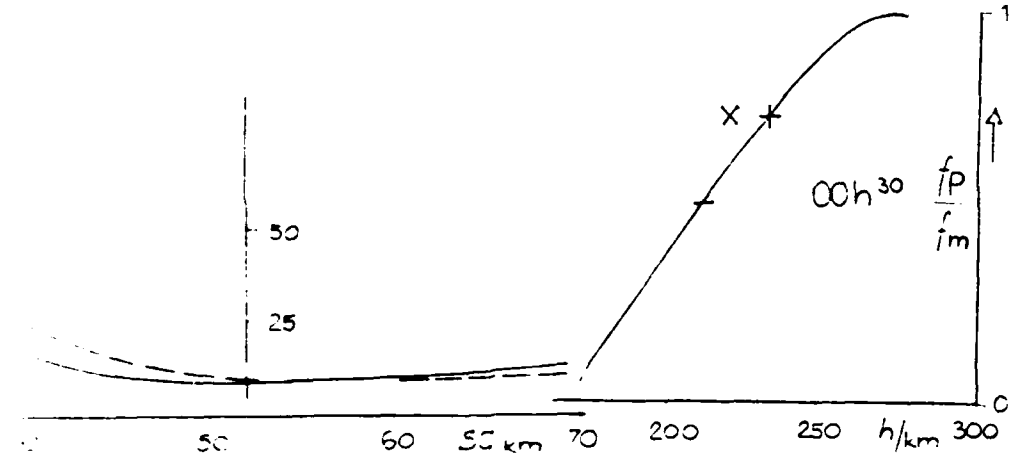
50
25
50
60
SC km
70
200
250
h/km
300
1
0
00h30
fp/fm

12b

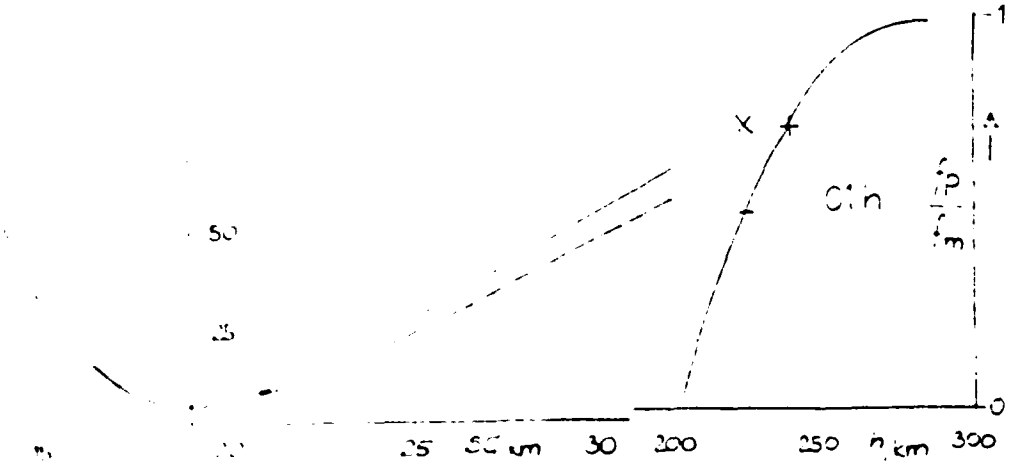
50
25
25
SC km
30
200
250
h km
300
1
0
01h
fp/fm

12c

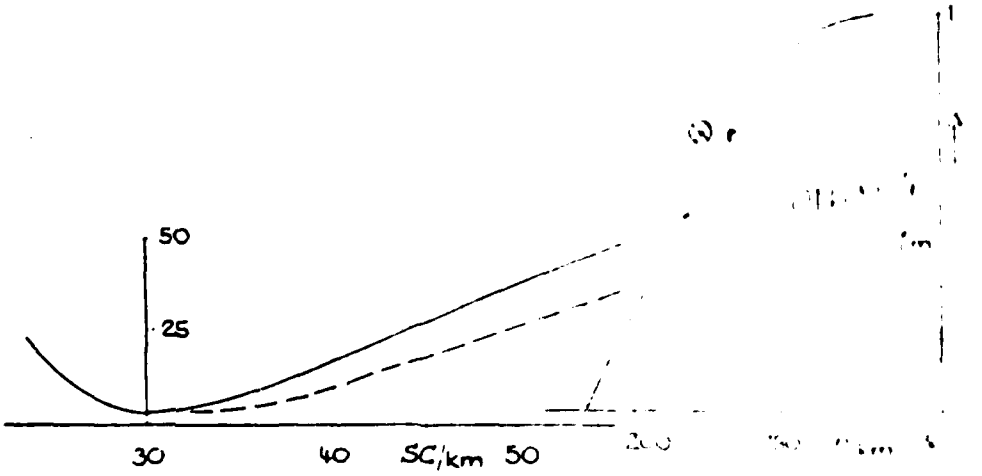
50
25
30
40
SC/km
50

12d

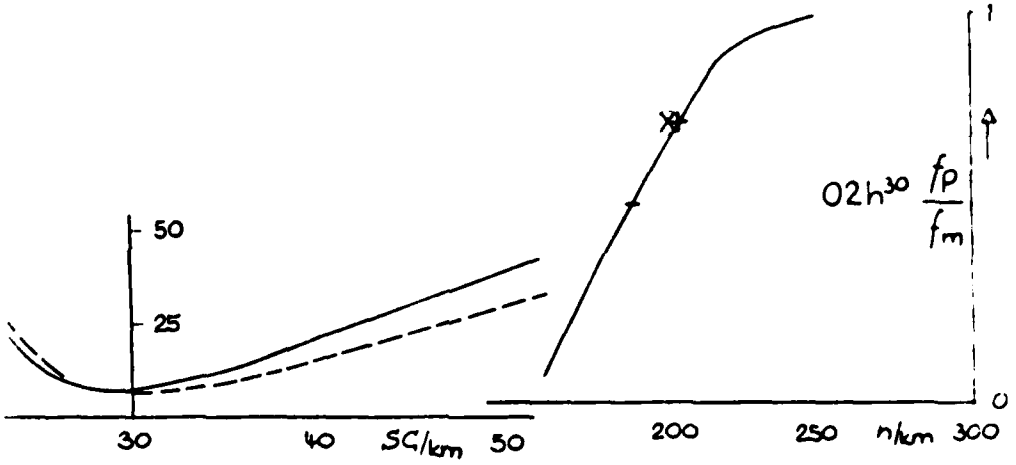
50
25
30
40
SC/km
50
200
250
n/km
300
02h30
fp/fm
1
0

12e

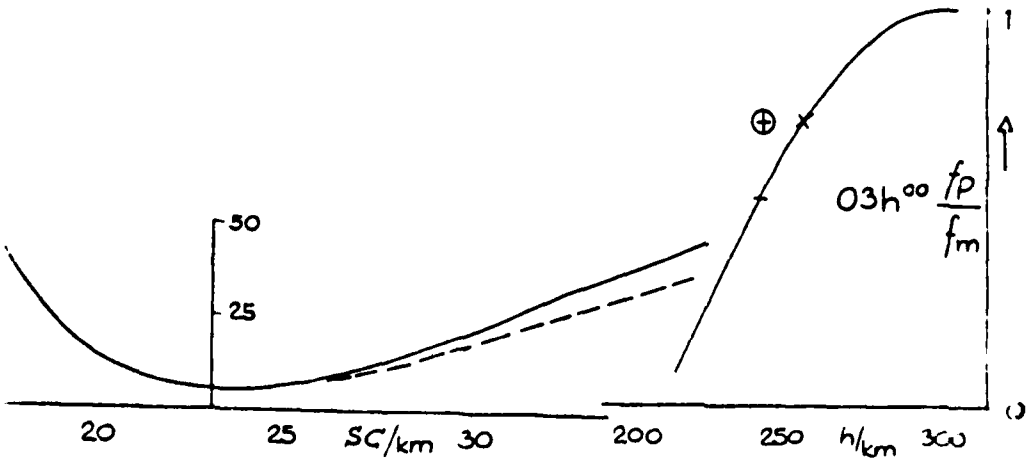
50
25
20
25
SC/km
30
200
250
h/km
300
03h00
fp/fm
1
0

12f

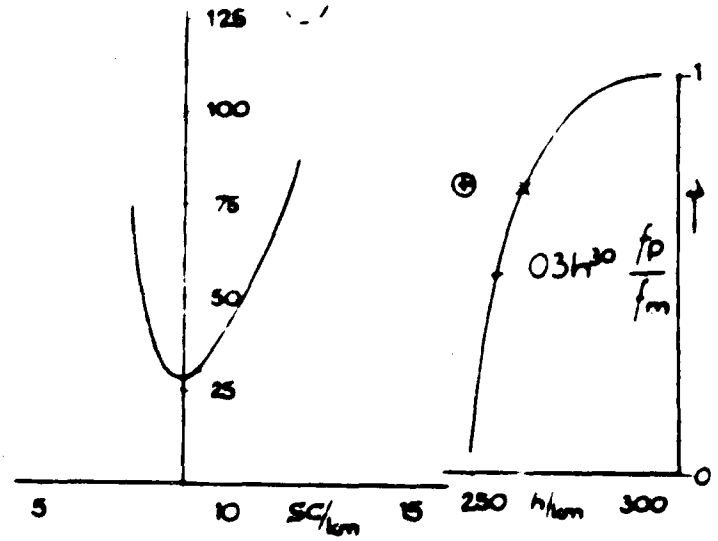
125
100
75
50
25
5
10
SC/km
15
1
0
03h^30 fp/fm
250
h/km
300

12g

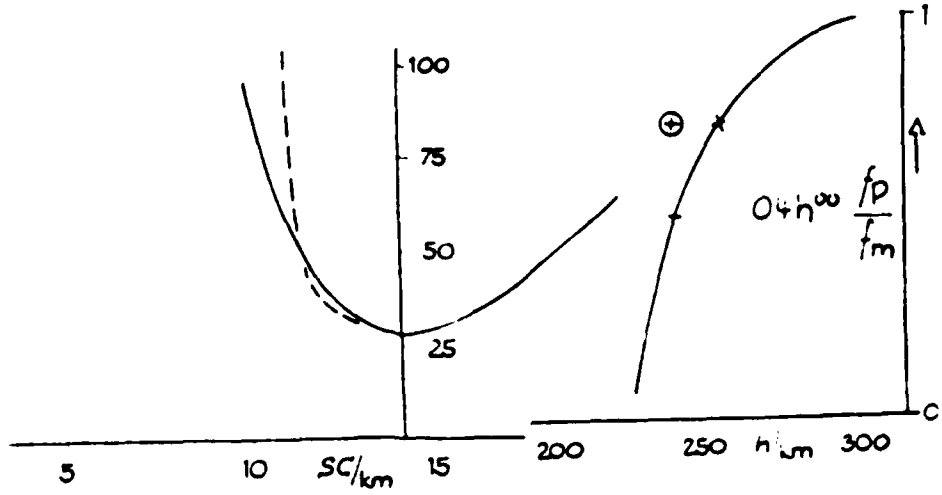
100
75
50
25
5
10
SC/km
15
1
0
04h^00 fp/fm
200
250
h/km
300

12h

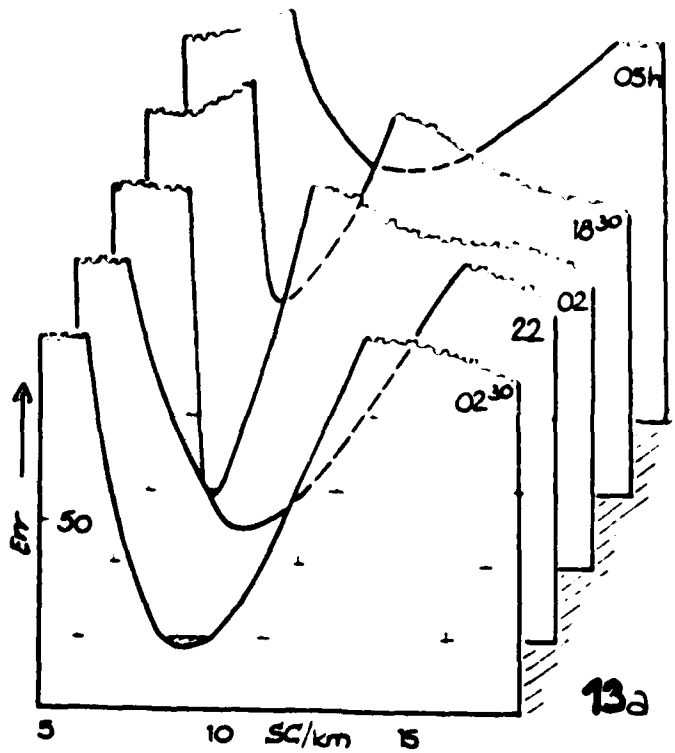
05h
18 30
02
22
02 30
Err
50
5
10
SC/km
15

13a

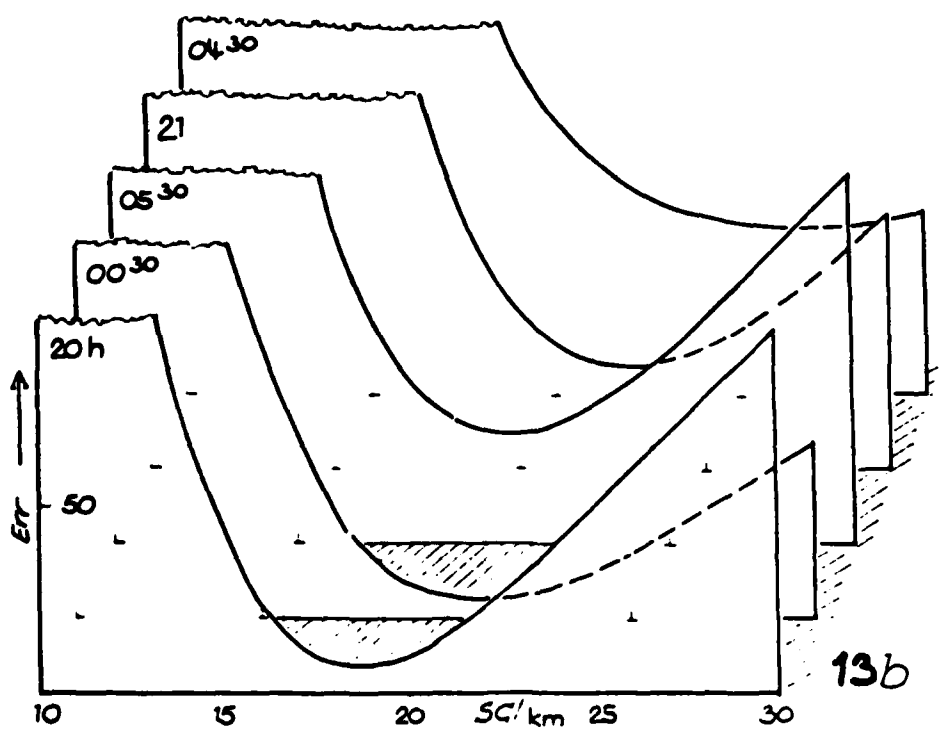
04 30
21
05 30
00 30
20 h
Err
50
10
15
20
SC/km
25
30

13b

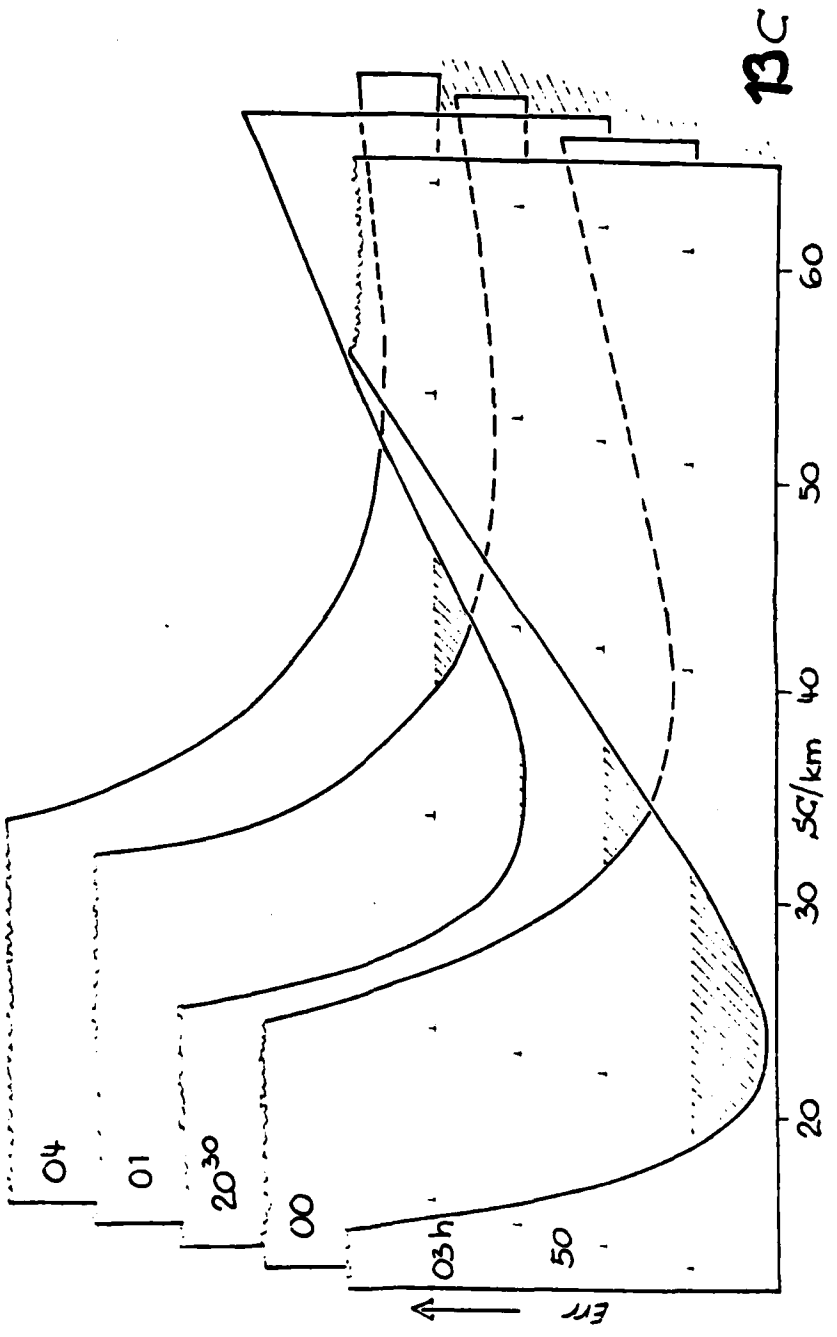
13C
60
50
40
30
20
SC/km
03h
50
00
20^30
01
04
Err

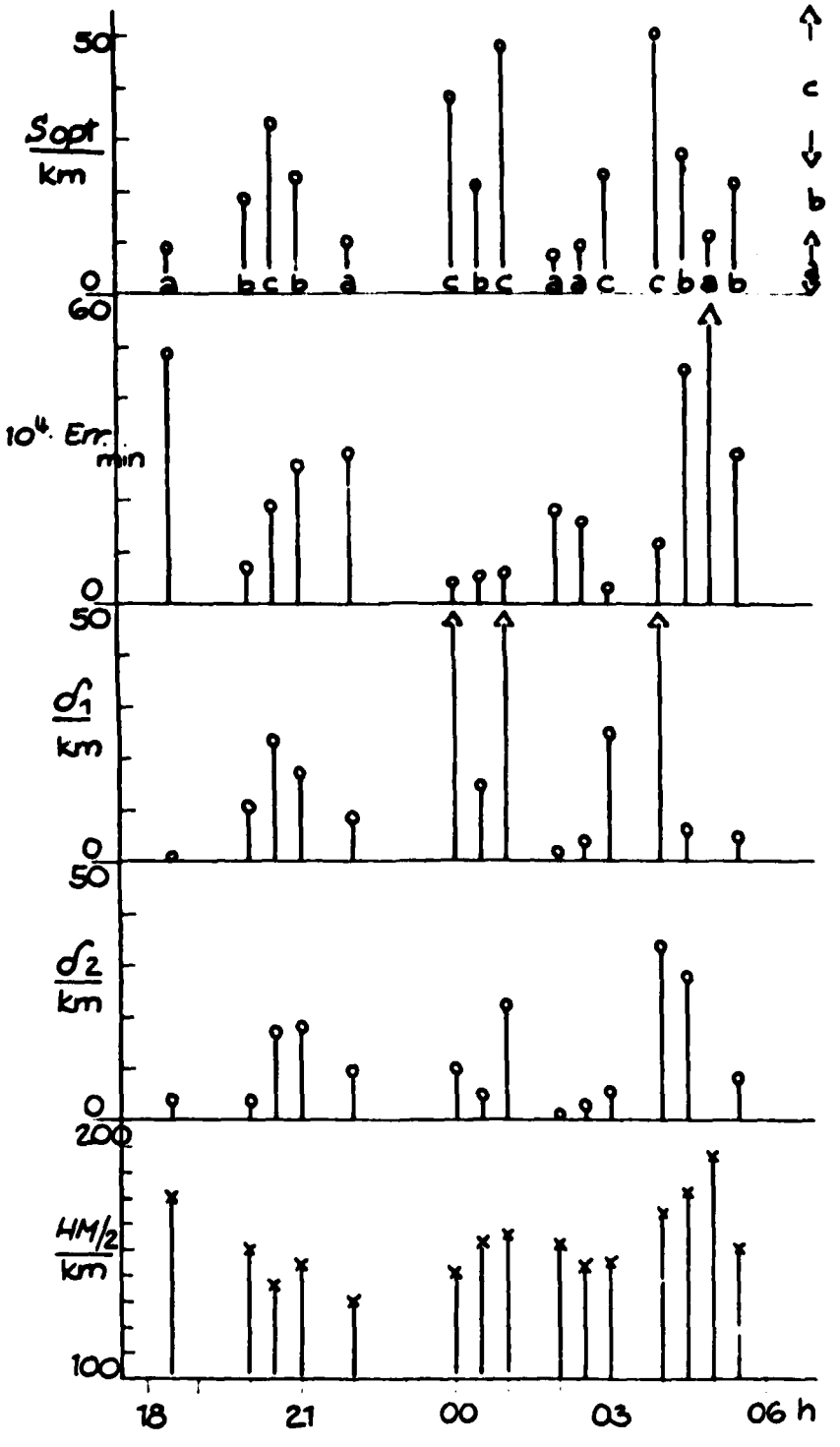
50
Sopt
km
0
a
b c b
a
c b c
a a
c
c
b a
b
c
b
a
60
10⁴. Err.
min
0
50
σ1
km
0
50
σ2
km
0
200
HM/2
km
100
18
21
00
03
06 h

14

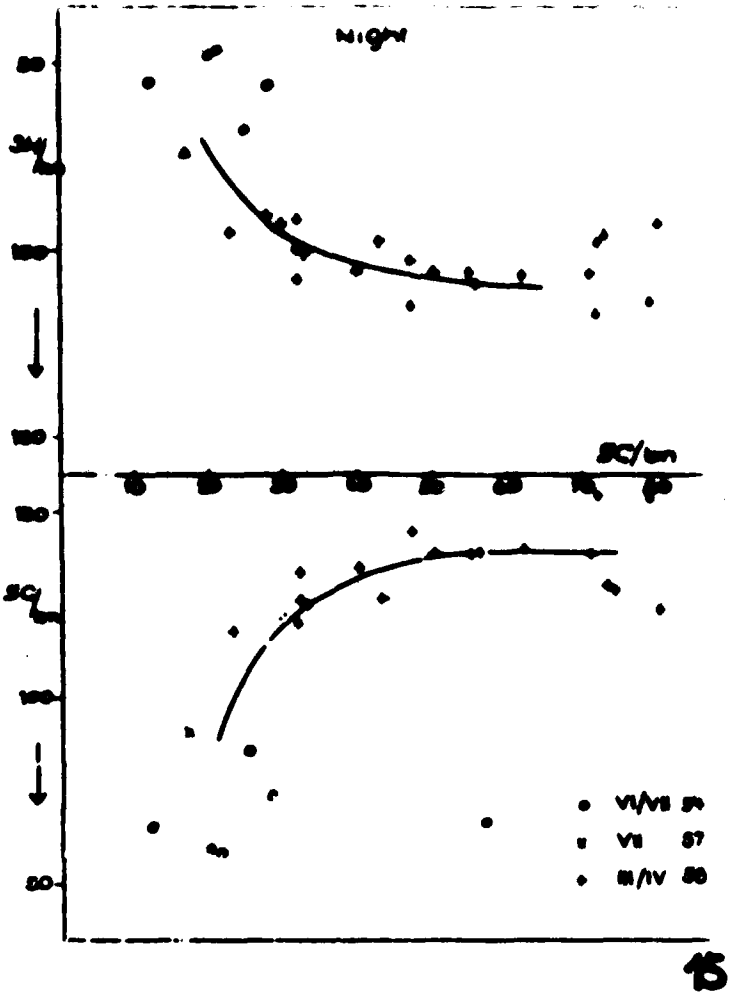
Night
SC/km
VI/VII
VII
III/IV

15

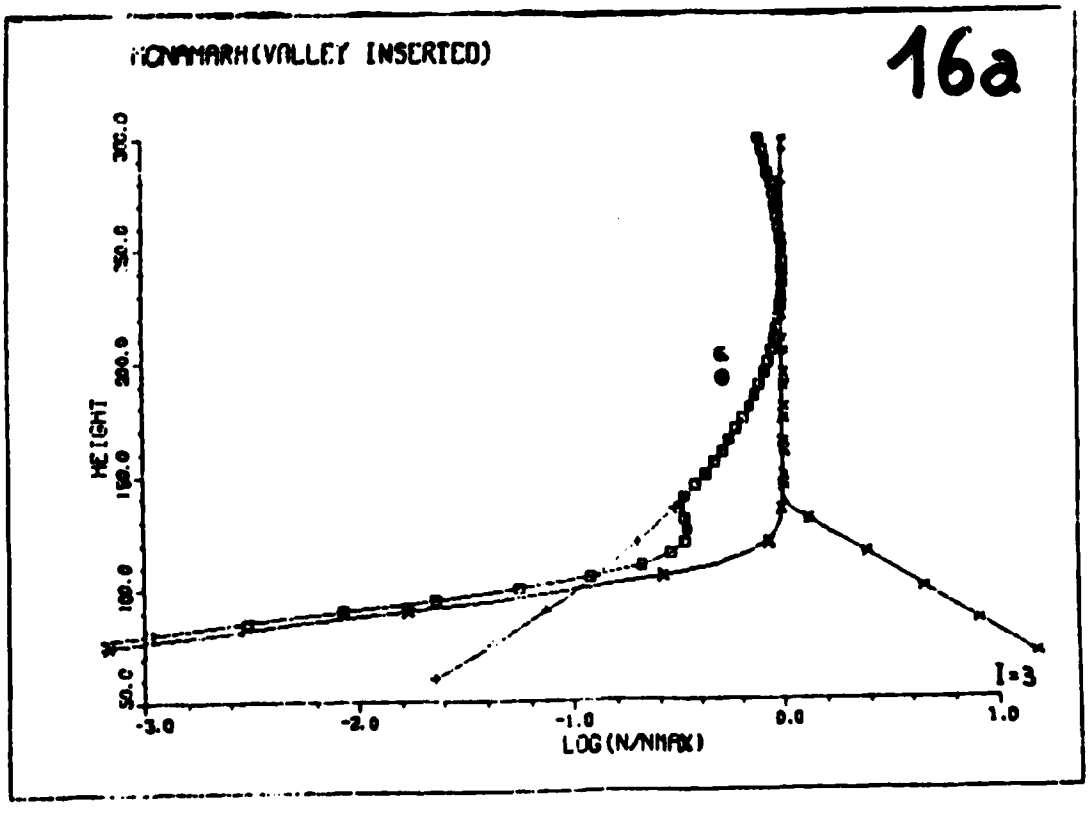
IONMARH(VALLEY INSERTED)
16a
HEIGHT
300.0
250.0
200.0
150.0
100.0
50.0
I=3
-3.0
-2.0
-1.0
0.0
1.0
LOG(N/NMAX)

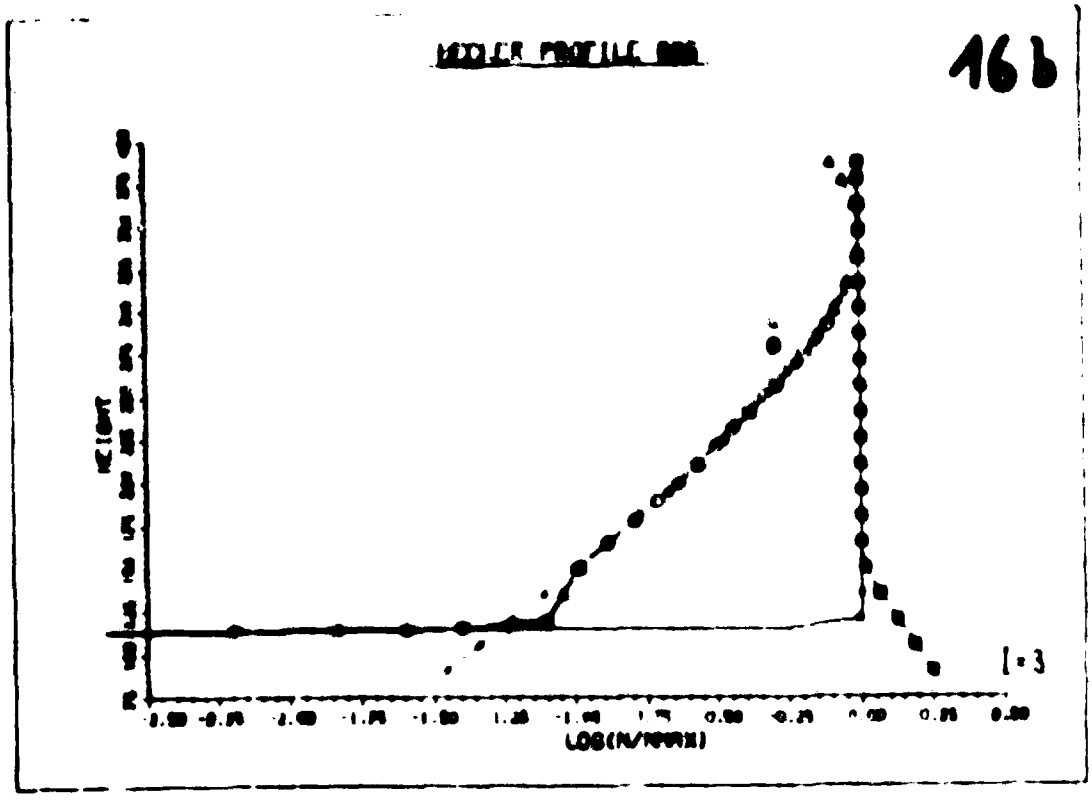
16b
HEIGHT
I=3
LOG(N/NMAX)

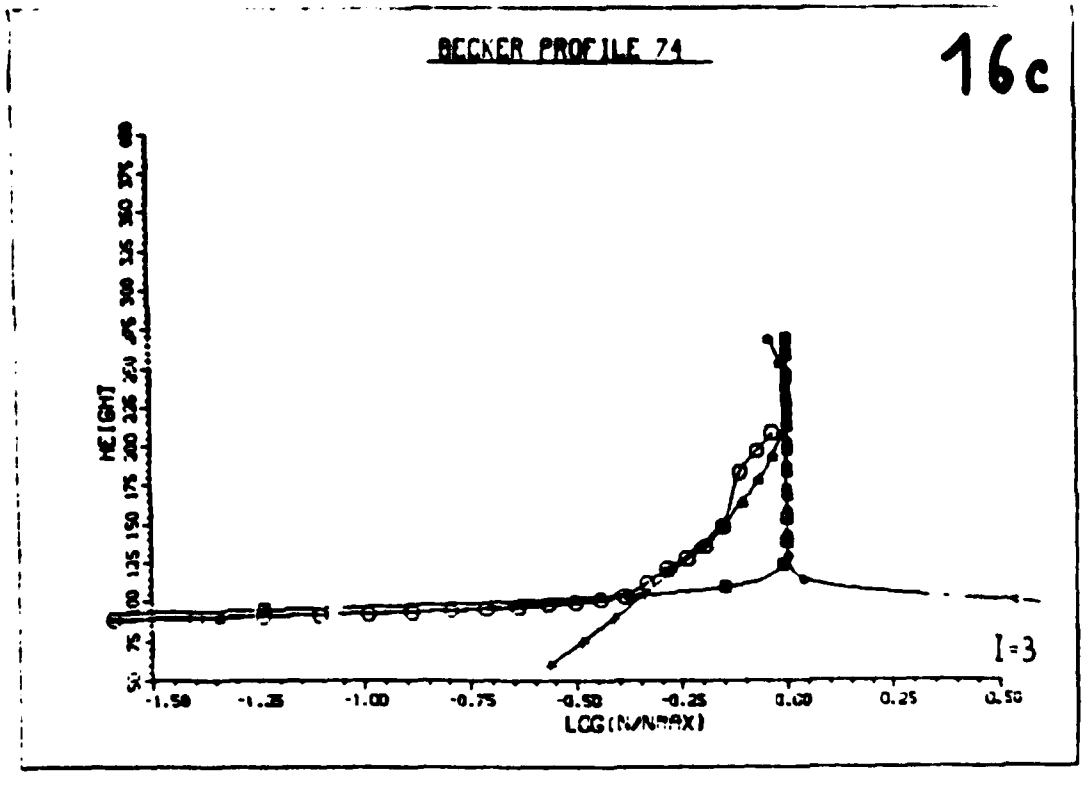
BECKER PROFILE 74
16c
HEIGHT
I=3
-1.50
-1.25
-1.00
-0.75
-0.50
-0.25
0.00
0.25
0.50
LOG(N/NMAX)

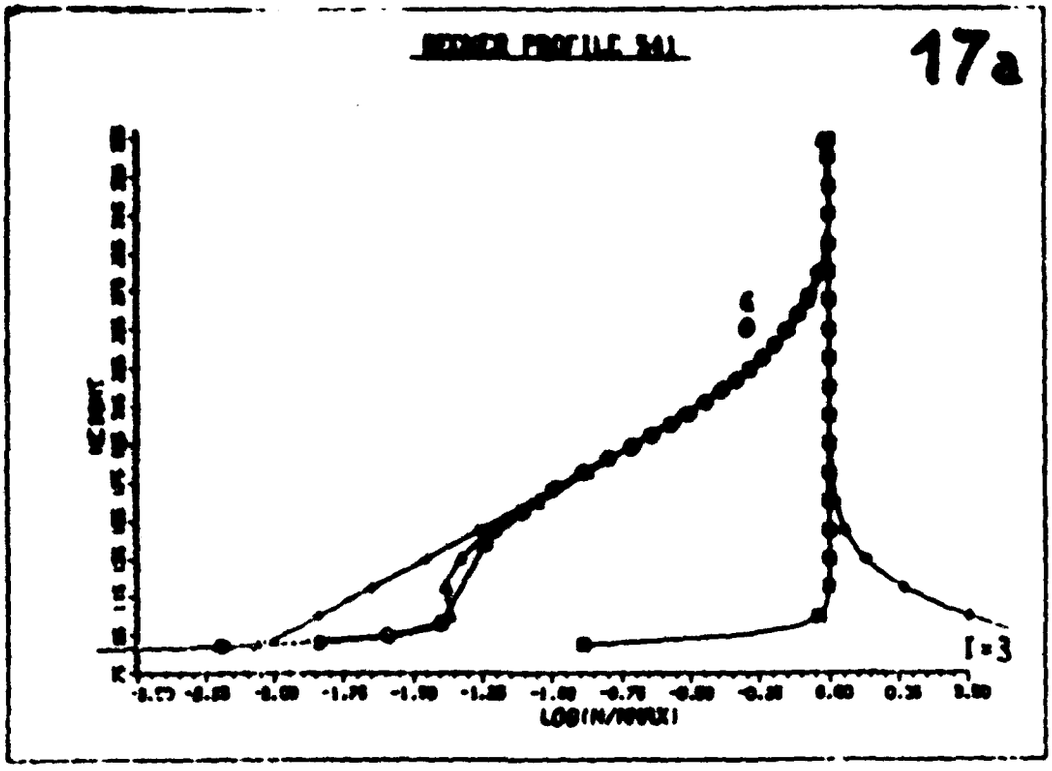
17a
I=3
LOG(N/NMAX)

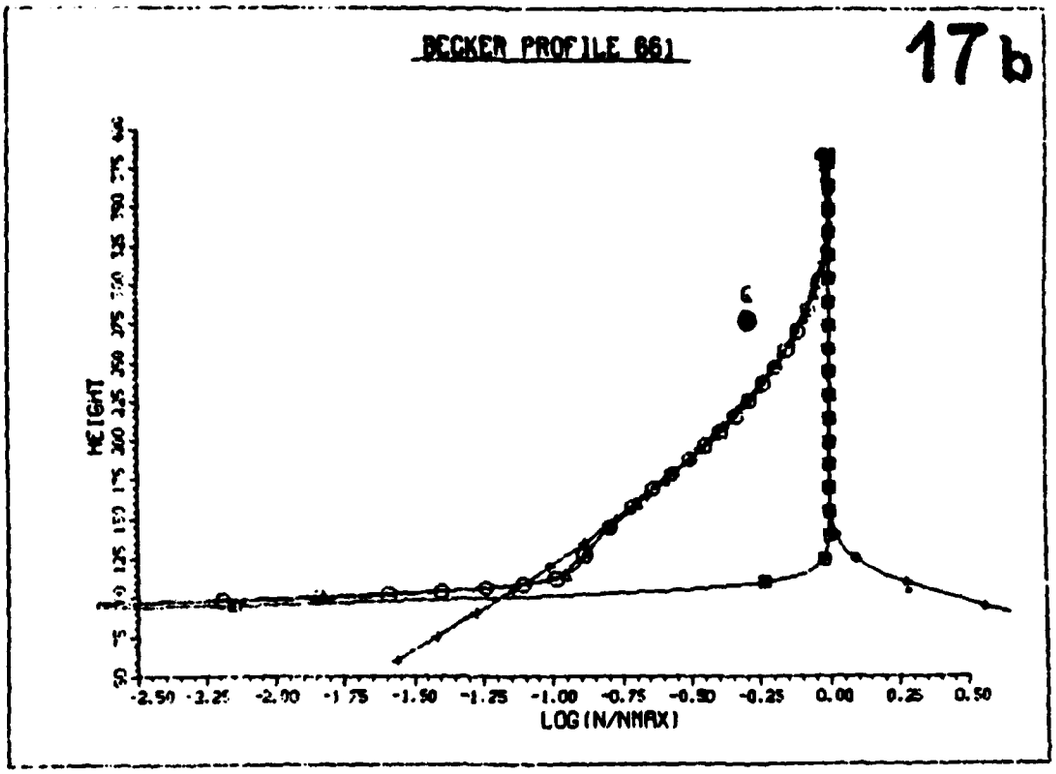
BECKER PROFILE 861
17b
HEIGHT
-2.50 -2.25 -2.00 -1.75 -1.50 -1.25 -1.00 -0.75 -0.50 -0.25 0.00 0.25 0.50
LOG(N/NMAX)

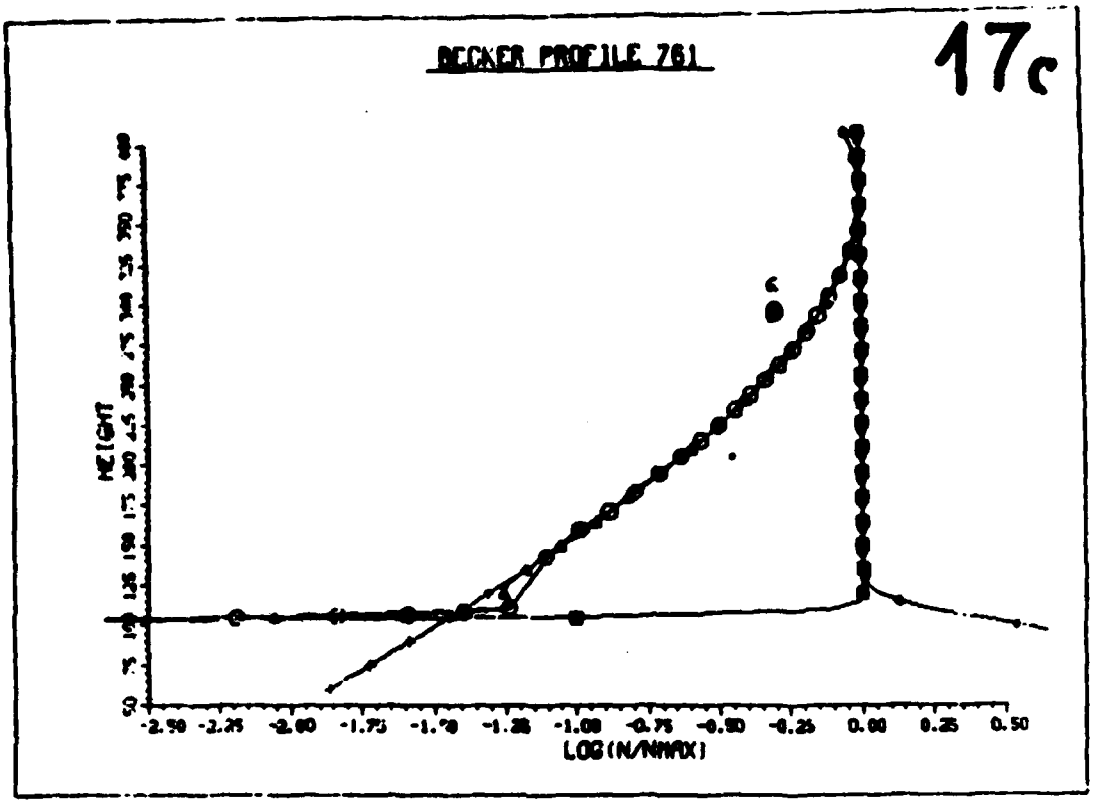
BECKER PROFILE 761
17c
HEIGHT
LOG(N/NMAX)

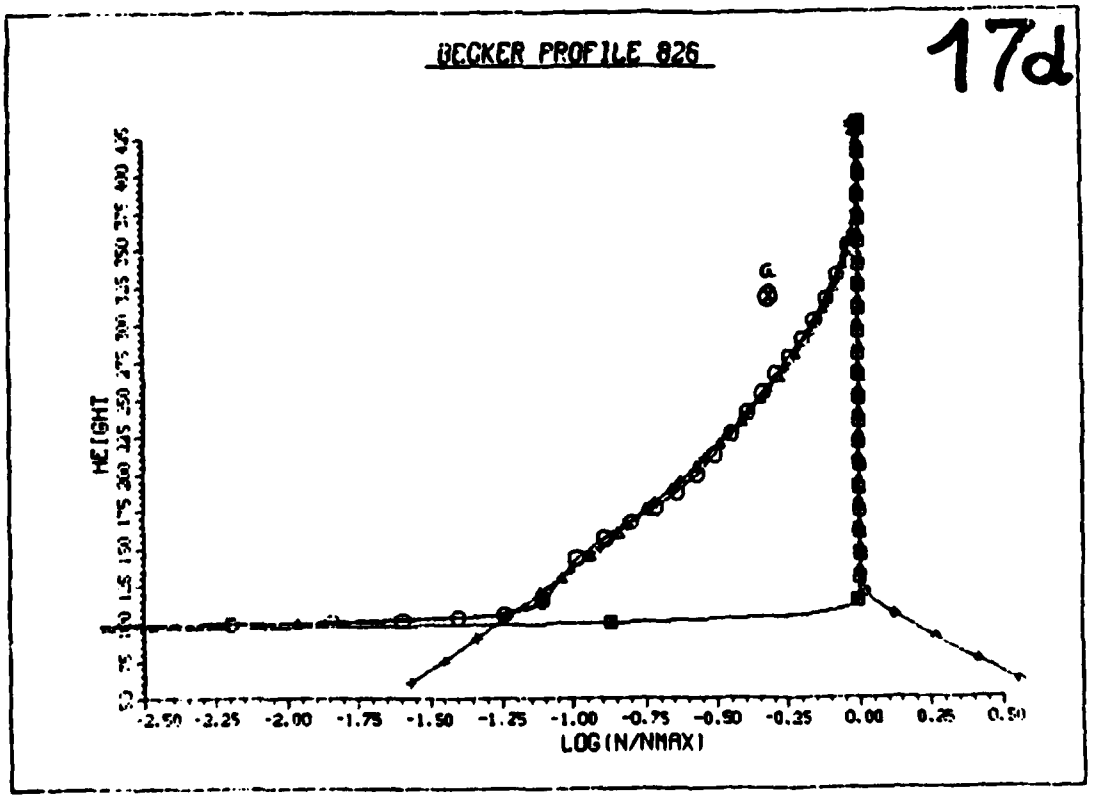
BECKER PROFILE 826
17d
HEIGHT
-2.50 -2.25 -2.00 -1.75 -1.50 -1.25 -1.00 -0.75 -0.50 -0.25 0.00 0.25 0.50
LOG(N/NMAX)

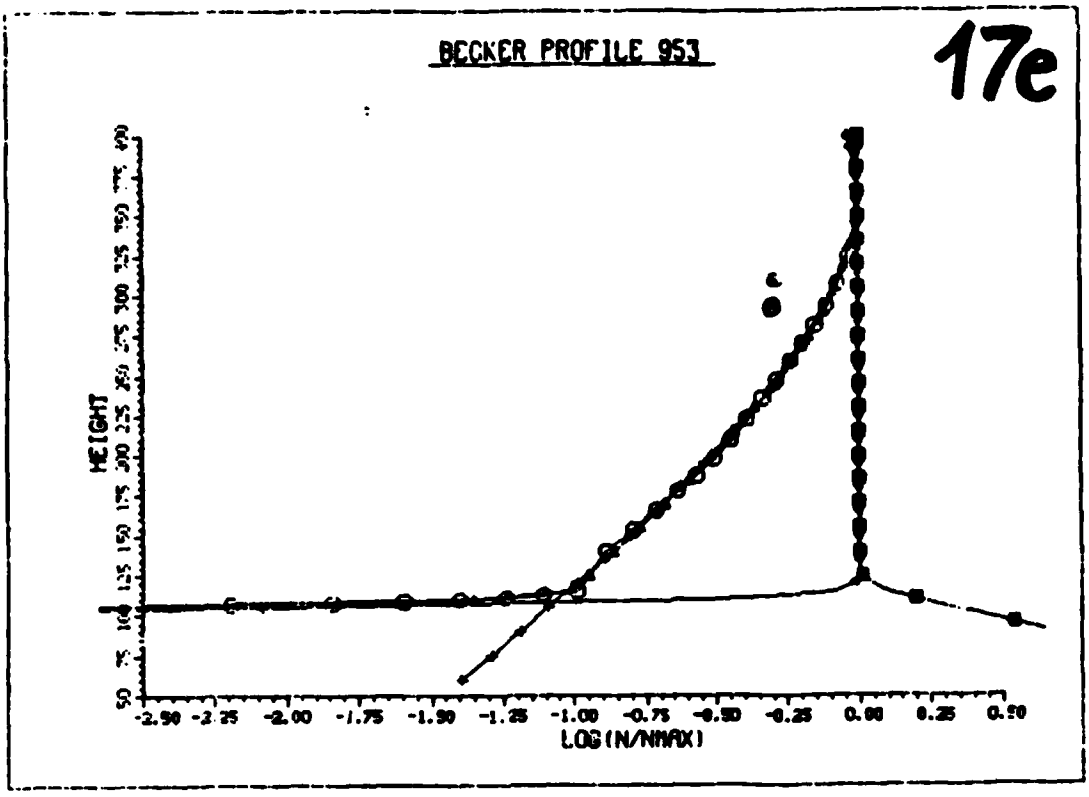
BECKER PROFILE 953
17e
HEIGHT
LOG(N/NMAX)

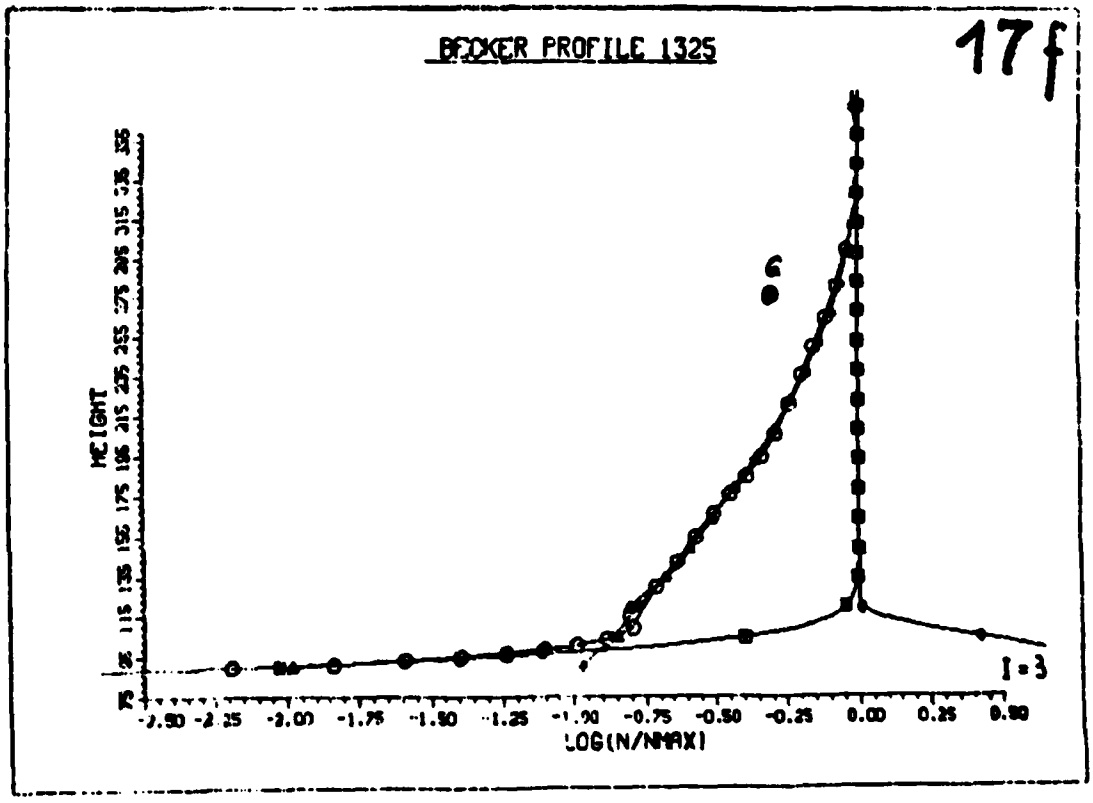
BECKER PROFILE 1325
17f
HEIGHT
LOG(N/NMAX)
I=3

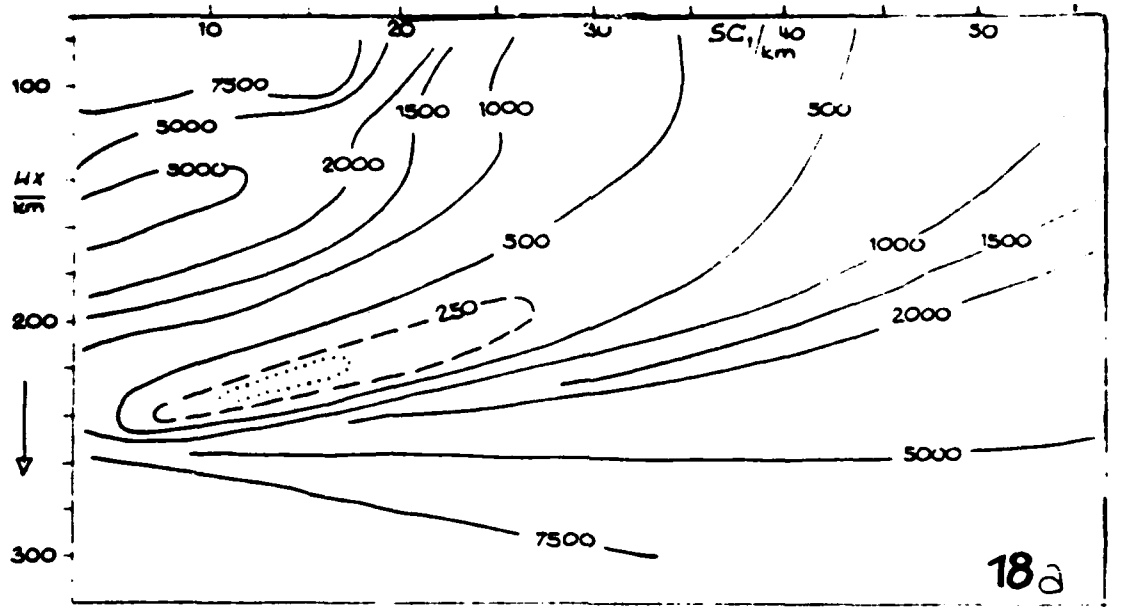
10
20
30
40
50
SC₁/km
100
200
300
Hx/km
7500
5000
3000
2000
1500
1000
500
250
18a

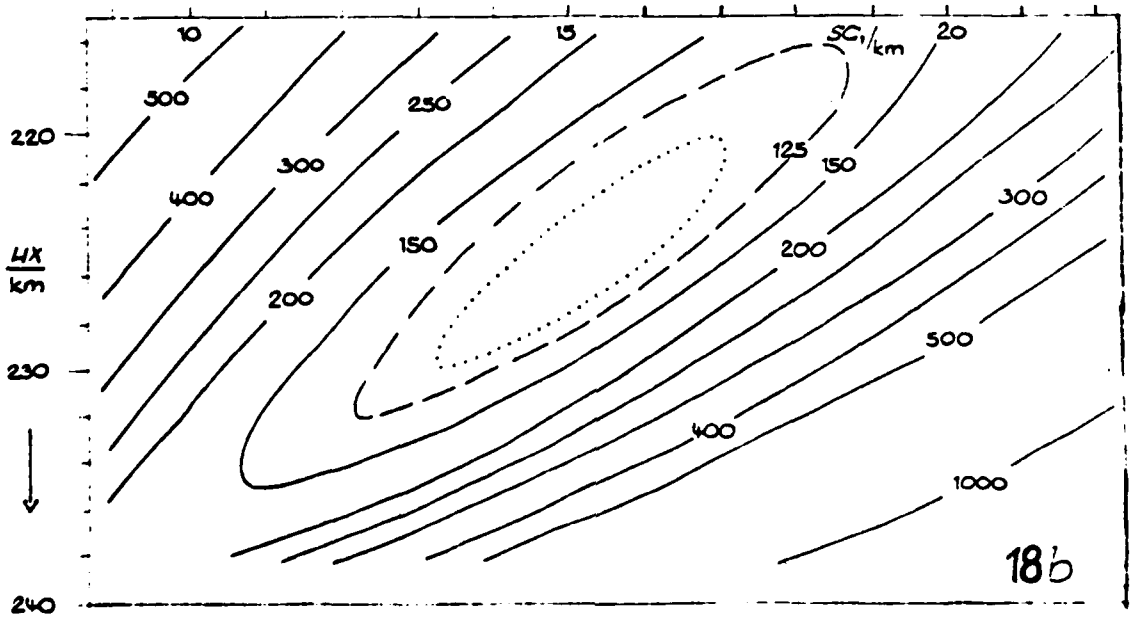
10
15
20
SC₁/km
220
230
240
Hx/km
500
400
300
250
200
150
125
1000
18b

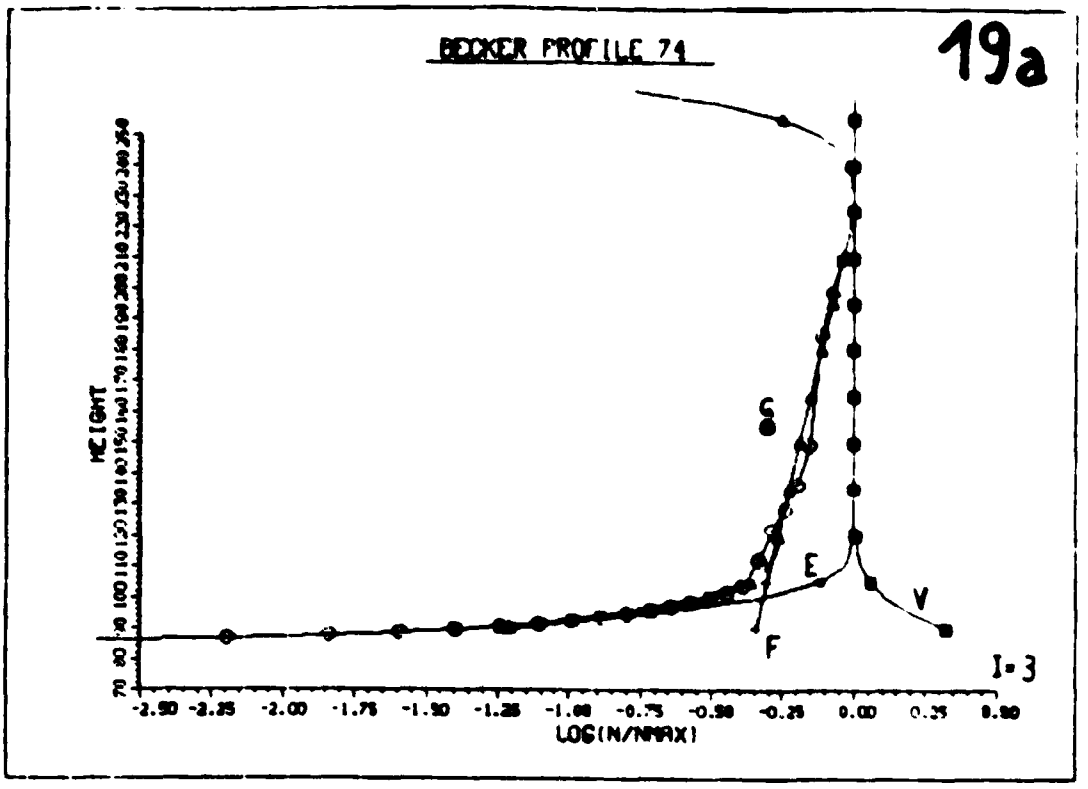
BECKER PROFILE 74
19a
HEIGHT
S
E
V
F
I=3
LOG(N/NMAX)

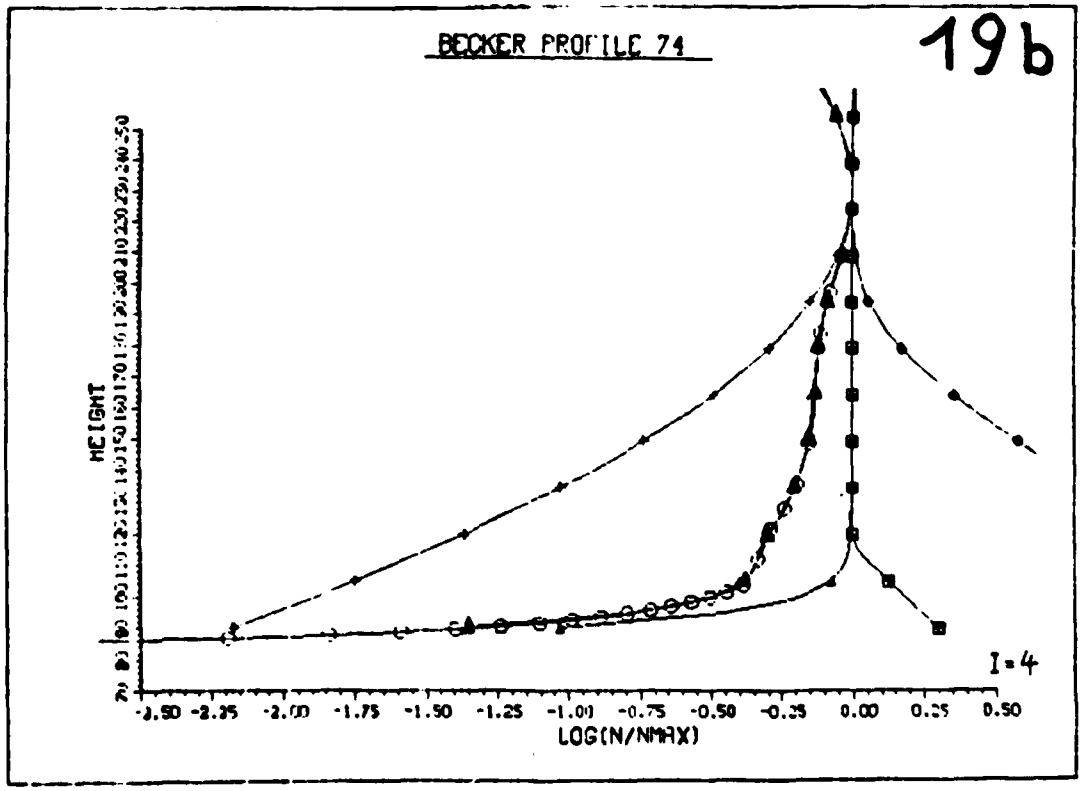
BECKER PROFILE 74
19b
HEIGHT
I=4
LOG(N/NMAX)

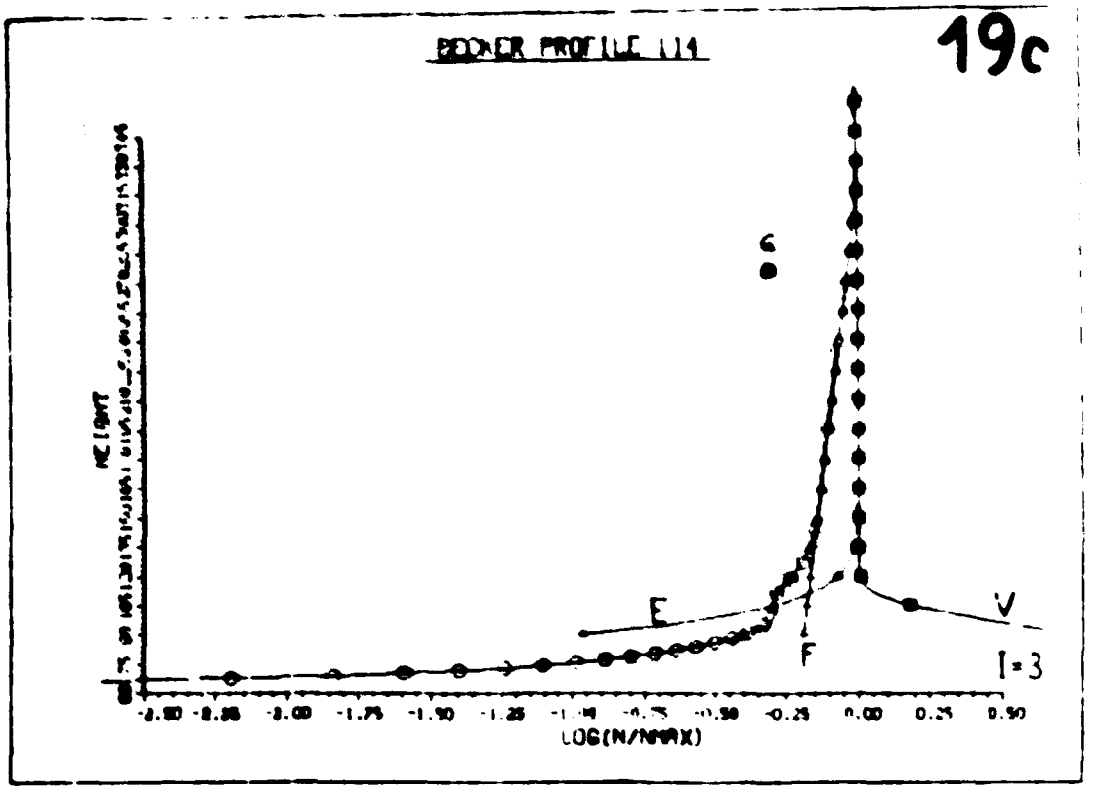
BECKER PROFILE 114
19c
WEIGHT
E
F
V
I = 3
LOG(N/NMAX)

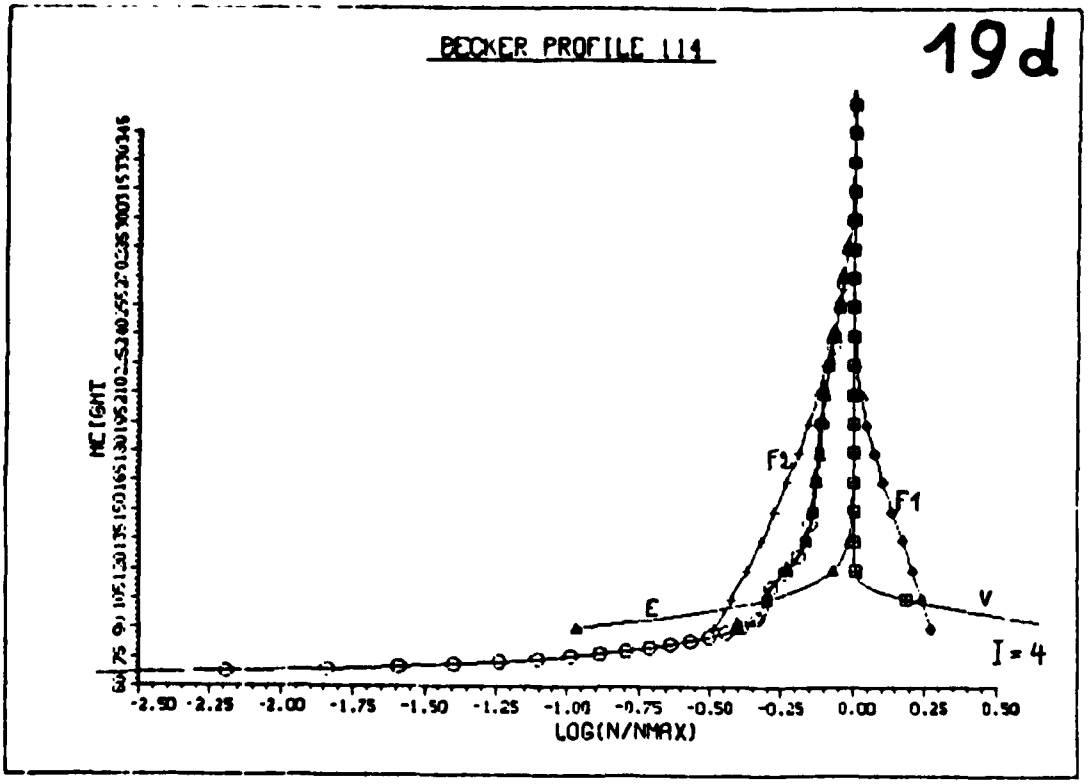
BECKER PROFILE 114
19d
WEIGHT
F2
F1
E
V
I = 4
-2.50 -2.25 -2.00 -1.75 -1.50 -1.25 -1.00 -0.75 -0.50 -0.25 0.00 0.25 0.50
LOG(N/NMAX)

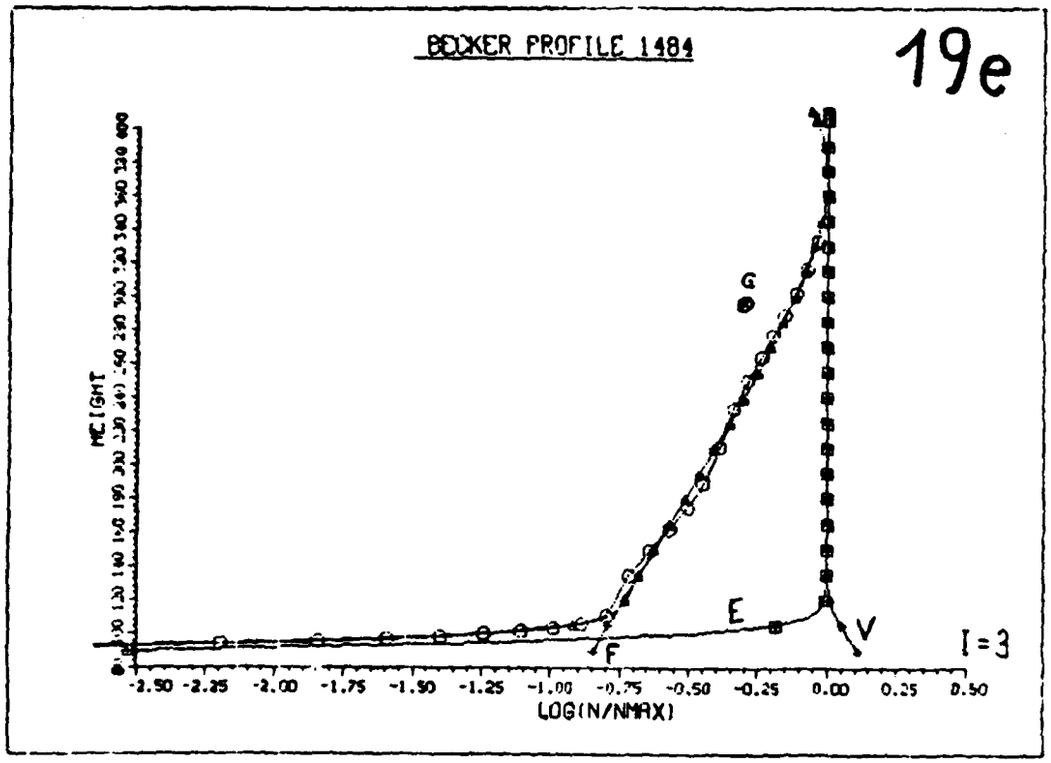
BECKER PROFILE 1484
19e
G
E
V
F
I=3
LOG(N/NMAX)

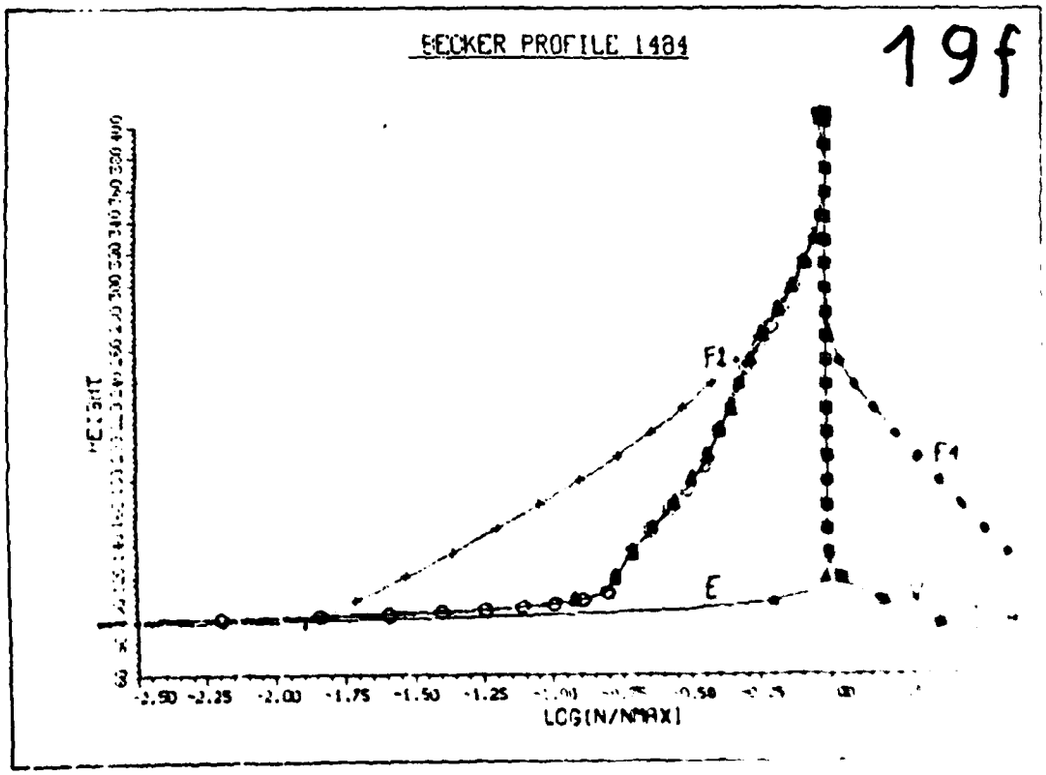
BECKER PROFILE 1484
19f
F1
F1
E
LOG(N/NMAX)

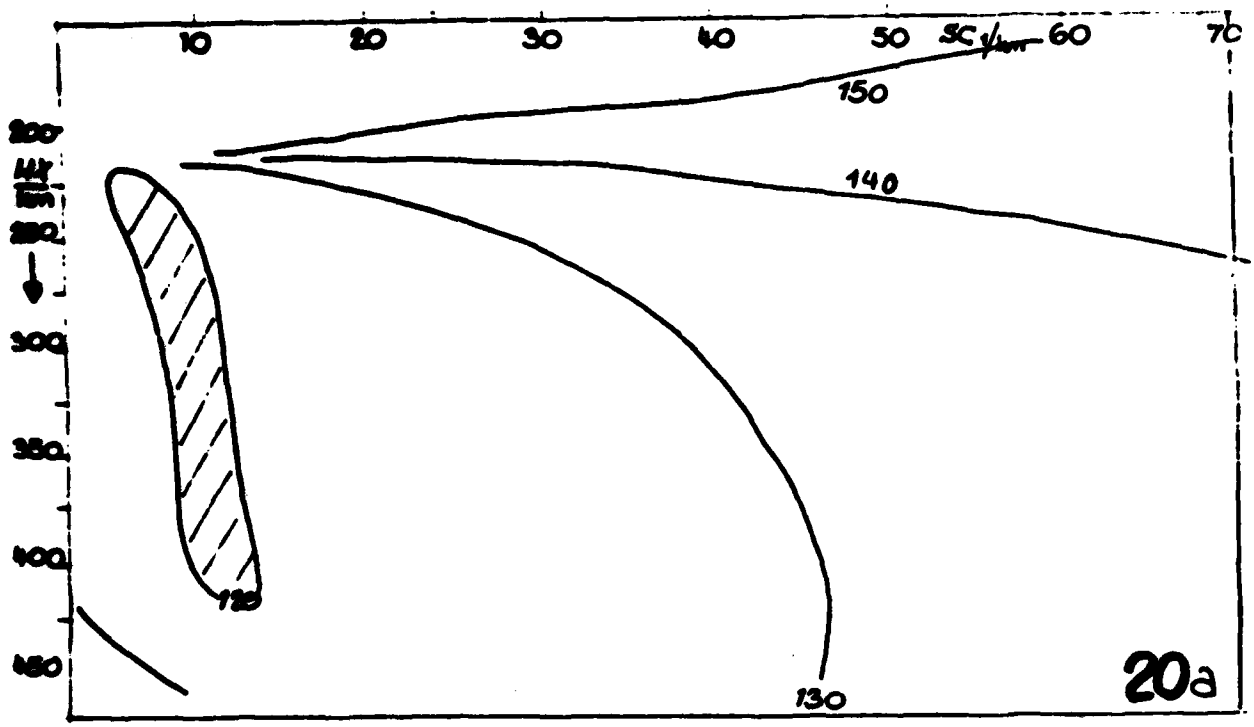
10
20
30
40
50
SC/km
60
70
150
140
130
Alt km
200
250
300
350
400
450
20a

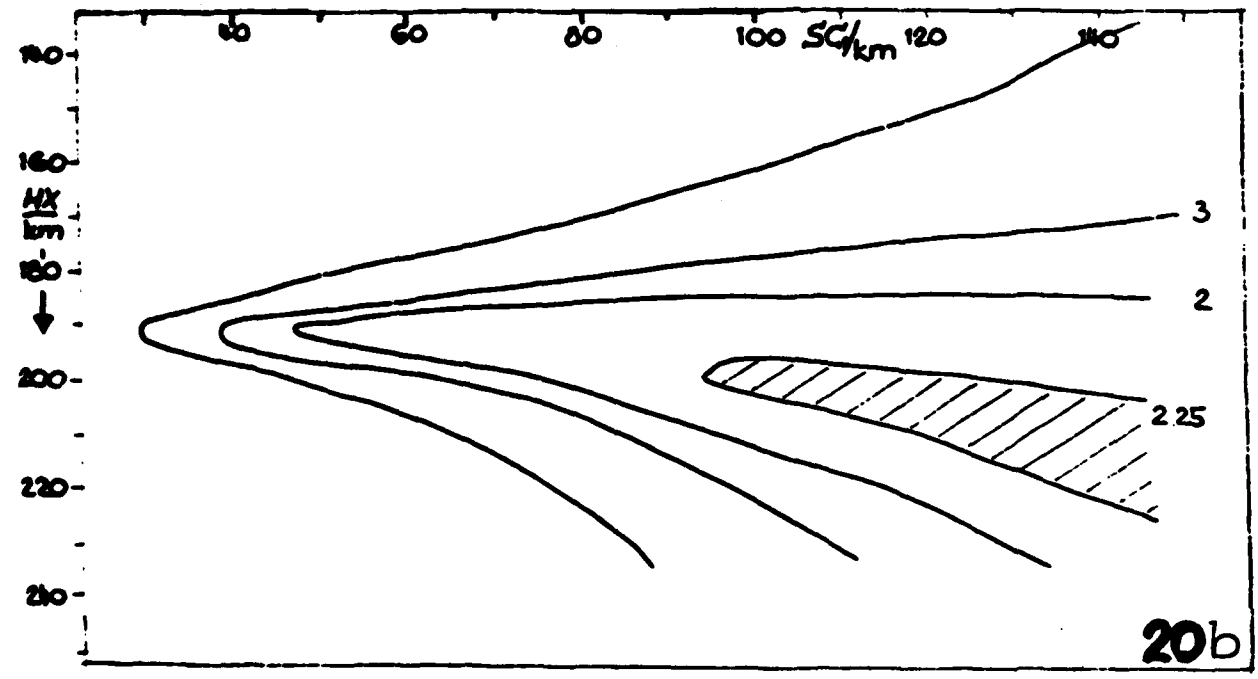
40
60
80
100
SC/km
120
140
160
Alt km
180
200
220
240
3
2
2.25
20b

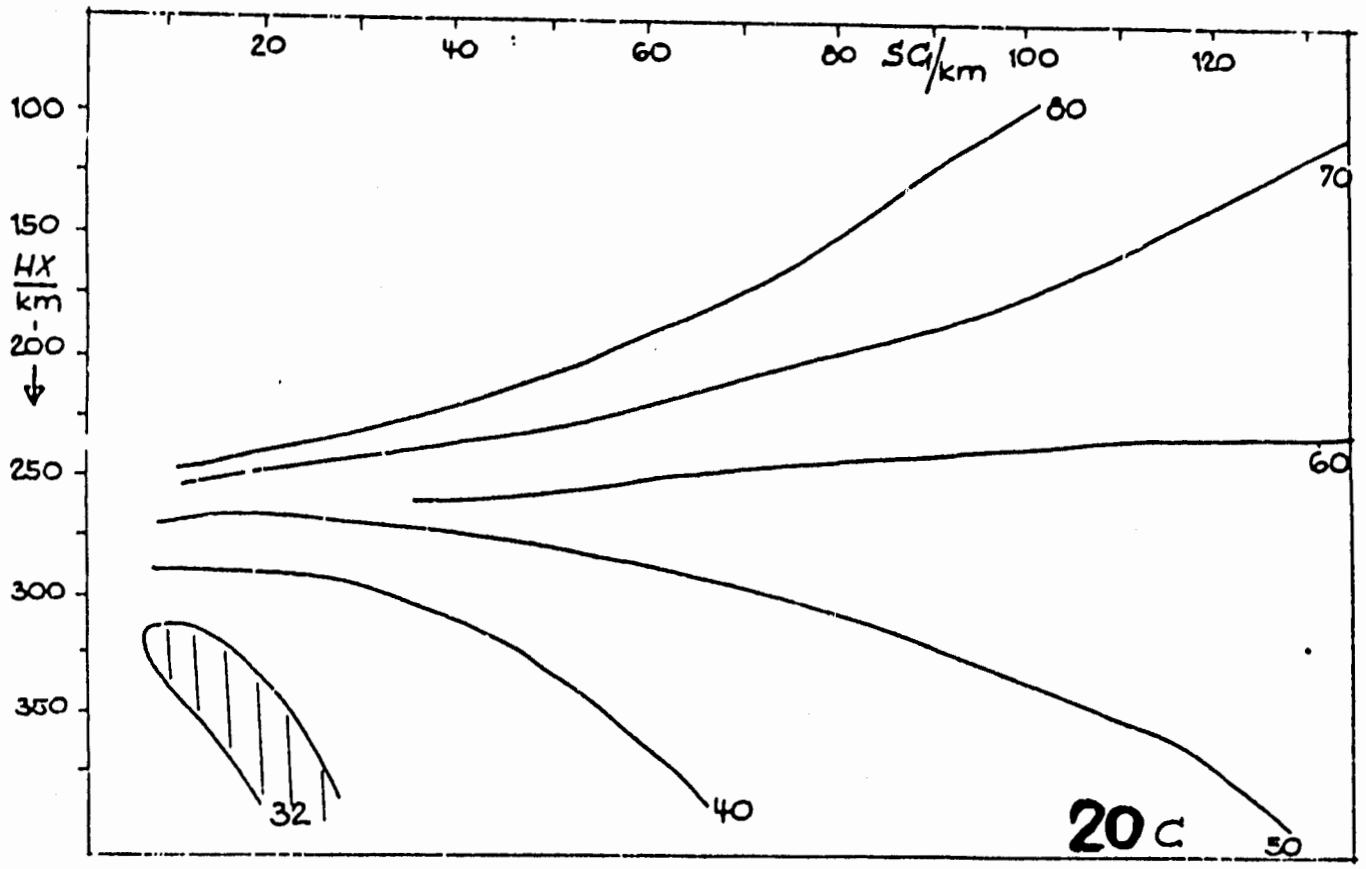
20
40
60
80 SC/km
100
120
100
150
HX
km
200
250
300
350
80
70
60
50
40
32
20 c

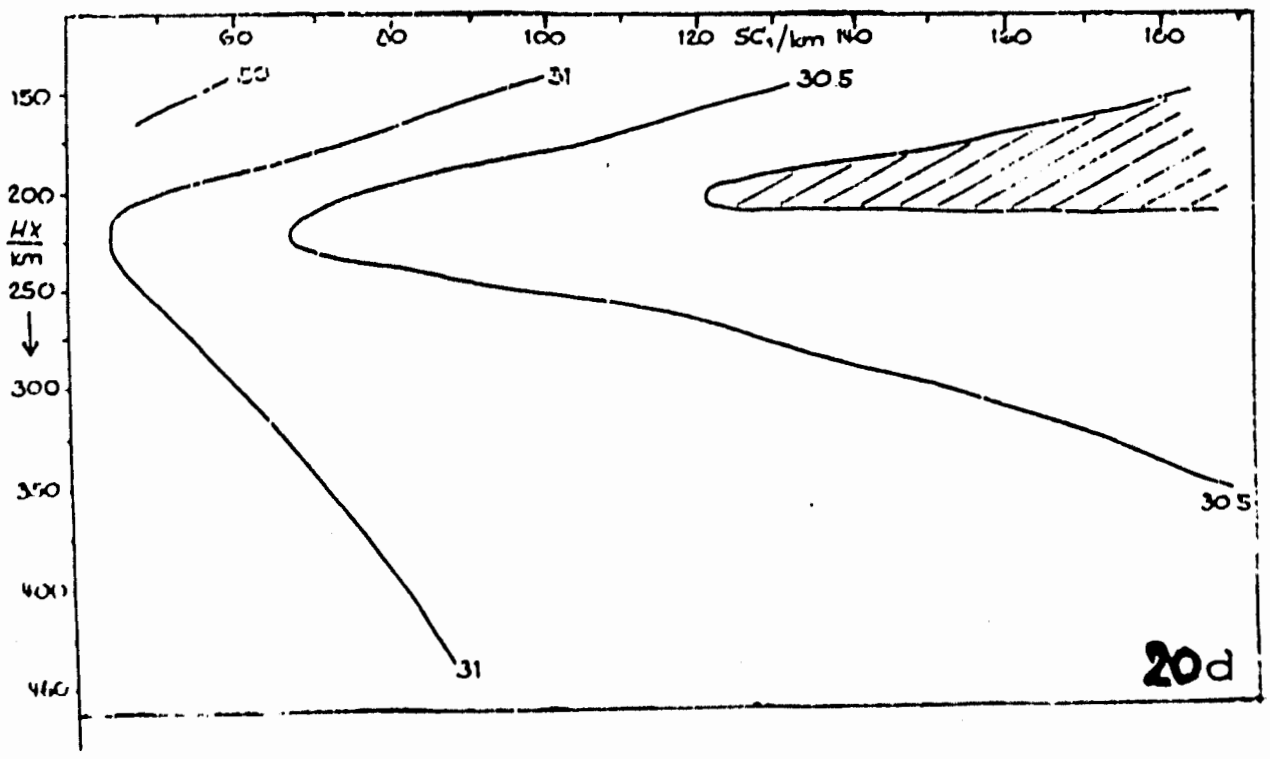
60
80
100
120 SC1/km
140
160
180
150
200
HX
km
250
300
350
400
460
31
31
30.5
30.5
20d

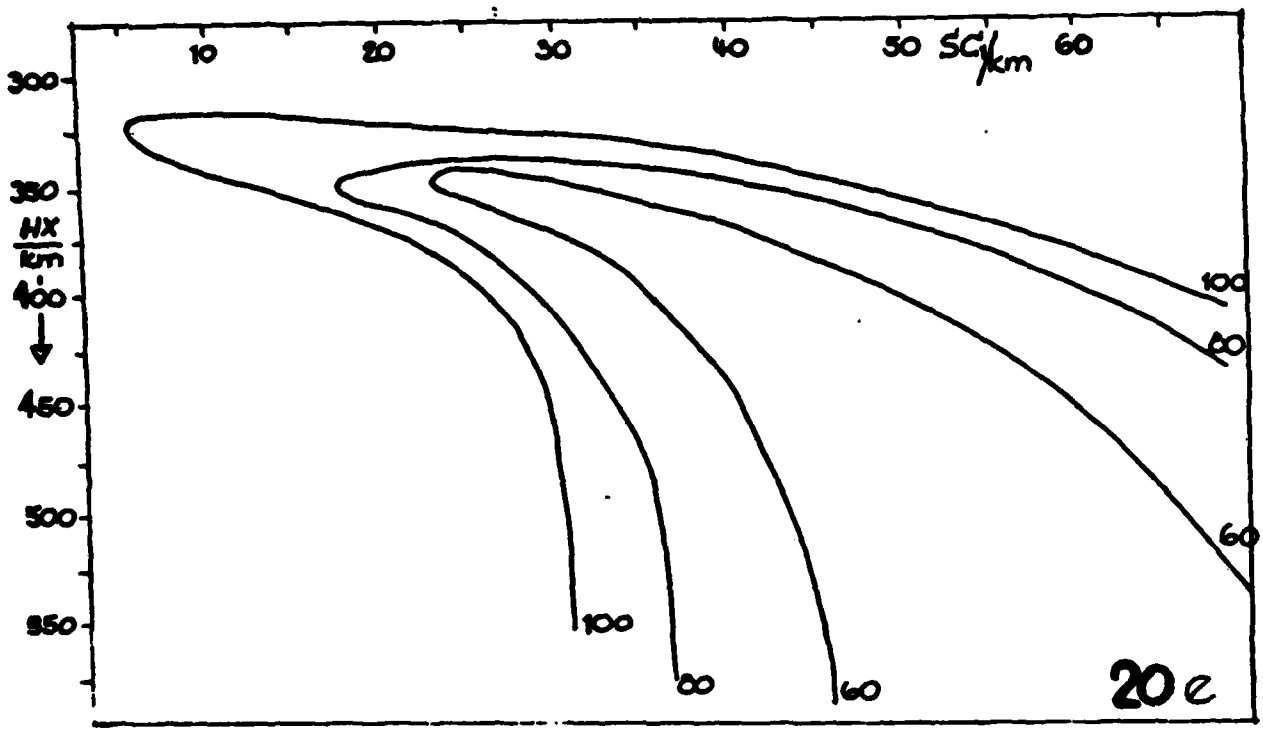
10
20
30
40
50 SC/km
60
300
350
HX/km
400
450
500
550
100
80
60
100
80
60
20e

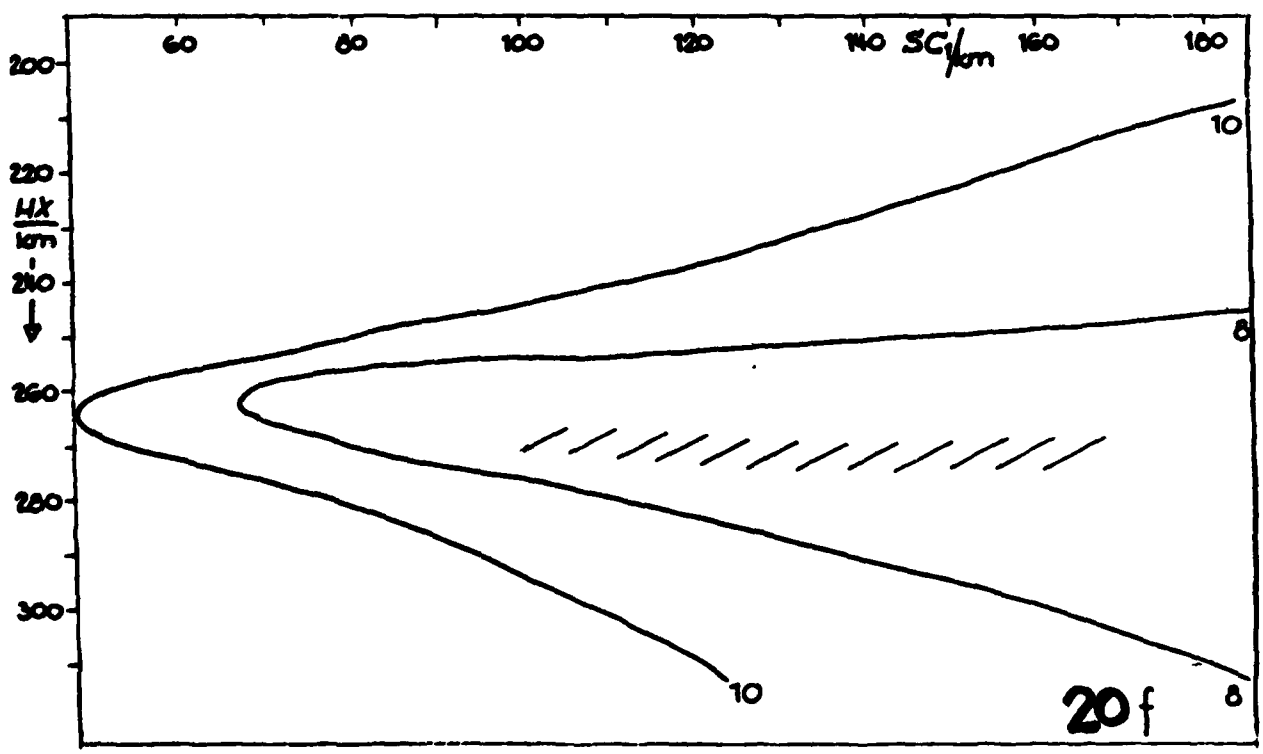
60
80
100
120
140 SC/km
160
180
200
220
HX/km
240
260
280
300
10
8
10
8
20f

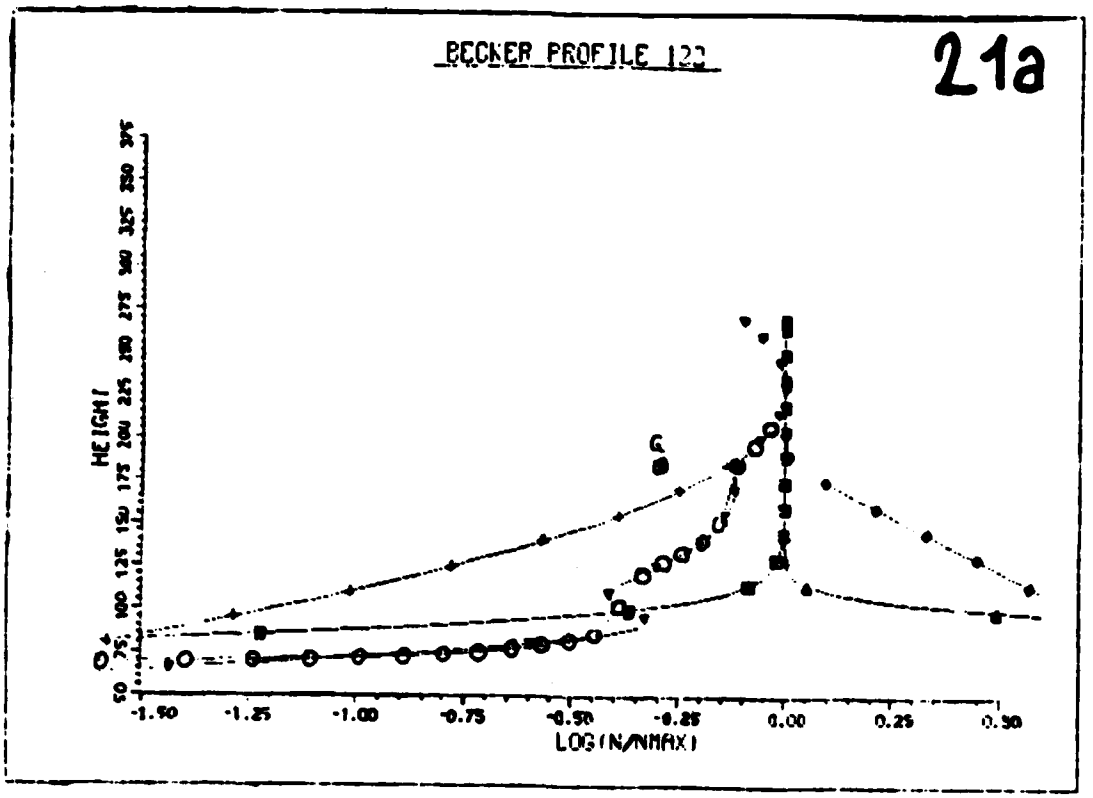
BECKER PROFILE 122
21a
HEIGHT
LOG(N/NMAX)

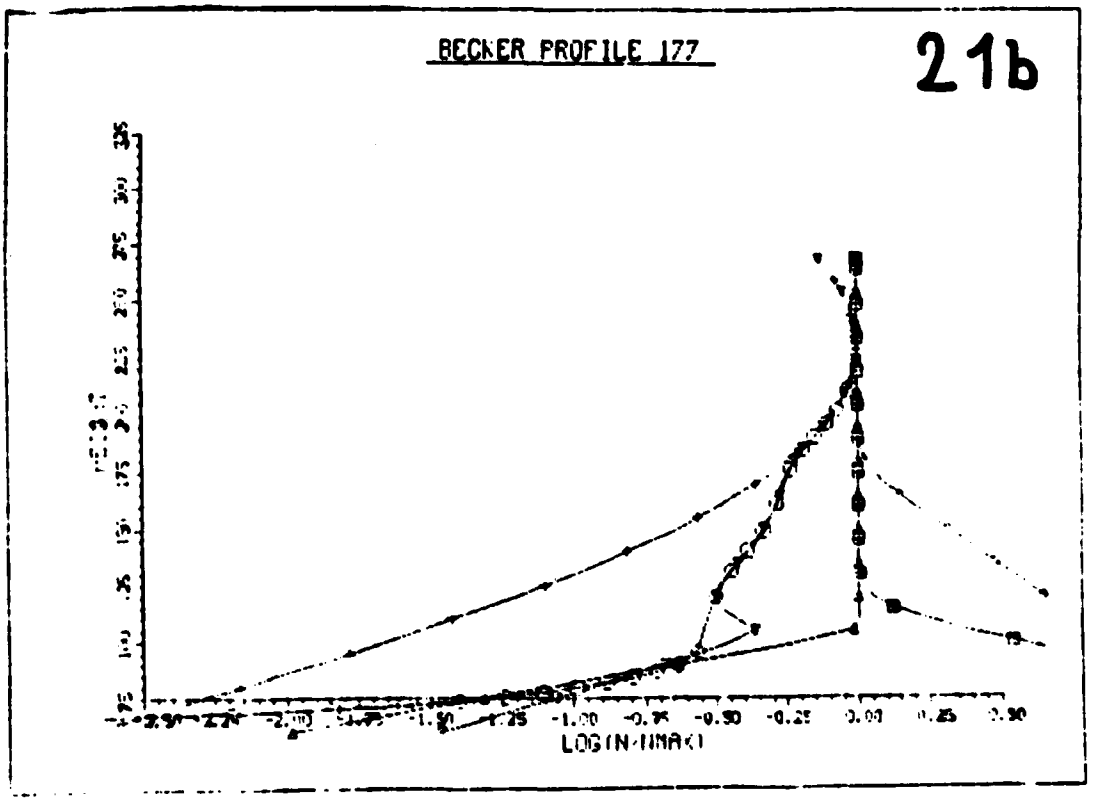
BECKER PROFILE 177
21b
LOG(N/NMAX)

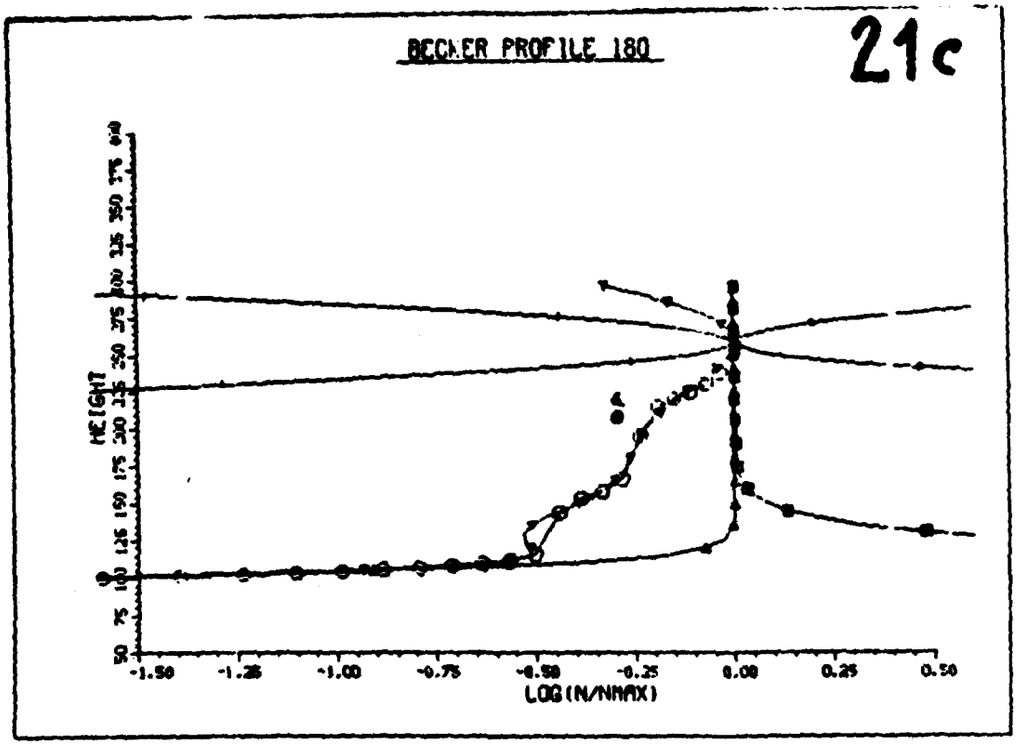
BECKER PROFILE 180
21c
HEIGHT
LOG(N/NMAX)

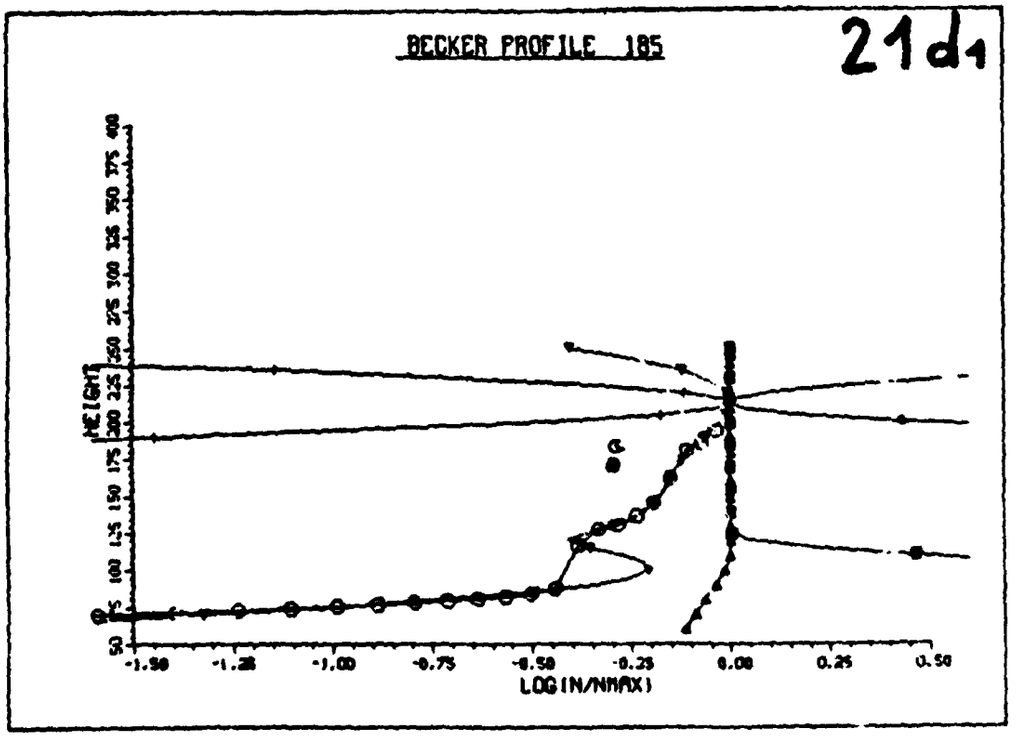
BECKER PROFILE 185
21d1
HEIGHT
LOG(N/NMAX)

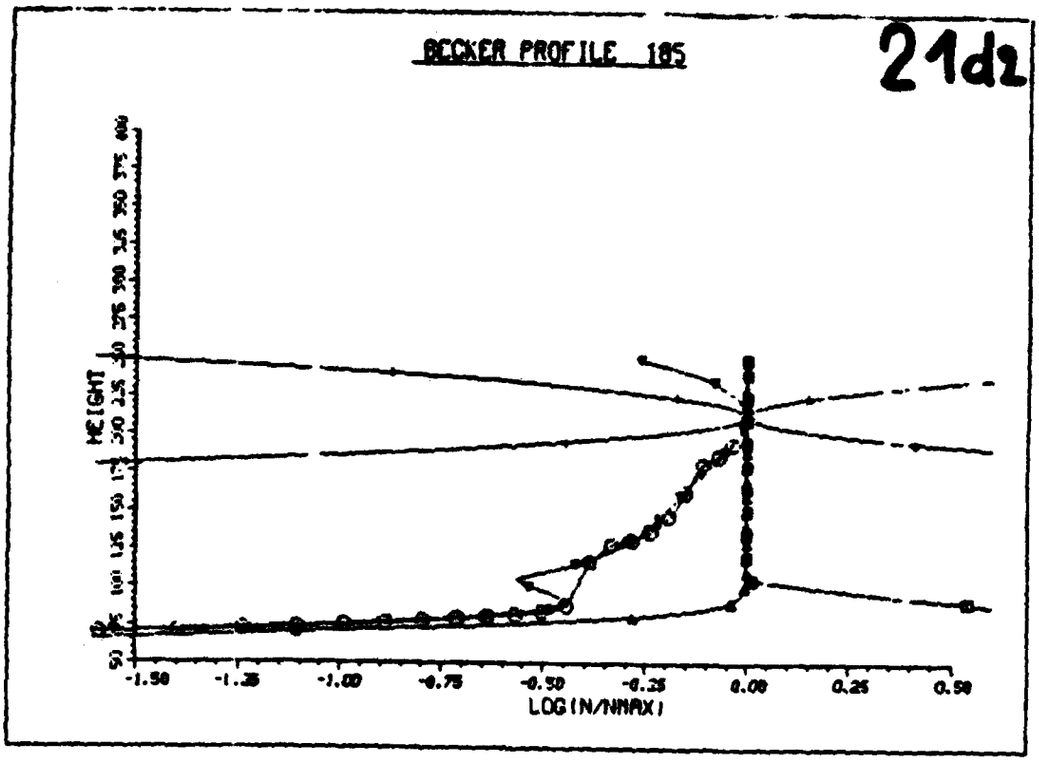
BECKER PROFILE 185
21d2
HEIGHT
LOG(N/NMAX)

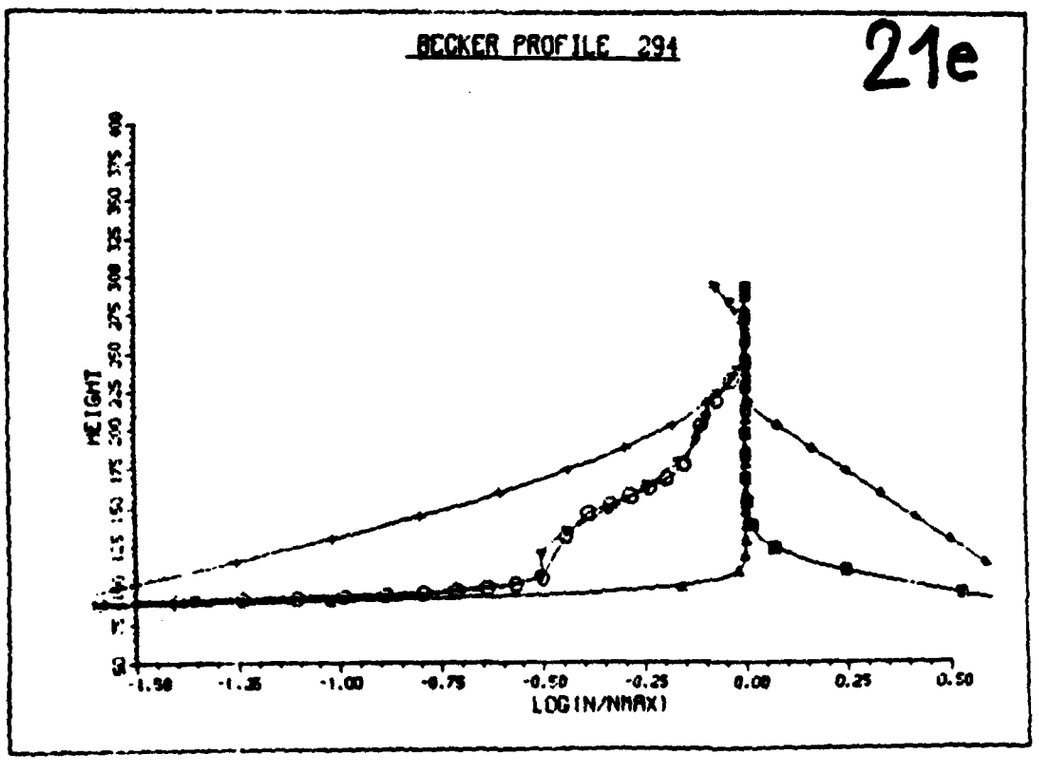
BECKER PROFILE 294
21e
HEIGHT
LOG(N/NMAX)

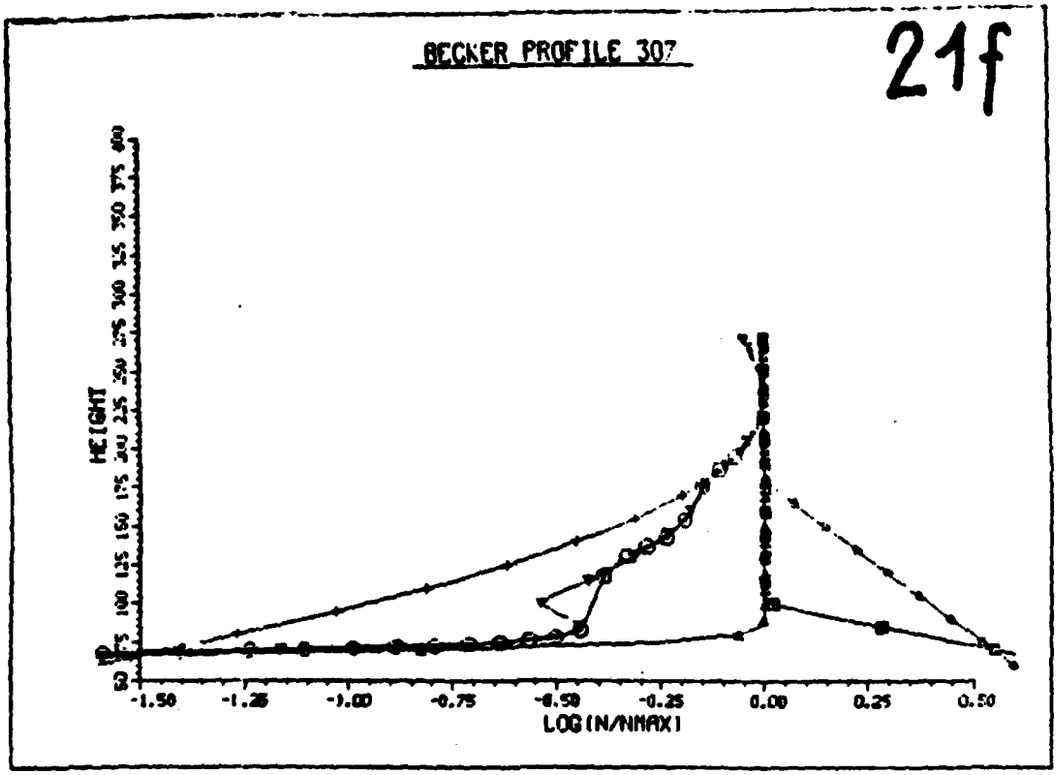
BECKER PROFILE 307
21f
HEIGHT
LOG(N/NMAX)

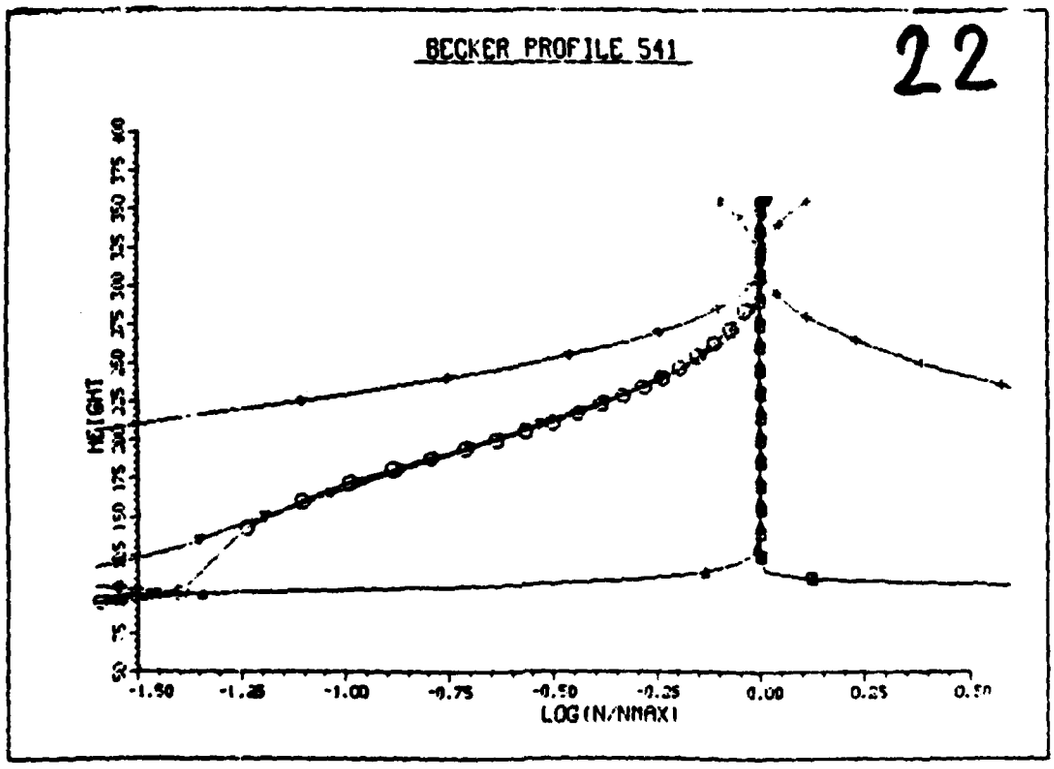
BECKER PROFILE 541
22
HEIGHT
LOG(N/NMAX)

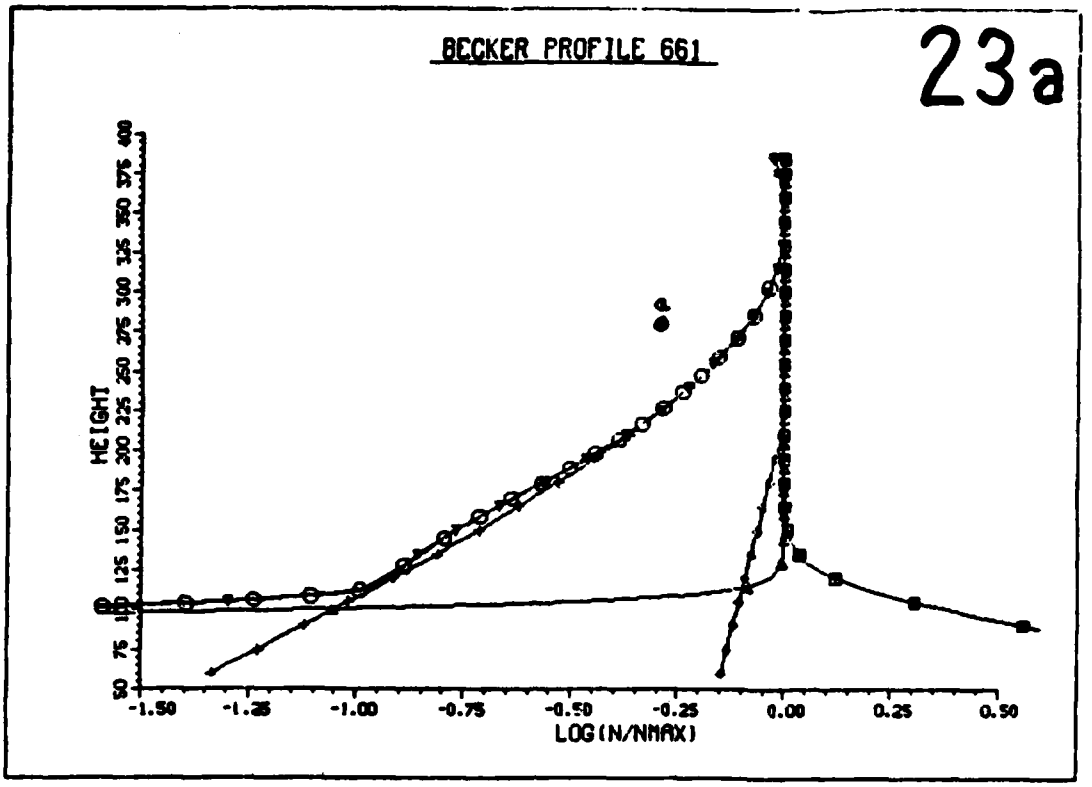
BECKER PROFILE 661
23a
HEIGHT
LOG(N/NMAX)

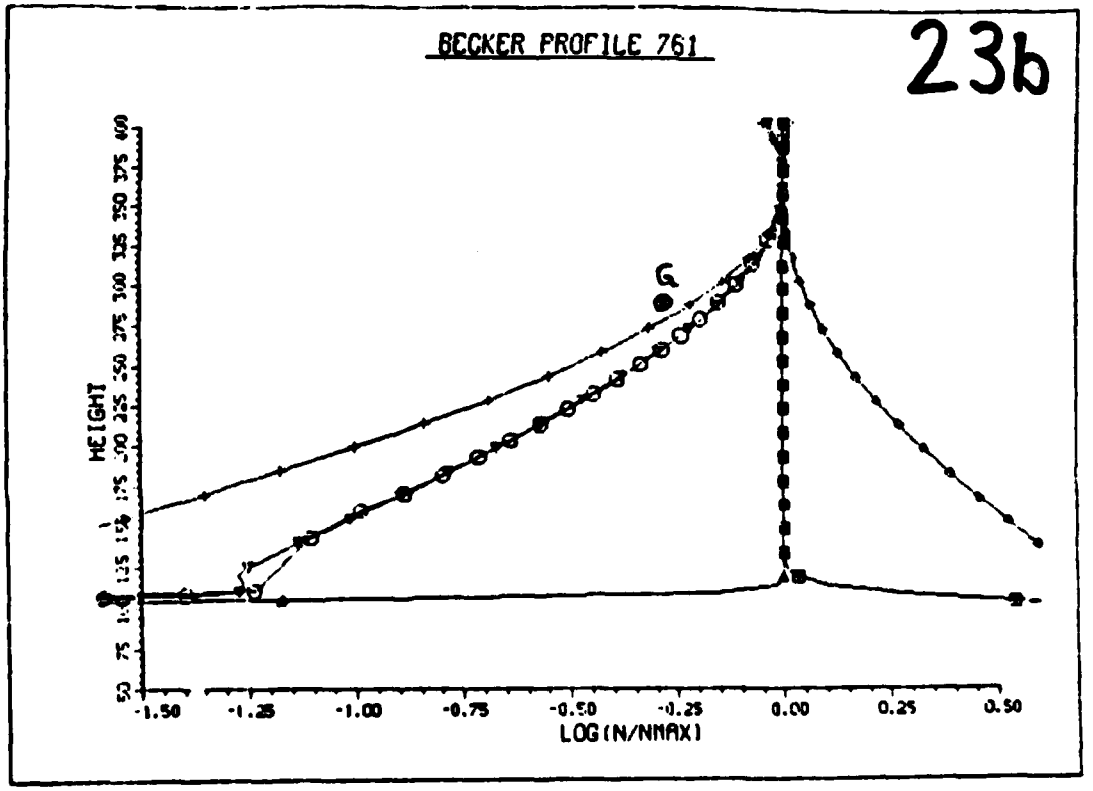
BECKER PROFILE 761
23b
HEIGHT
LOG(N/NMAX)

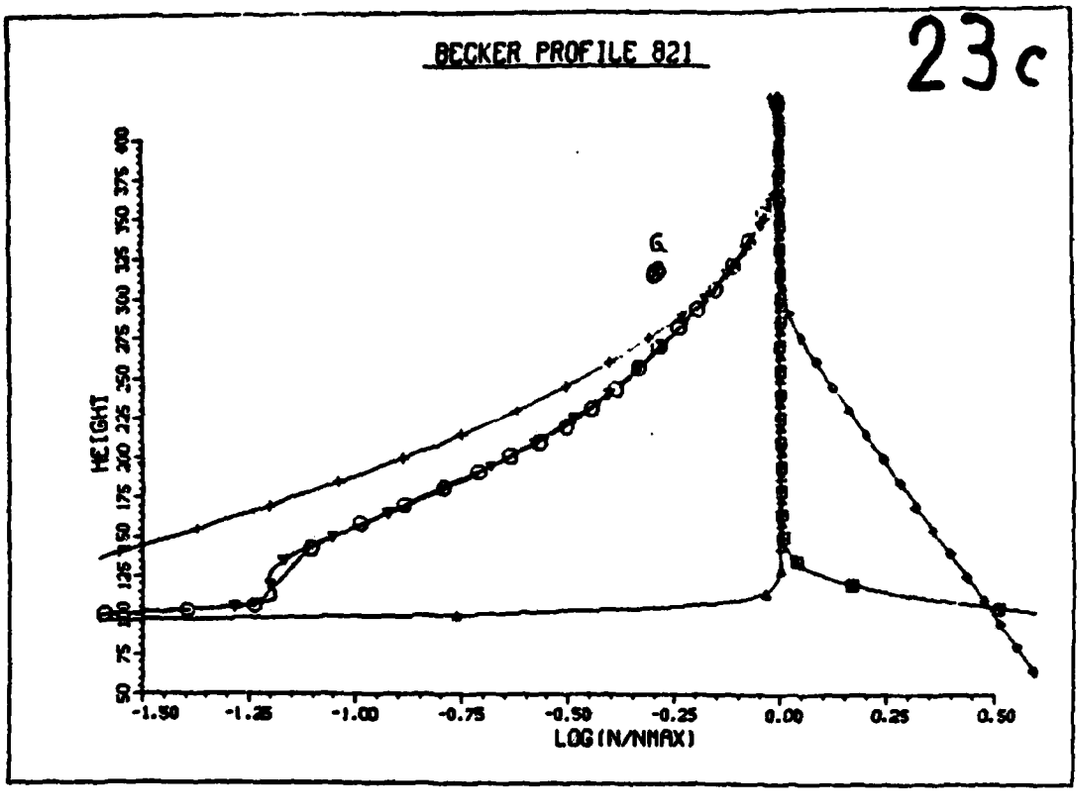
BECKER PROFILE 821
23c
HEIGHT
LOG(N/NMAX)

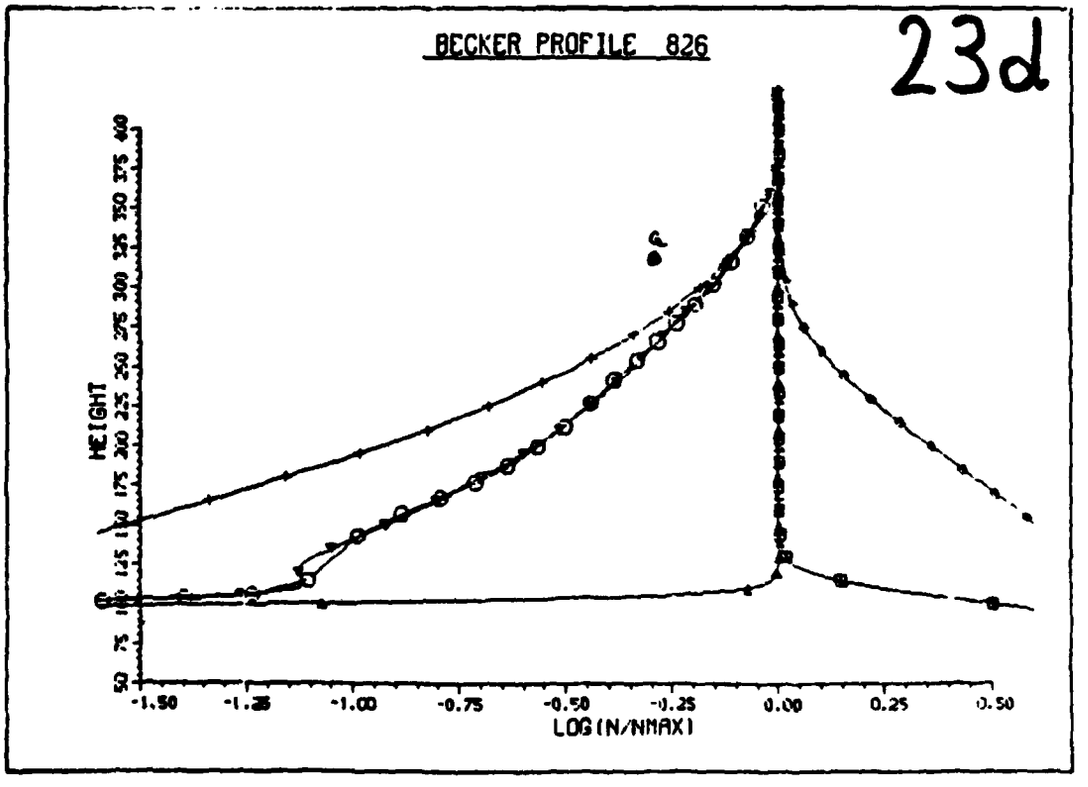
BECKER PROFILE 826
23d
HEIGHT
LOG(N/NMAX)

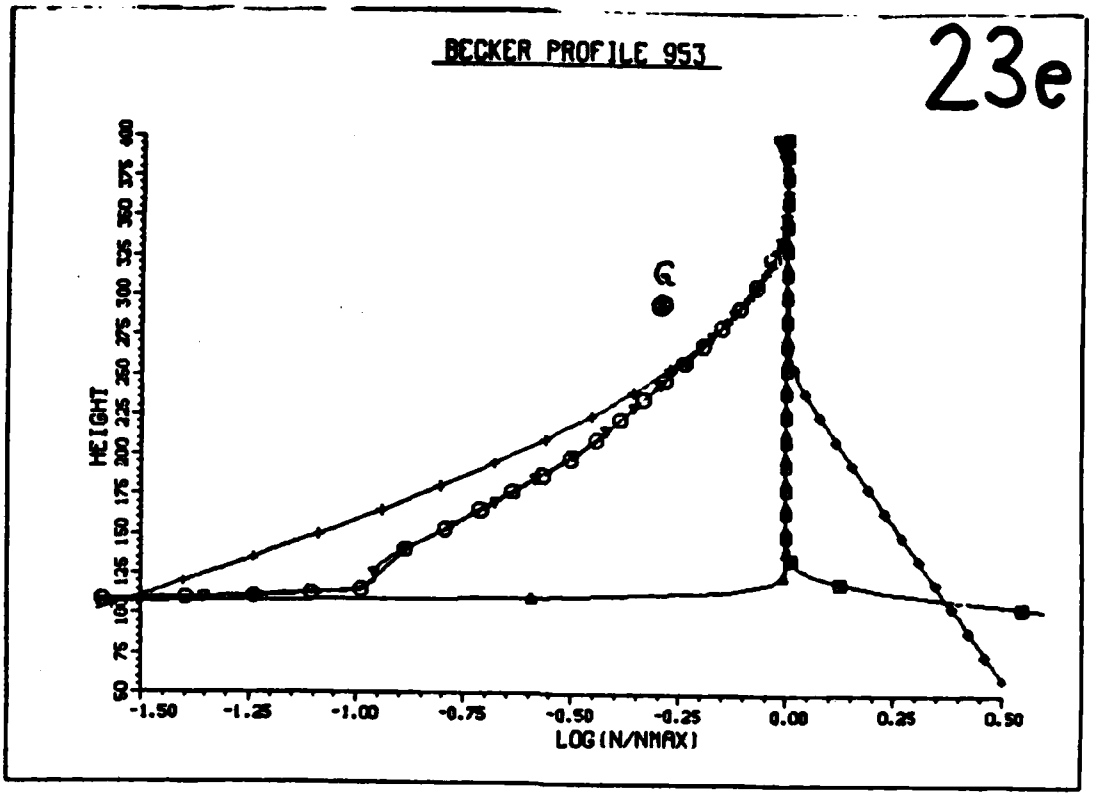
BECKER PROFILE 953
23e
HEIGHT
LOG(N/NMAX)

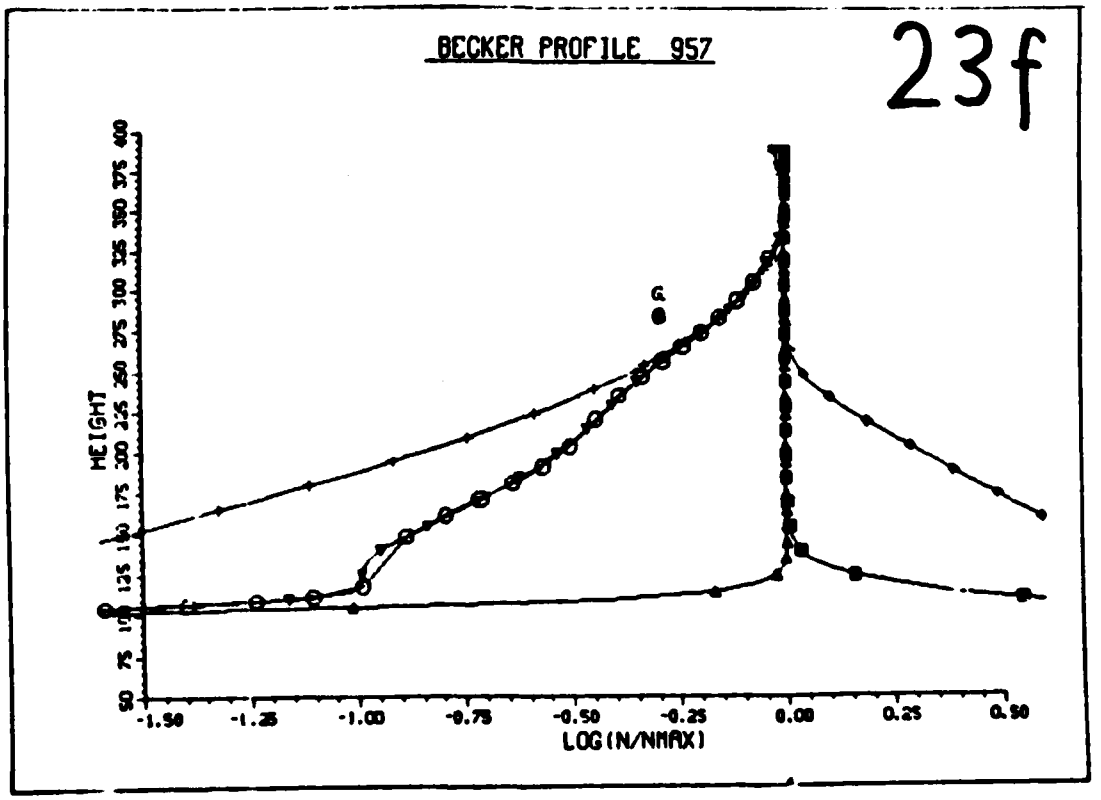
BECKER PROFILE 957
23f
HEIGHT
LOG(N/NMAX)

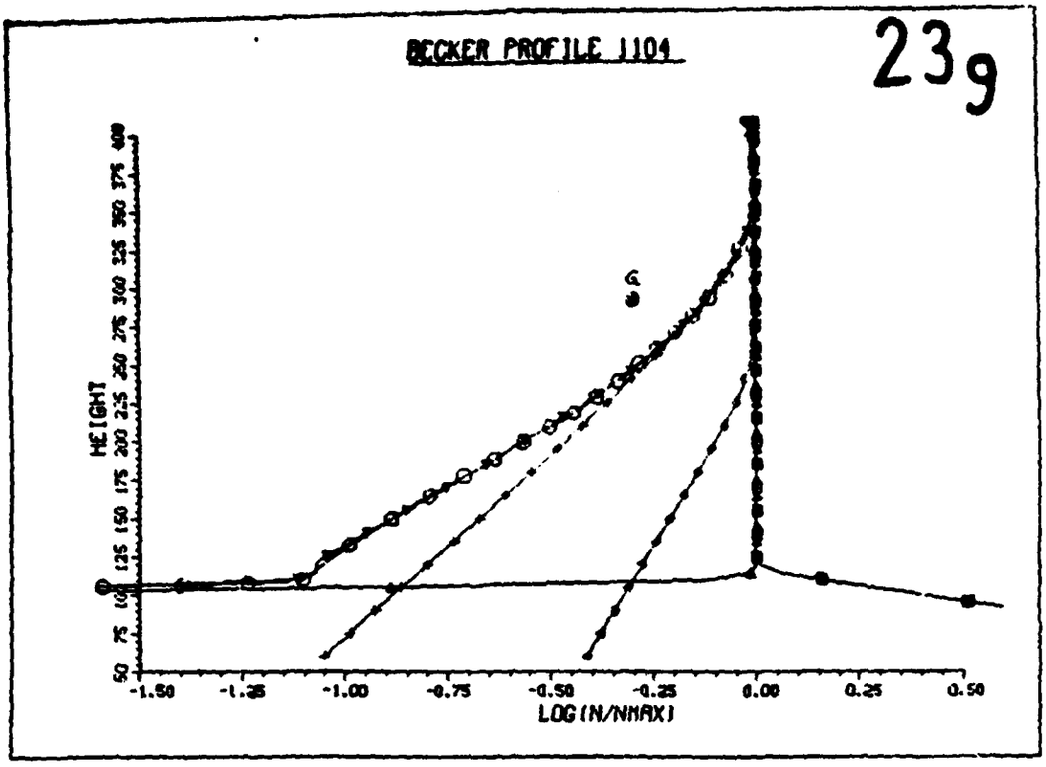
BECKER PROFILE 1104
23g
HEIGHT
LOG(N/NMAX)

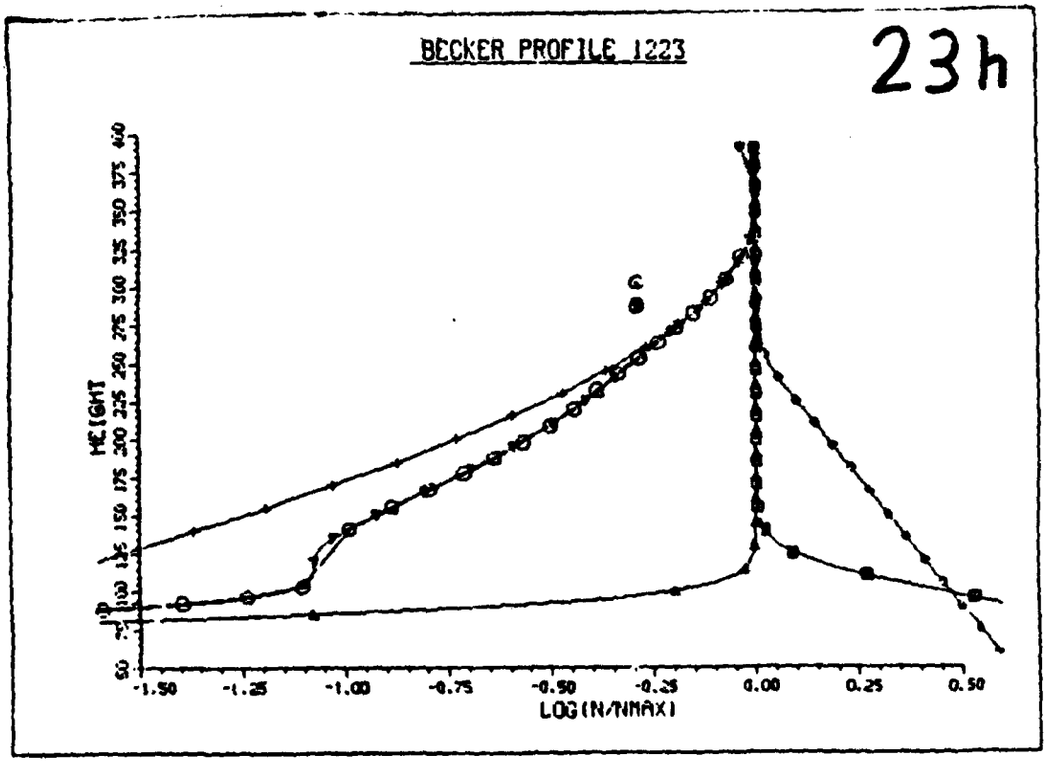
BECKER PROFILE 1223
23h
HEIGHT
LOG(N/NMAX)

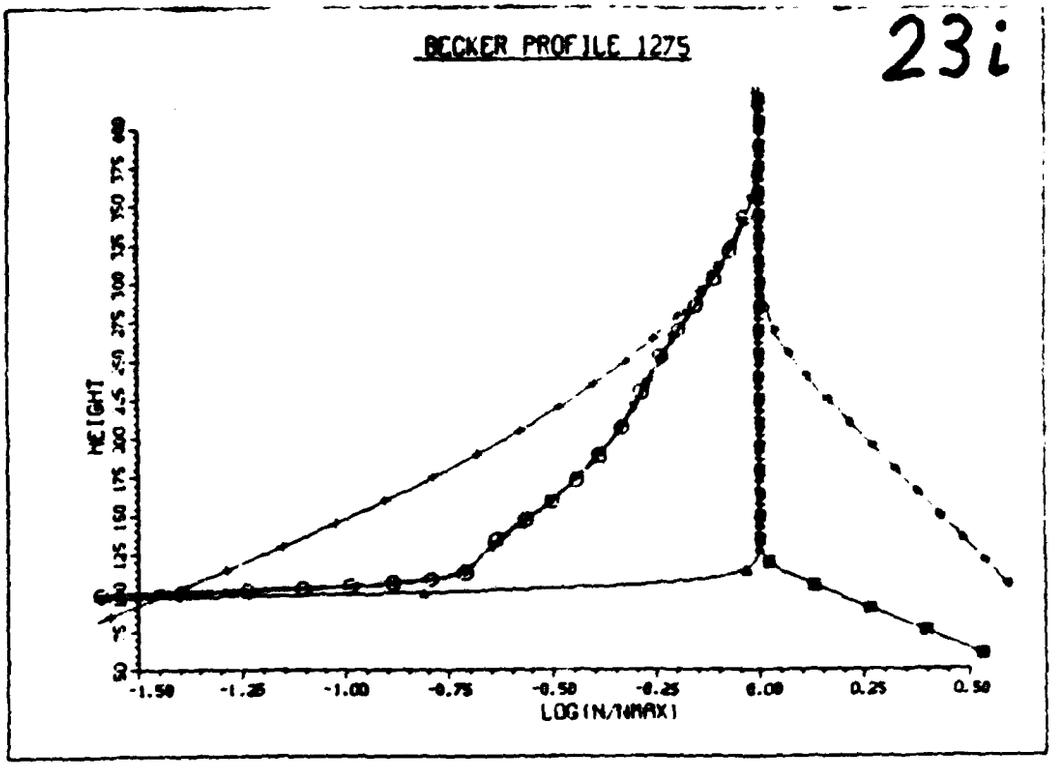
BECKER PROFILE 1275
23i
HEIGHT
-1.50
-1.25
-1.00
-0.75
-0.50
-0.25
0.00
0.25
0.50
LOG(N/NMAX)

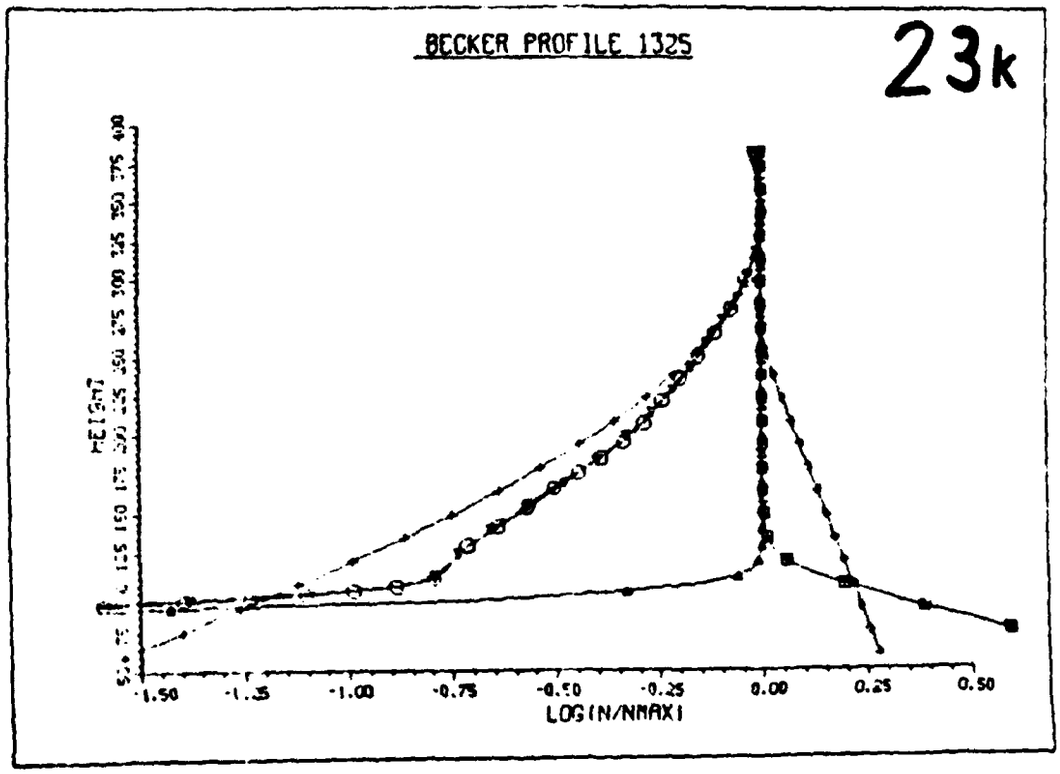
BECKER PROFILE 1325
23k
HEIGHT
-1.50
-1.00
-0.75
-0.25
0.00
0.25
0.50
LOG(N/NMAX)

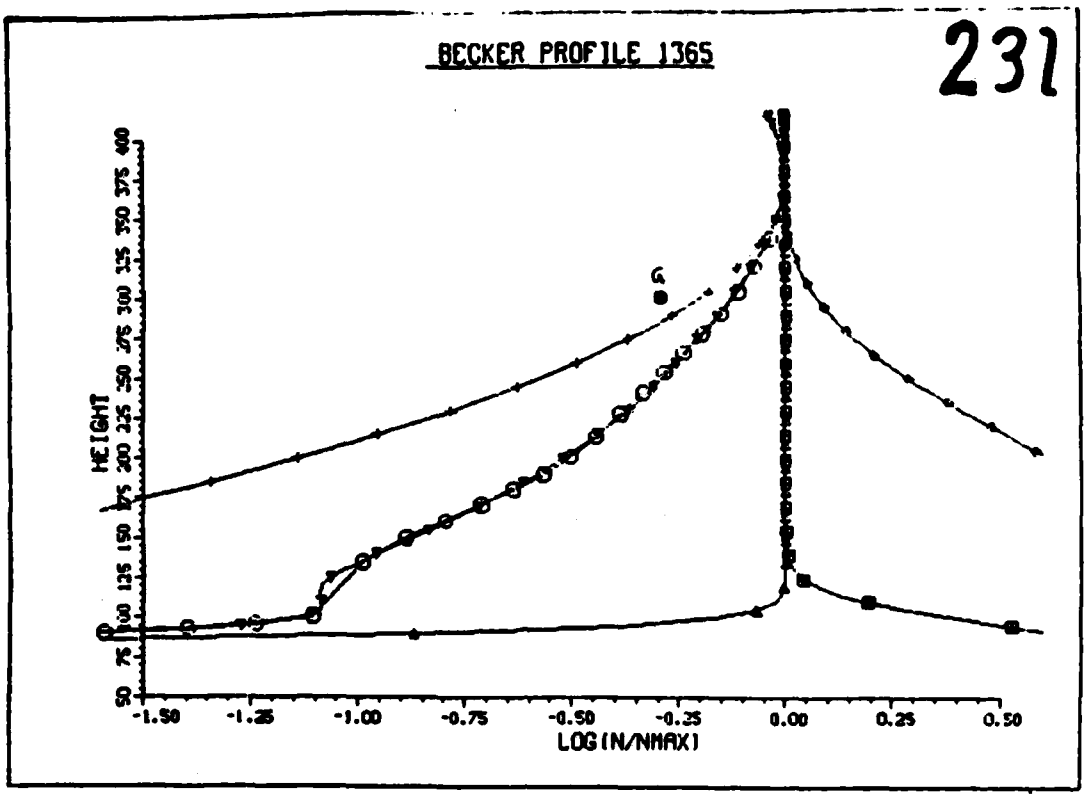
BECKER PROFILE 1365
231
HEIGHT
LOG(N/NMAX)

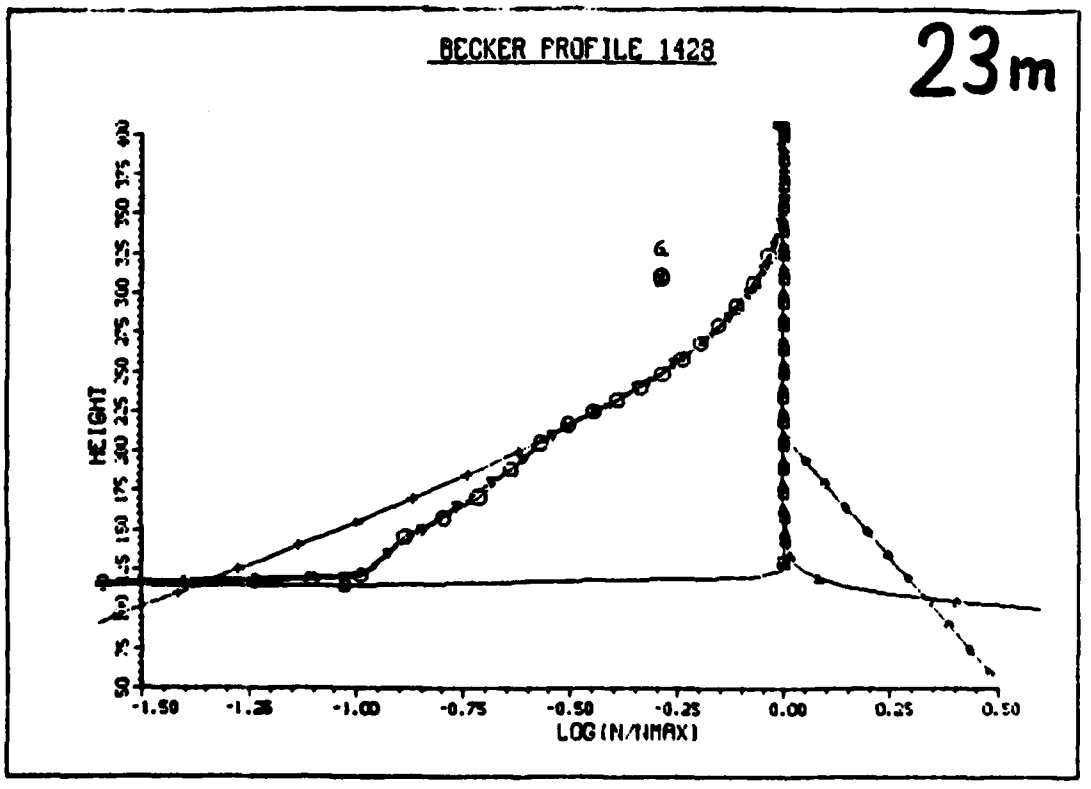
BECKER PROFILE 1428
23m
HEIGHT
LOG(N/NMAX)

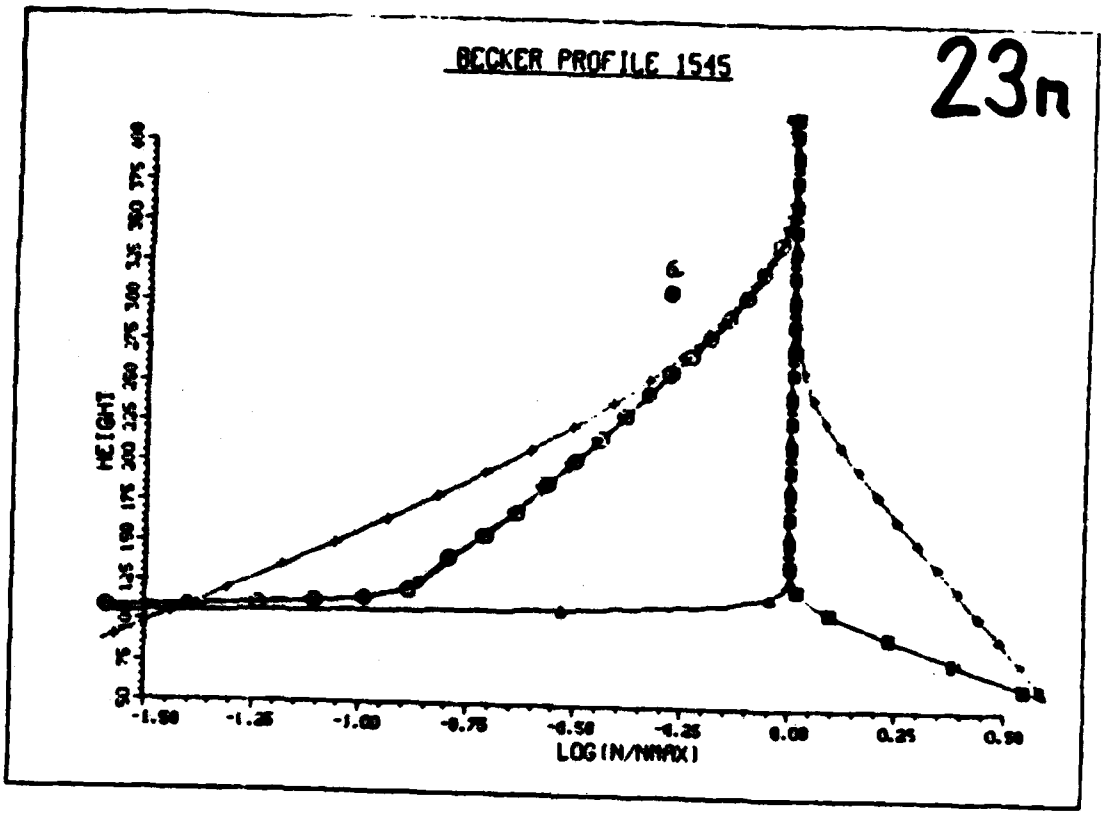
BECKER PROFILE 1545
23n
HEIGHT
LOG(N/NMAX)

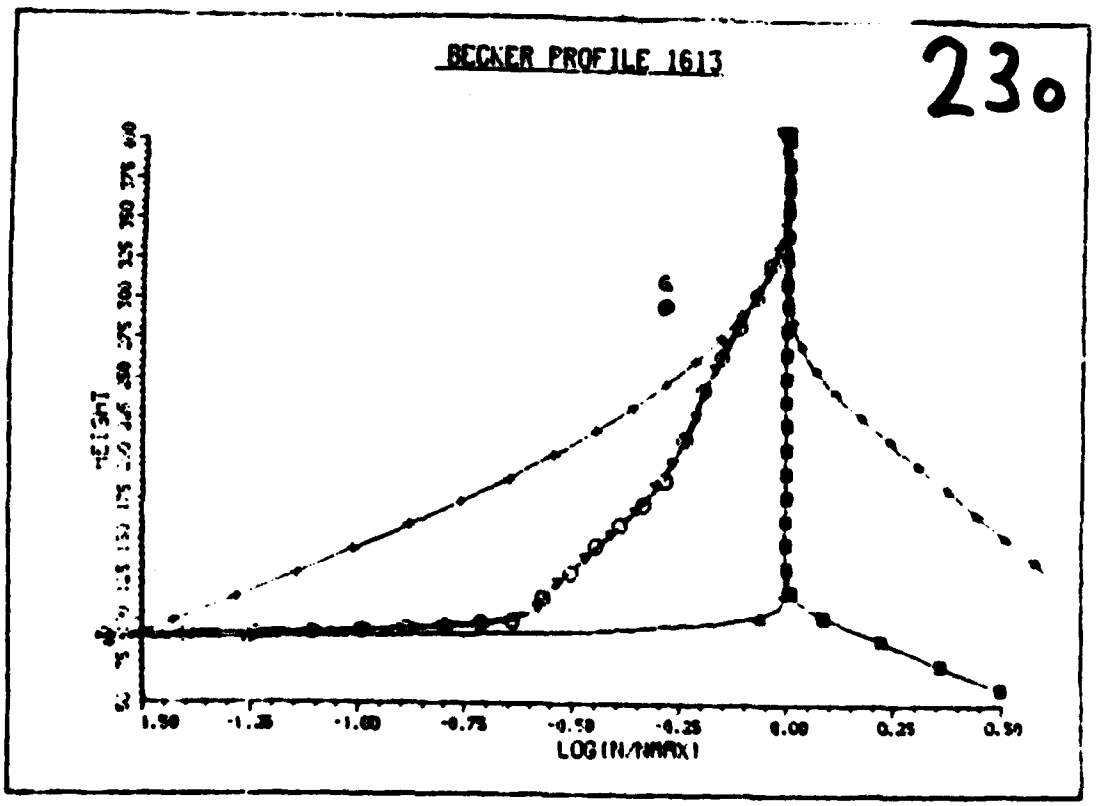
BECKER PROFILE 1613
23o
LOG(N/NMAX)

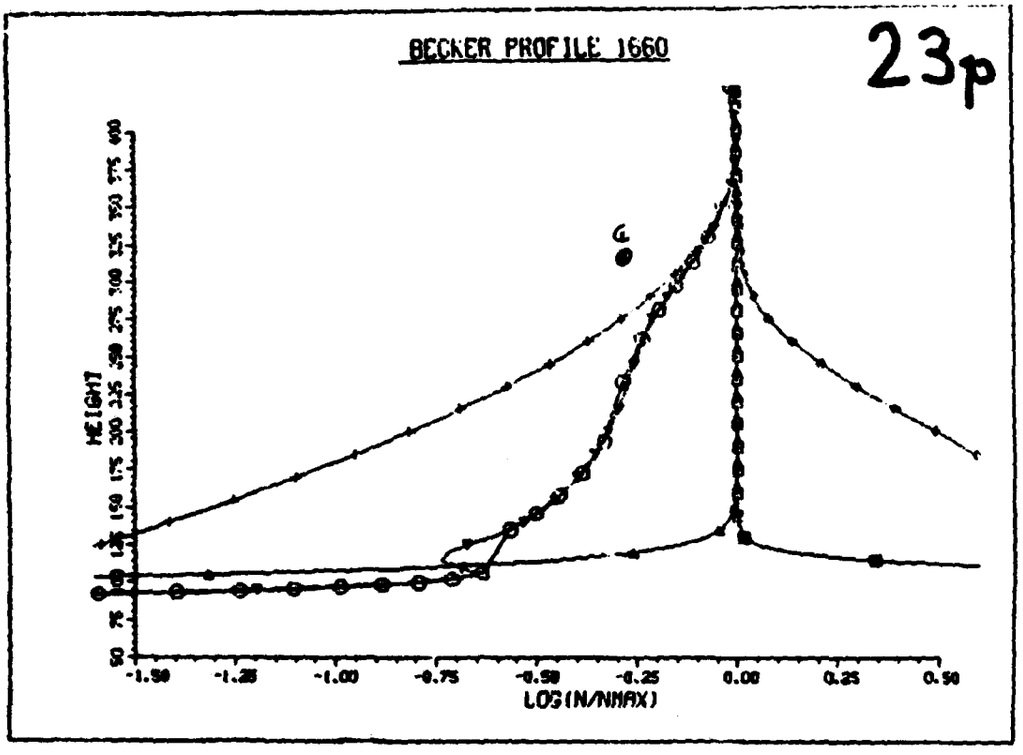

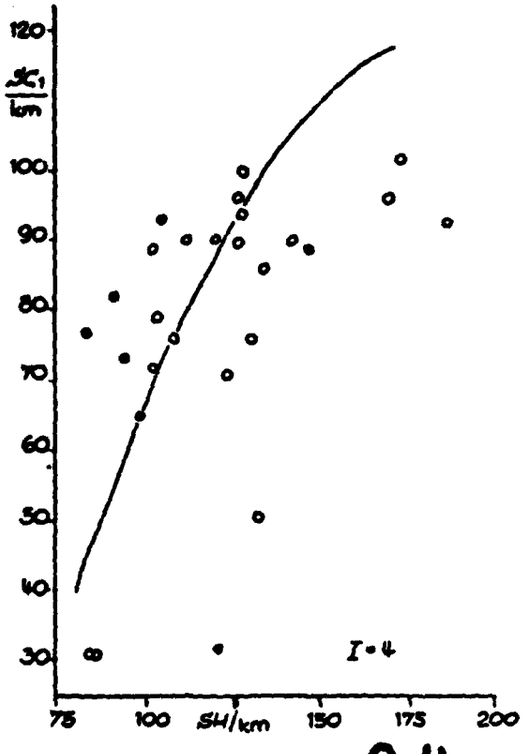

24

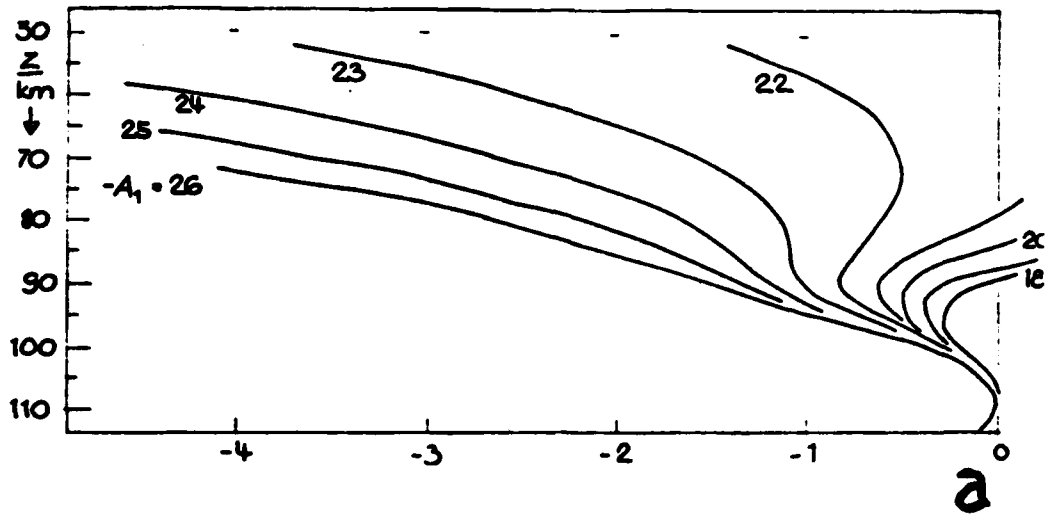
30
Z
km
↓
70
80
90
100
110
23
22
24
25
-A1 = 26
2α
1e
-4
-3
-2
-1
0

a

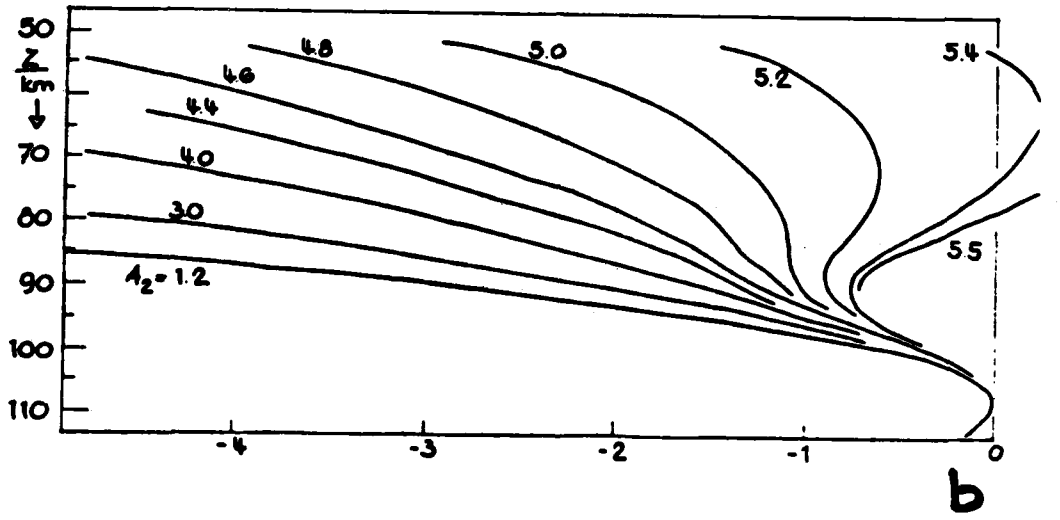
50
Z
km
↓
70
80
90
100
110
4.8
5.0
5.4
4.6
5.2
4.4
4.0
5.5
3.0
A2 = 1.2
-4
-3
-2
-1
0

b

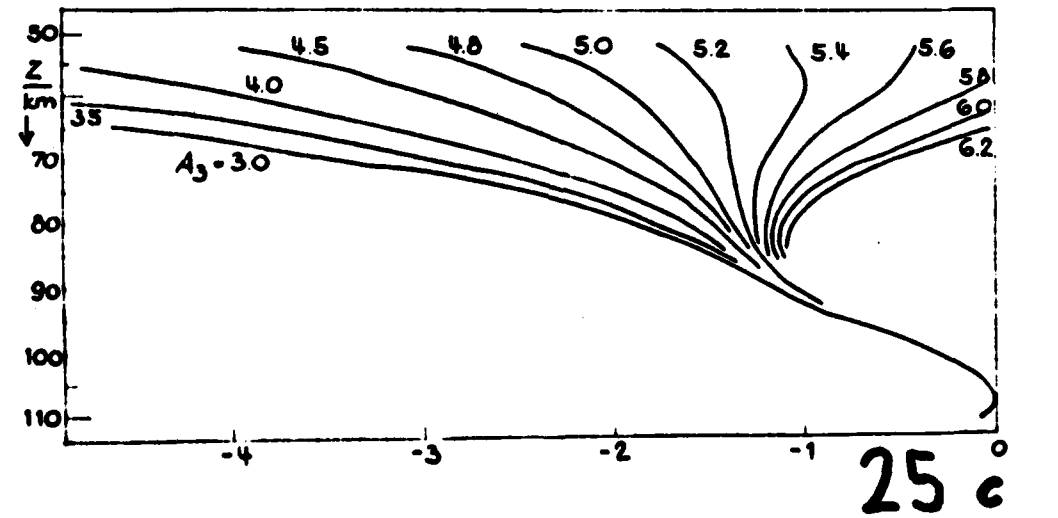
50
Z
km
↓
70
80
90
100
110
4.5
4.8
5.0
5.2
5.4
5.6
4.0
5.8
6.0
3.5
6.2
A3 = 3.0
-4
-3
-2
-1
0

25 c

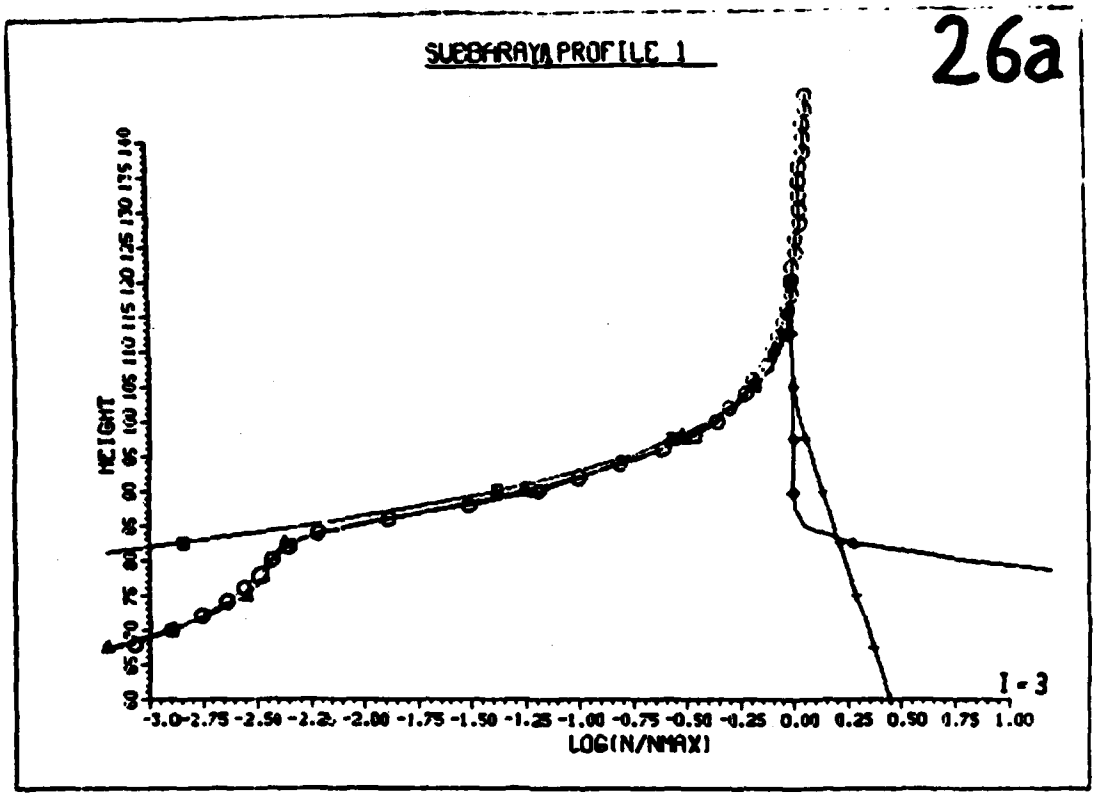
SUBBARAY PROFILE 1
26a
HEIGHT
I = 3
-3.0 -2.75 -2.50 -2.25 -2.00 -1.75 -1.50 -1.25 -1.00 -0.75 -0.50 -0.25 0.00 0.25 0.50 0.75 1.00
LOG(N/NMAX)

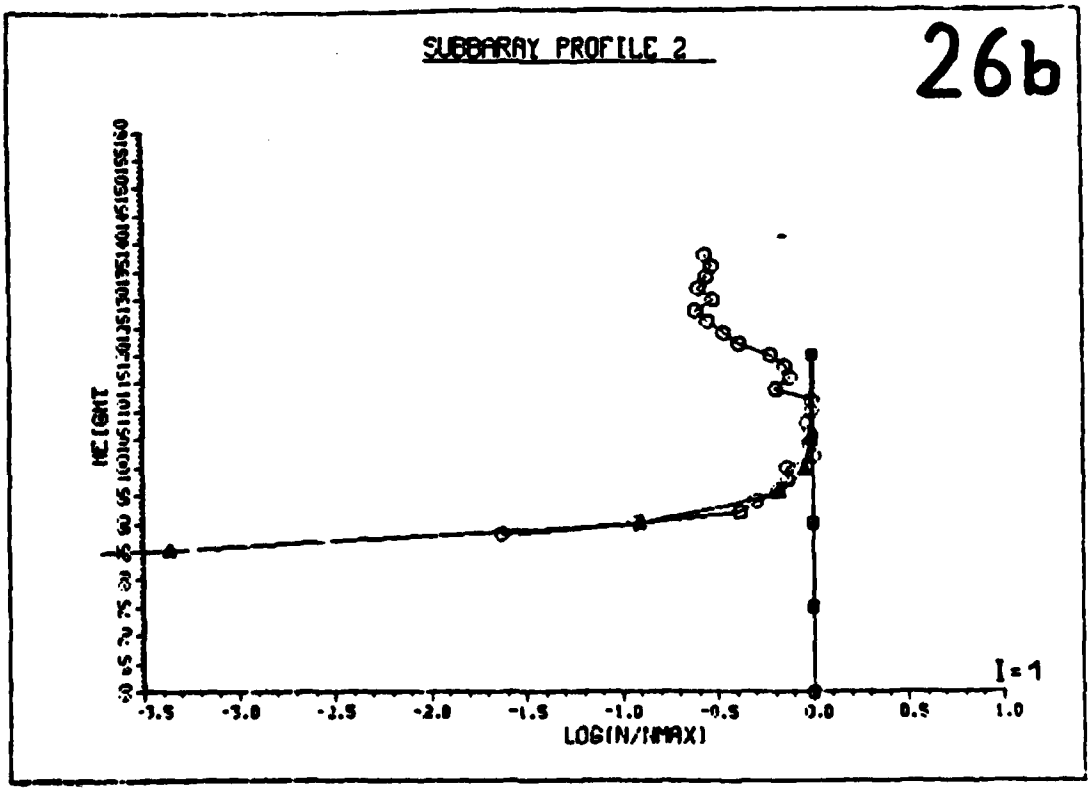
SUBBARAY PROFILE 2
26b
HEIGHT
I = 1
-3.5 -3.0 -2.5 -2.0 -1.5 -1.0 -0.5 0.0 0.5 1.0
LOG(N/NMAX)

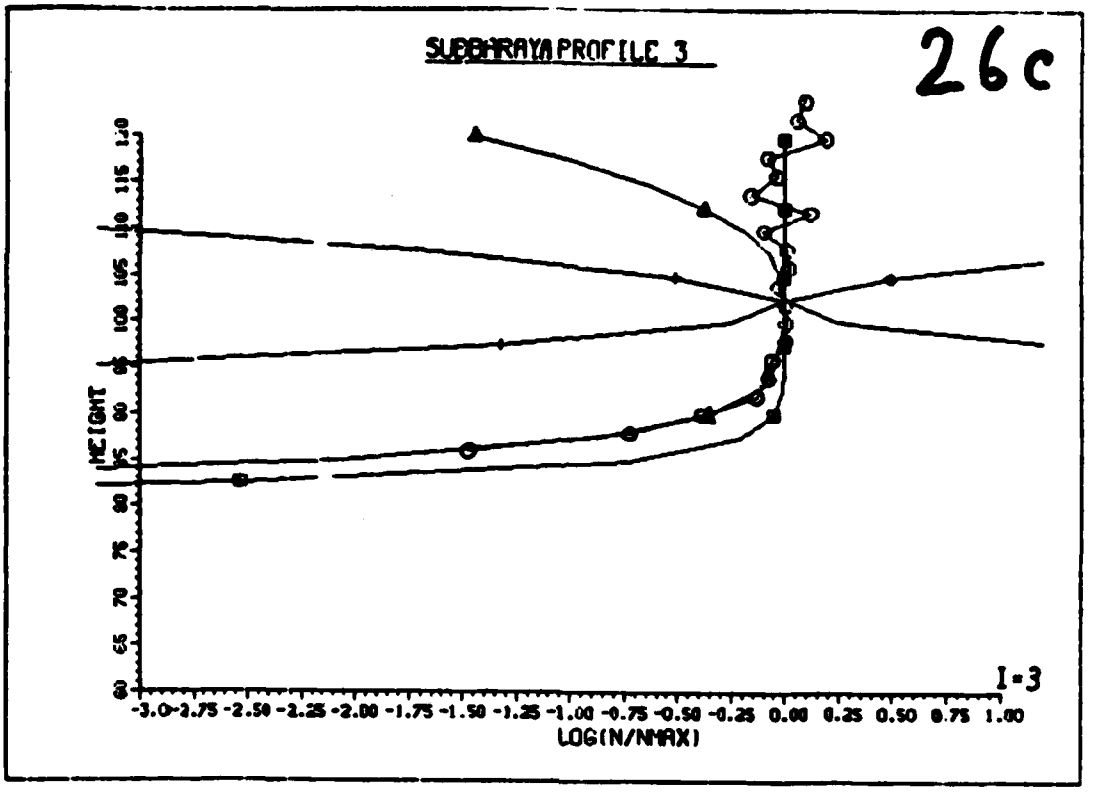
SUBBARAYA PROFILE 3
26c
HEIGHT
I=3
-3.0 -2.75 -2.50 -2.25 -2.00 -1.75 -1.50 -1.25 -1.00 -0.75 -0.50 -0.25 0.00 0.25 0.50 0.75 1.00
LOG(N/NMAX)

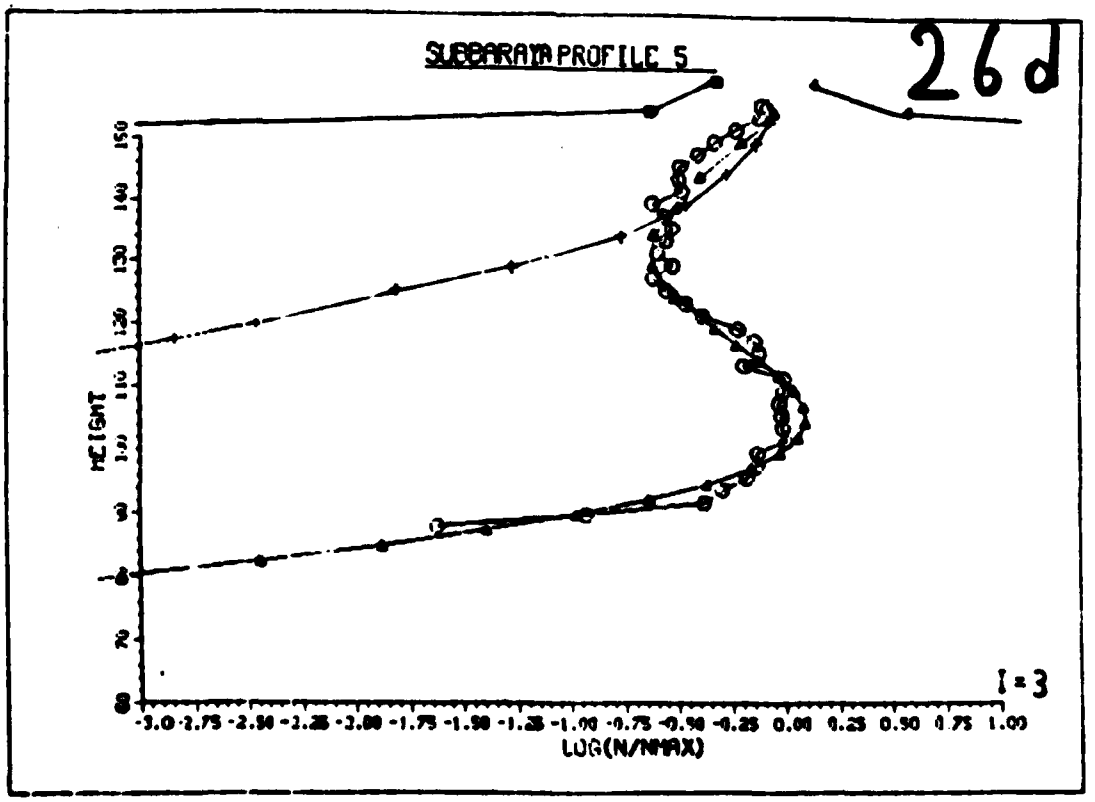
SUBBARAYA PROFILE 5
26d
HEIGHT
I=3
LOG(N/NMAX)

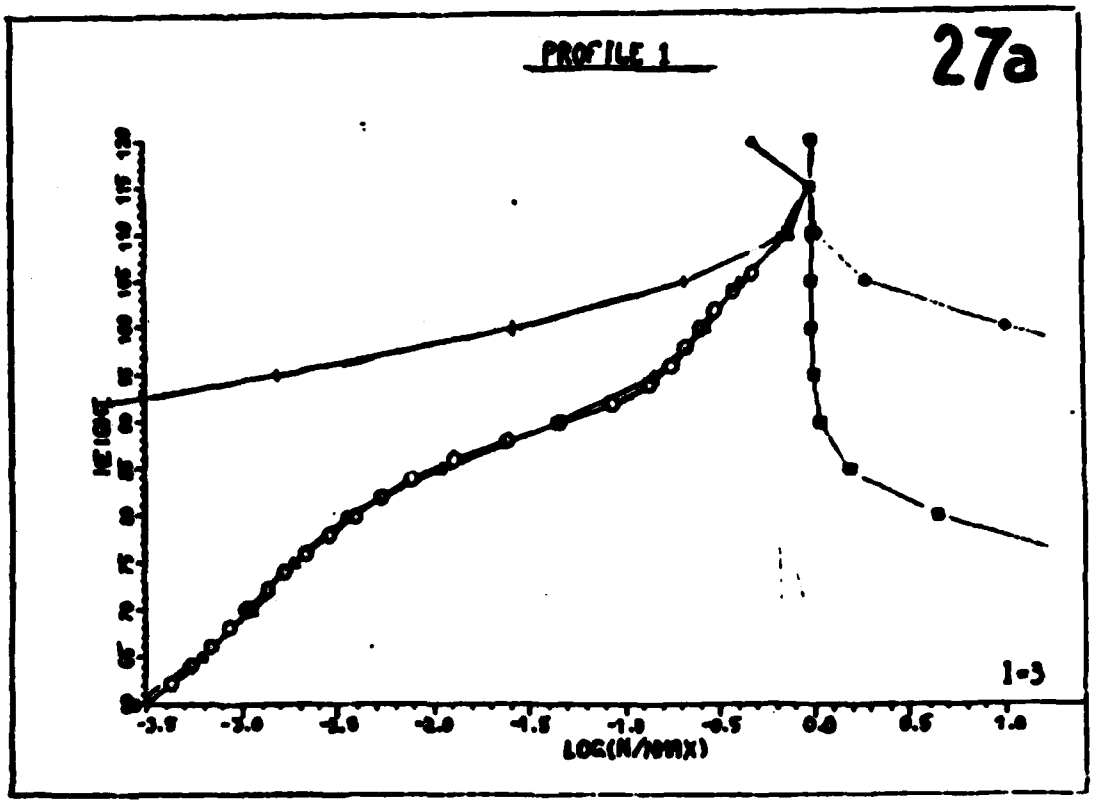
PROFILE 1
27a
HEIGHT
LOG(N/NMAX)
I=3

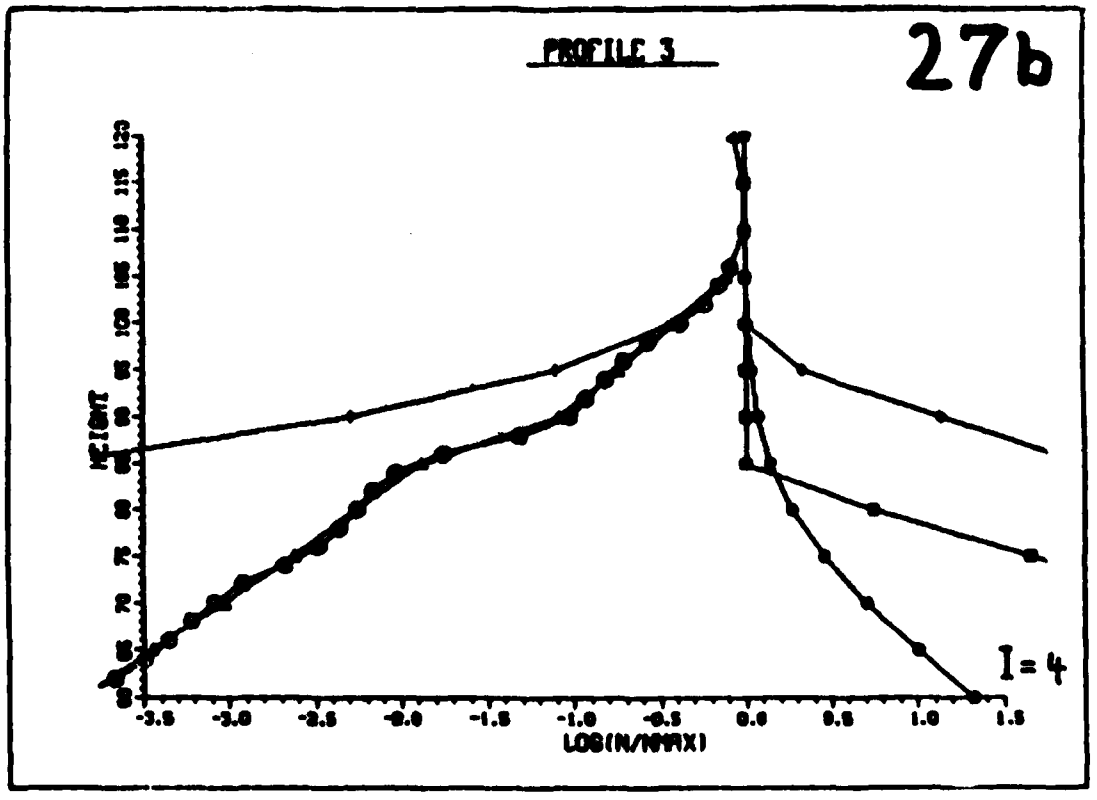
PROFILE 3
27b
HEIGHT
LOG(N/NMAX)
I=4

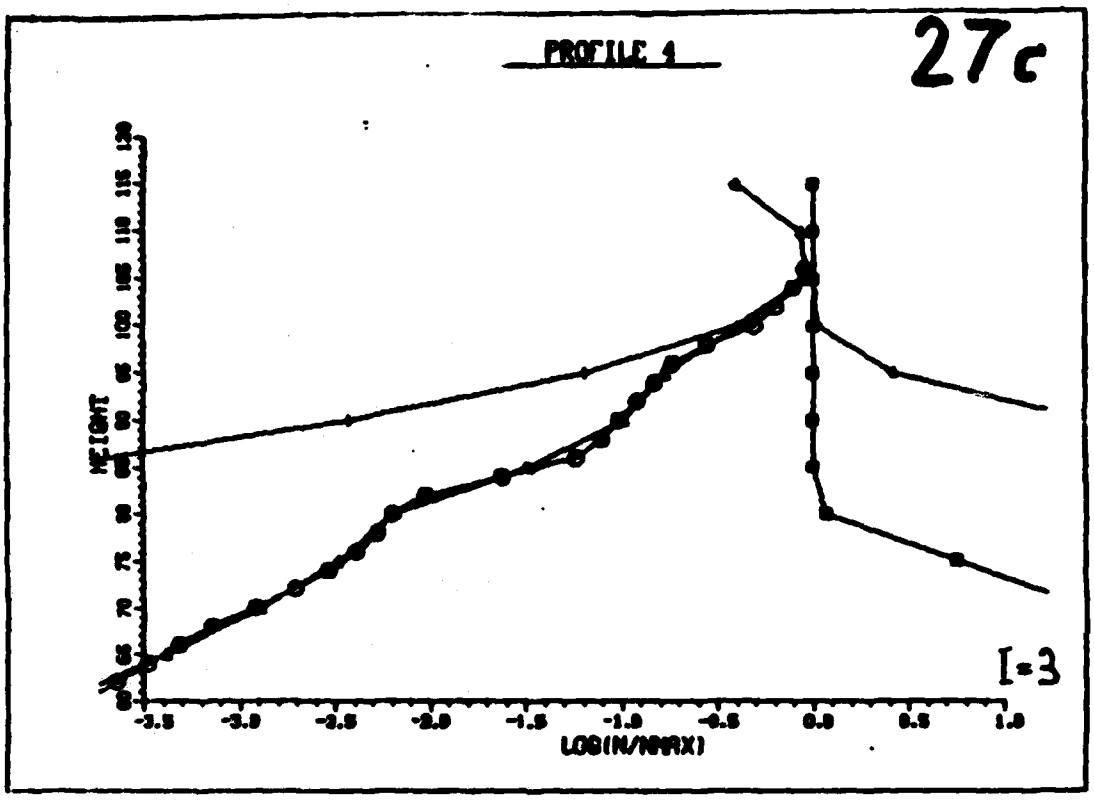
PROFILE 4
27c
HEIGHT
I=3
LOG(N/NMAX)

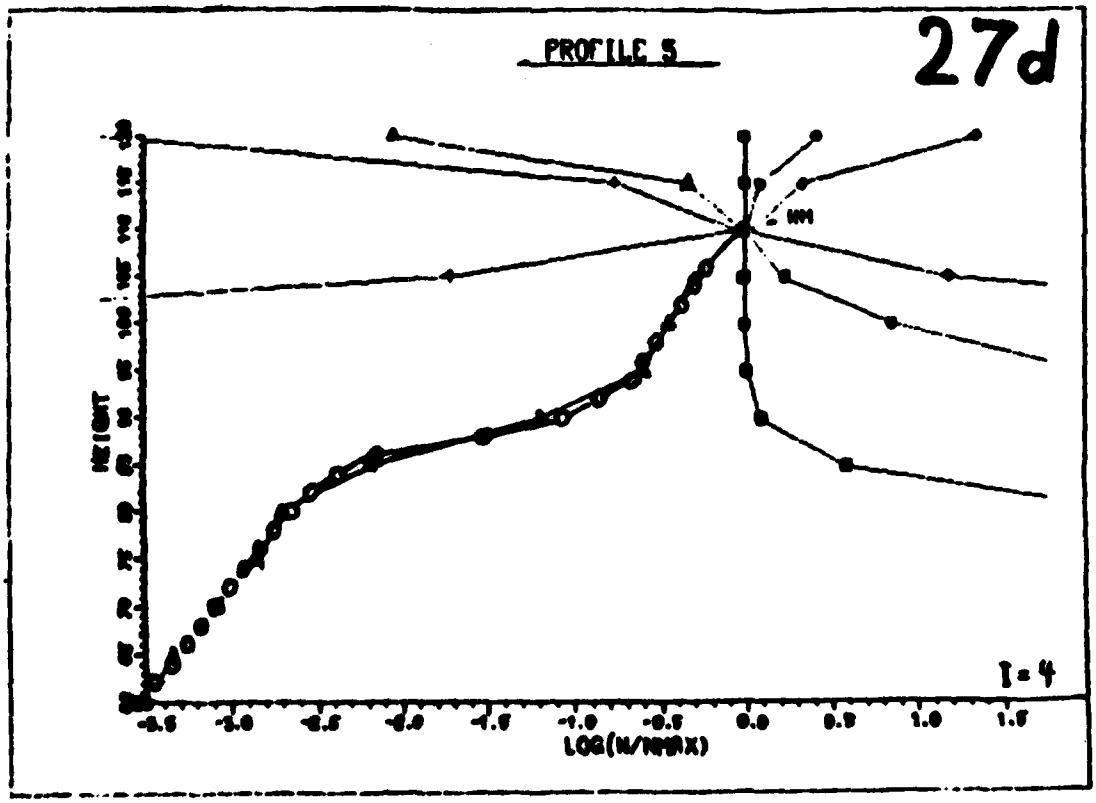
PROFILE 5
27d
HEIGHT
I=4
LOG(N/NMAX)

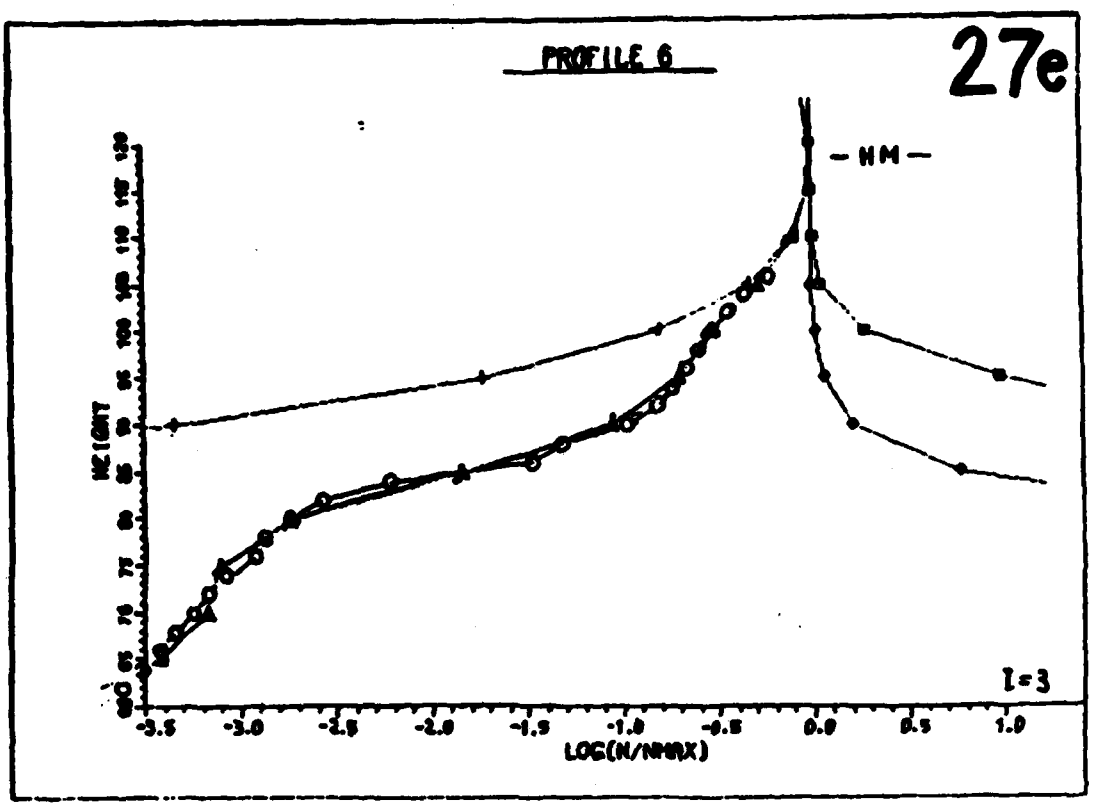
PROFILE 6
27e
- HM -
I=3
HEIGHT
LOG(N/NMAX)

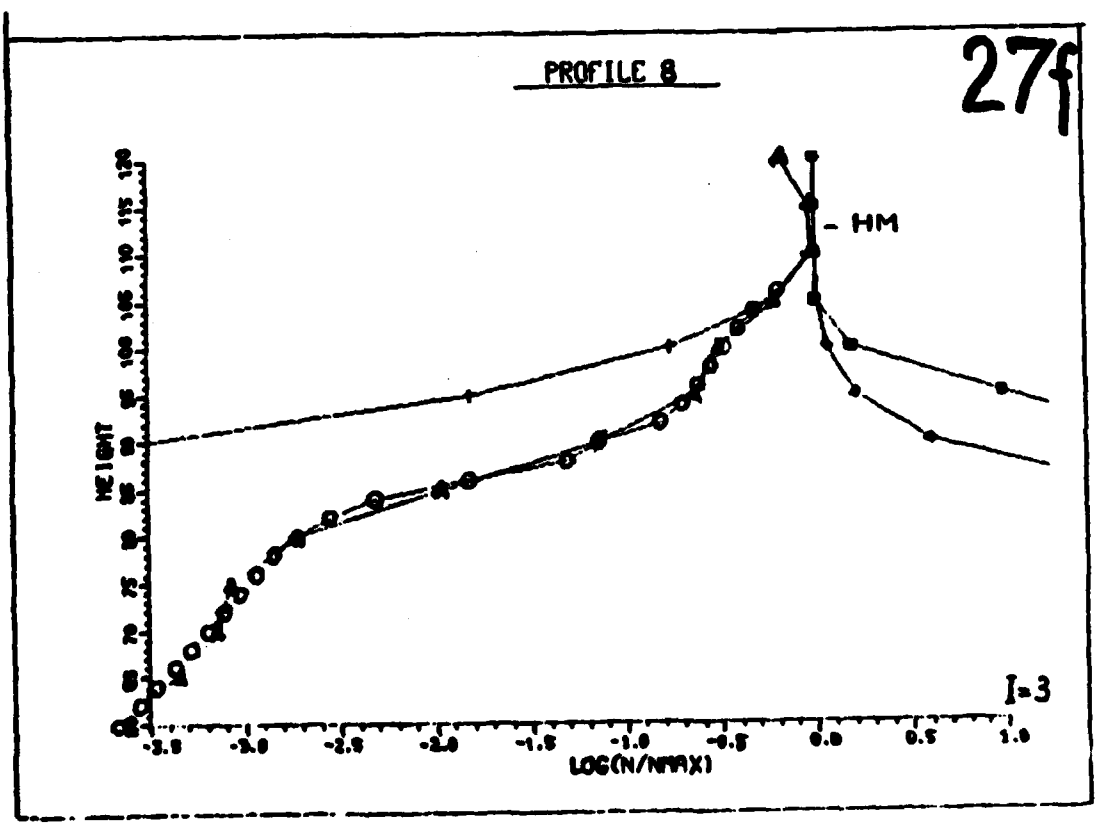
PROFILE 8
27f
- HM
I=3
HEIGHT
LOG(N/NMAX)

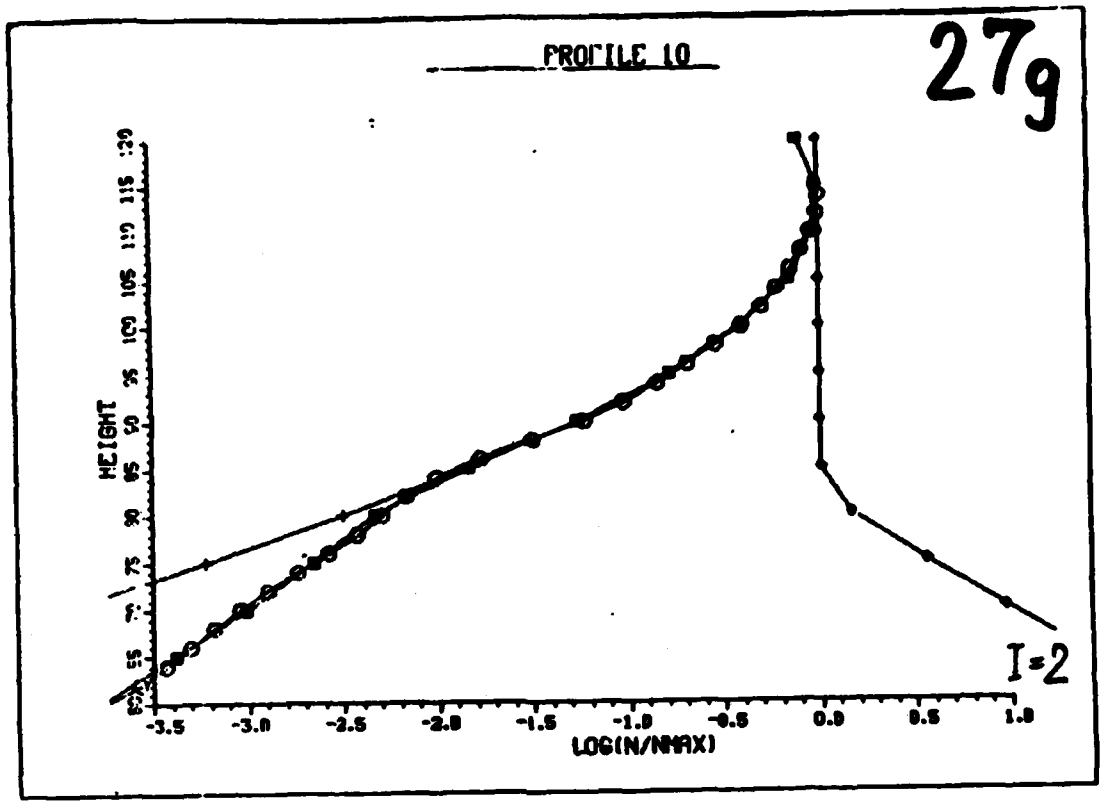
PROFILE 10
27g
HEIGHT
LOG(N/NMAX)
I=2

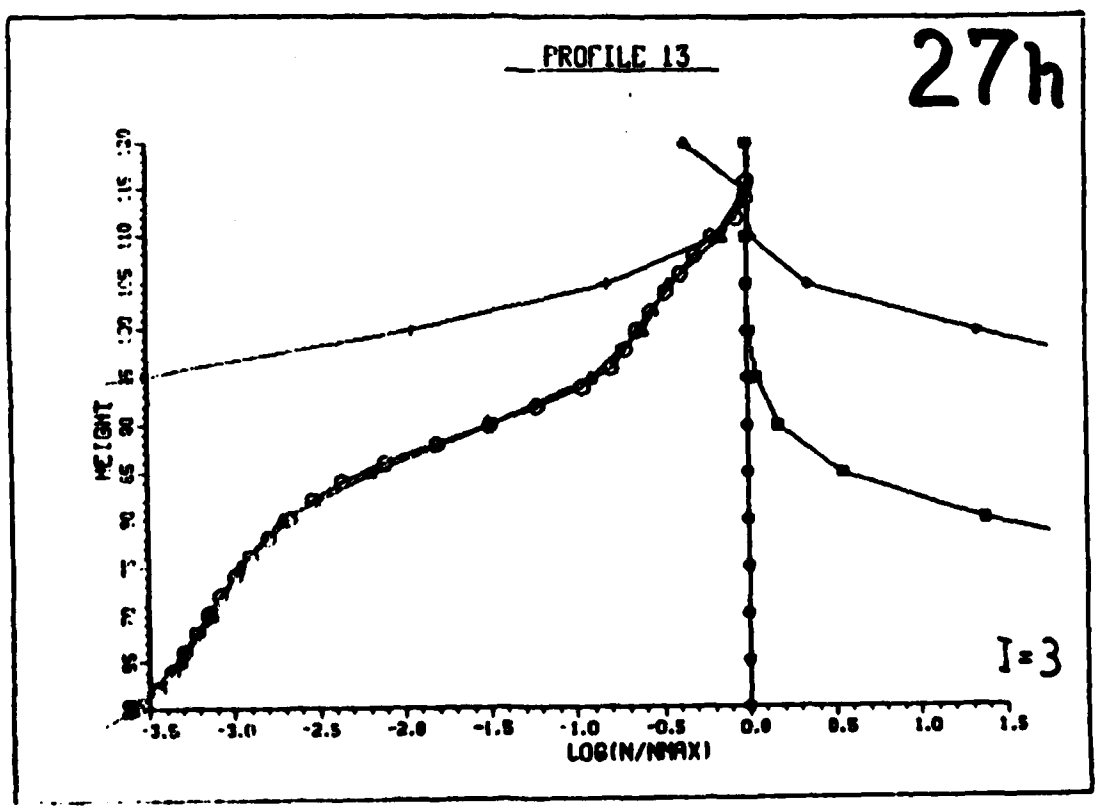
PROFILE 13
27h
HEIGHT
LOG(N/NMAX)
I=3

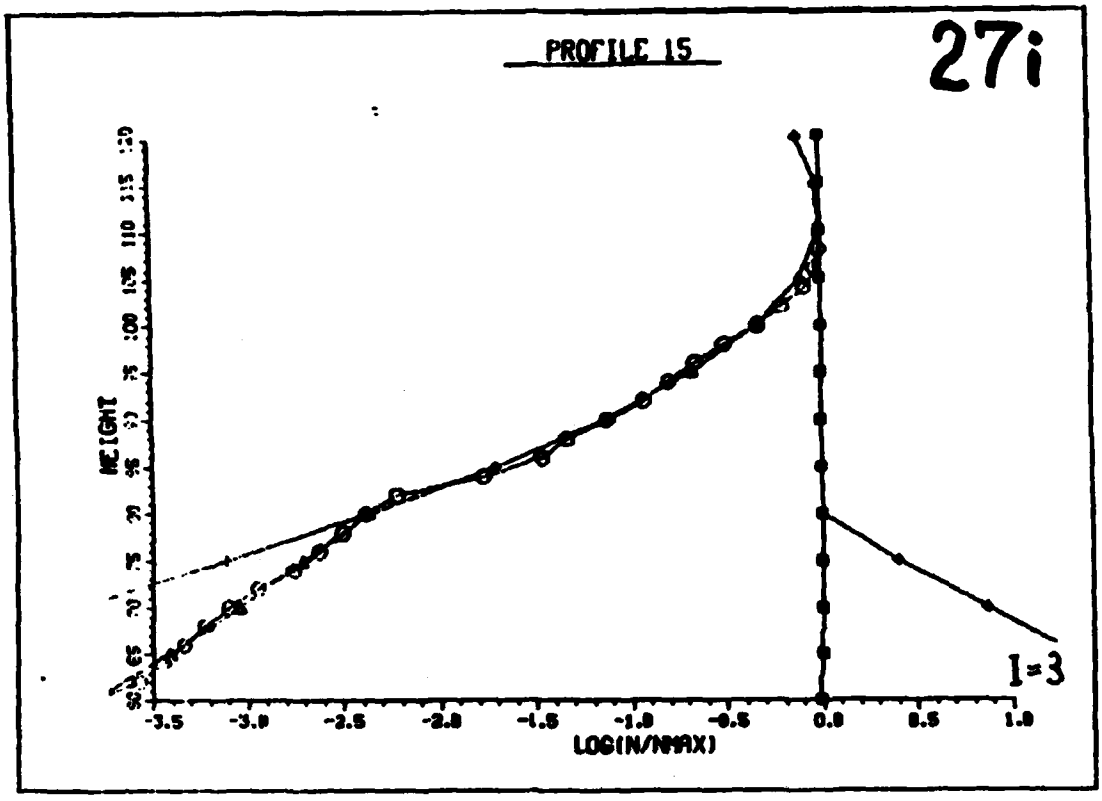
PROFILE 15
27i
HEIGHT
I=3
-3.5
-3.0
-2.5
-2.0
-1.5
-1.0
-0.5
0.0
0.5
1.0
LOG(N/NMAX)

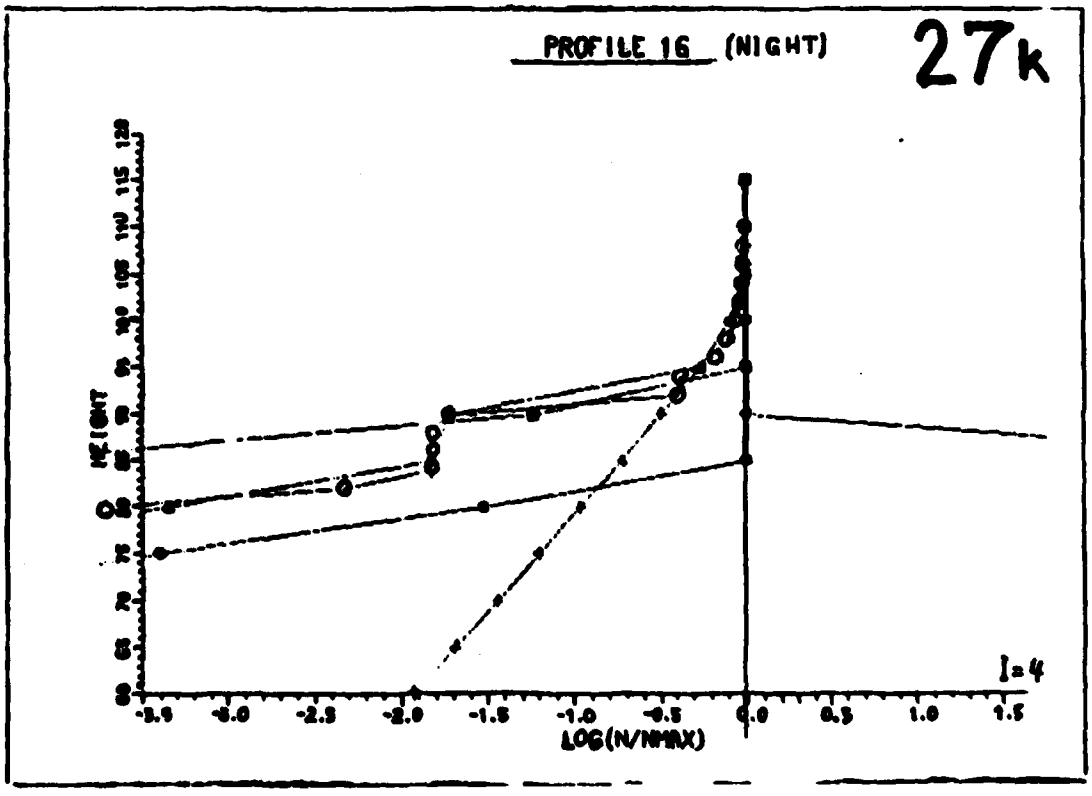
PROFILE 16 (NIGHT)
27k
HEIGHT
I=4
-3.5
-3.0
-2.5
-2.0
-1.5
-1.0
-0.5
0.0
0.5
1.0
1.5
LOG(N/NMAX)